10/3-9-92 (1)

SANDIA REPORT

SAND91—0790
Unlimited Release
Printed January 1992

Yucca Mountain Site Characterization Project

Estimation of the Limitations for Surficial Water Addition Above a Potential High Level Radioactive Waste Repository at Yucca Mountain, Nevada

Merton E. Fewell, Steven R. Sobolik, John H. Gauthier

Prepared by
Sandia National Laboratories
Albuquerque, New Mexico 87185 and Livermore, California 94550
for the United States Department of Energy
under Contract DE-AC04-76DP00789

"Prepared by Yucca Mountain Site Characterization Project (YMSCP) participants as part of the Civilian Radioactive Waste Management Program (CRWM). The YMSCP is managed by the Yucca Mountain Project Office of the U.S. Department of Energy, DOE Field Office, Nevada (DOE/NV). YMSCP work is sponsored by the Office of Geologic Repositories (OGR) of the DOE Office of Civilian Radioactive Waste Management (OCRWM)."

Issued by Sandia National Laboratories, operated for the United States Department of Energy by Sandia Corporation.

Available to DOE and DOE contractors from
Office of Scientific and Technical Information
PO Box 62
Oak Ridge, TN 37831

Prices available from (615) 576-8401, FTS 626-8401

Available to the public from
National Technical Information Service
US Department of Commerce
5285 Port Royal Rd
Springfield, VA 22161

NTIS price codes
Printed copy: A05
Microfiche copy: A01

SAND--91-0790

DE92 008454

SAND91-0790
Unlimited Release
Printed January 1992

Estimation of the Limitations for Surficial Water Addition Above a Potential High Level Radioactive Waste Repository at Yucca Mountain, Nevada

Merton E. Fewell, Steven R. Sobolik, and John H. Gauthier
Performance Assessment Development Division 6313
Sandia National Laboratories
Albuquerque, New Mexico 87185

Abstract

The Yucca Mountain Site Characterization Project is studying Yucca Mountain in southwestern Nevada as a potential site for a high-level nuclear waste repository. Site characterization includes surface-based and underground testing. Analyses have been performed to design site characterization activities with minimal impact on the ability of the site to isolate waste, and on tests performed as part of the characterization process. One activity of site characterization is the construction of an Exploratory Studies Facility, consisting of underground shafts, drifts, and ramps, and the accompanying surface pad facility and roads. The information in this report addresses the following topics: (1) a discussion of the potential effects of surface construction water on repository performance, and on surface and underground experiments; (2) one-dimensional numerical calculations predicting the maximum allowable amount of water that may infiltrate the surface of the mountain without affecting repository performance; and (3) two-dimensional numerical calculations of the movement of that amount of surface water and how the water may affect repository performance and experiments. The results contained herein should be used with other site data and scientific/ engineering judgement in determining controls on water usage at Yucca Mountain. This document contains information that has been used in preparing Appendix I of the Exploratory Studies Facility Design Requirements document for the Yucca Mountain Site Characterization Project.

The work reported here was conducted under Work Breakdown Structure (WBS) 1.2.1.4.7.

Acknowledgements

The authors would like to acknowledge the work of the following people who assisted in creating this document:

Sharon Shannon, who produced many of the graphs in this report directly from the NORIA-SP computational solutions;

Roger Eaton and Polly Hopkins, who gave the authors a sympathetic ear and some helpful advice in running NORIA-SP;

Tom Hinkebein and Franz Lauffer, who reviewed this document and the work contained herein.

Table of Contents

List of Tables

List of Figures

1. INTRODUCTION

The Yucca Mountain Site Characterization Project (YMP) is studying Yucca Mountain in southwestern Nevada as a potential site for a high-level nuclear waste repository. Site characterization includes both surface-based and underground testing. Underground testing is to be facilitated by the construction of an Exploratory Studies Facility (ESF).[1] Water will be placed on the surface of the mountain above the proposed location of a potential repository during construction of the ESF. The water will be used for construction-related operations, such as compaction of fill material and for dust control during construction of roads and pads for the ESF, and for surface-based testing. Because ground water has the potential for reducing the ability of the site to safely isolate waste, there is concern that water applied at the surface of the mountain will degrade repository performance. This report describes calculations that were performed to estimate the maximum amount of water that can enter the surface of Yucca Mountain above the repository without compromising the ability of the site to safely store radioactive waste. Also, additional water might influence experiments conducted in the ESF. This report also describes calculations performed to determine the maximum lateral extent of water entering the surface of the mountain. The results of these calculations will be used to support ESF design, will be incorporated into the Exploratory Studies Facility Design Requirements document (ESF DR), and will be available for guidance in controlling the application of surficial water.

These calculations constitute one of eleven ESF analyses being performed in support of the ESF DR. The particular analysis described in this report is ESF Analysis Number 1, and it evaluated the movement of water used for all ESF surface-based activities to be conducted over the repository. The calculations and analyses performed for ESF Analysis Number 1 were conducted as Quality-Related in accordance with Sandia National Laboratories' implementation of the Yucca Mountain Project Quality Assurance plan and were controlled by Problem Definition Memos (PDM) 72-28 and 72-29. The work reported here was conducted under Work Breakdown Structure (WBS) 1.2.1.4.7.

These calculations are based on available data and on the present conceptual understanding of the processes and mechanisms perceived active at Yucca Mountain. Due to this limited knowledge of Yucca Mountain prior to site characterization, the hydrogeological conceptual model, existing conceptual models of the physical processes, and the mathematical models used in these analyses are not validated. Therefore, considerable uncertainty exists in these results. Recommendations based on the results of these analyses are intended to provide guidance for applying engineering judgment during the design, construction, and operation of the ESF, and therefore must provide relevant results to the architects and engineers who design the ESF. Refinement of the results is an ongoing and iterative process, which must complement site characterization. These calculations may be refined as better understanding evolves through site characterization and through additional analyses, which will address uncertainties and the sensitivity of the results to alternate conceptual models.

---

1. The Exploratory Shaft Facility was renamed the Exploratory Studies Facility in February 1991.

2. APPROACH

Calculations of water movement in layered, fractured, unsaturated porous media using the currently accepted mathematical models are complex and require sophisticated computer codes. Two-dimensional calculations can be extremely time-consuming and are, therefore, expensive while one-dimensional calculations are relatively inexpensive. Unfortunately, the results of one-dimensional calculations cannot be shown to be conservative a priori, and cannot be used to determine the lateral movement of water. Consequently, a combination of one- and two-dimensional calculations was used. A series of one-dimensional calculations was performed to estimate the maximum amount of water that can infiltrate the surface of the mountain without degrading repository performance. The resulting value was used as input to a two-dimensional calculation, which was used to corroborate the one-dimensional results, and to estimate the maximum lateral extent of the water infiltrating the surface of the mountain above the potential repository.

The computer programs TOSPAC [Dudley et al., 1988] and NORIA-SP [Hopkins et al., 1990] were used to perform the one-dimensional and two-dimensional calculations, respectively. In these calculations, the fractures and matrix were treated as an equivalent porous media via the composite-porosity model [Peters and Klavetter, 1988], and the van Genuchten model [van Genuchten, 1980] was used to describe the characteristic curves for the matrix and fractures. Multi-phase affects were assumed to be negligible.

Because only the water that enters the mountain can influence repository performance and underground tests, these calculations were posed in terms of the amount of water entering the surface rather than the amount of water that can be placed on the surface. Posing the calculations in this way avoids complications and uncertainties associated with surface water balances and scenarios for water application. In these calculations, it is also assumed that water entering the surface cannot leave the mountain. The physics associated with water transport at the surface is complicated and includes unpredictable variables such as the weather and surface topography. Thus, at the present time, the amount of water that will infiltrate the mountain is impossible to predict with certainty; however, because rainfall, surface evaporation, runoff, and the amount of water placed on the surface are measurable quantities, infiltration can be inferred from measurements and a surface water balance.

3. PERFORMANCE CRITERIA

Federal regulations 10 CFR 60 [NRC, 1987] and 10 CFR 960 [DOE, 1987] require that the pre-emplacement groundwater travel time (GWTT) from the disturbed zone surrounding the repository to the accessible environment shall not be less than 1000 years and specify acceptable limits for the release of radionuclides to the accessible environment during the 10,000 years following closure of the repository. These regulations provide the performance assessment criteria for measuring performance of the repository and are the basis for determining degradation in repository performance.

Complex processes may be induced by waste emplacement. The possibility that such processes can occur introduces uncertainties into the definition of the disturbed zone and into predicting the potential for increasing the

radionuclide releases due to surface water. Because these processes are not well defined at the present time, our ability to make calculations which include these effects are limited. For these reasons, indication of a precipitous change in GWTT is perhaps a more conservative and meaningful criterion for determining degradation in repository performance. However, to avoid these complications, it is assumed that for surface water to affect the release of radionuclides, an increase in moisture at the repository horizon must occur within 10,000 years. Because an increase in moisture at the repository is not a sufficient condition for an increase in the release of radionuclides to the accessible environment to occur, this assumption is conservative. Therefore, in these analyses, repository performance is considered to be degraded when one or more of three criteria are met:

- GWTT is less than 1000 years;
- A precipitous decrease in GWTT occurs;
- An increase in the total saturation (on the order of one-tenth of one percent) occurs at the repository horizon within 10,000 years.

4. CALCULATIONS

The problem is conceptualized as follows. The mountain as represented in Figure 1 is at the steady-state saturation conditions that correspond to a uniform infiltration of 0.01 mm/yr through the surface of the mountain.[2] At "time zero," a pulse of water begins to infiltrate portions of the top of the mountain at an elevated rate while water continues to infiltrate the mountain through the remaining surface at 0.01 mm/yr. After this pulse of water has entered the mountain, the infiltration into the mountain returns to a uniform 0.01 mm/yr. The movement of this pulse of water is followed through at least 10,000 years in the one- and two-dimensional calculations described below.

4.1 One-dimensional Analysis

PDM 72-28 describes the one-dimensional flow analysis, using TOSPAC [Dudley et al., 1988], to determine the maximum amount of water that infiltrates the mountain through the surface area under construction or maintenance without degrading repository performance. TOSPAC uses the finite difference method to numerically solve the one-dimensional Richards' equation for the transient flow of water in layered, unsaturated porous and fractured media. TOSPAC also simulates the transport of radioactive contaminants and performs ground water travel time (GWTT) calculations. GWTT is calculated by simulating the release of particles from specified locations and monitoring their progress until they

---

2. Montazer and Wilson (1984) estimate the percolation rate through the tuff matrix in the Topopah Spring unit to be between 10^{-4} and 10^{-7} mm/yr. Weeks and Wilson (1984) estimate the rate to be between 0.003 and 0.2 mm/yr. Based on these estimates, 0.01 mm/yr was chosen as a representative value for the steady-state surface infiltration. Also, saturation values obtained by the one- and two-dimensional steady-state calculations at 0.01 mm/yr are within the range of saturation values that presently reside in the Reference Information Base (RIB), with the exception of those reported for the vitric Paintbrush Tuff layer PTn (see the explanation in Section 4.1.1).

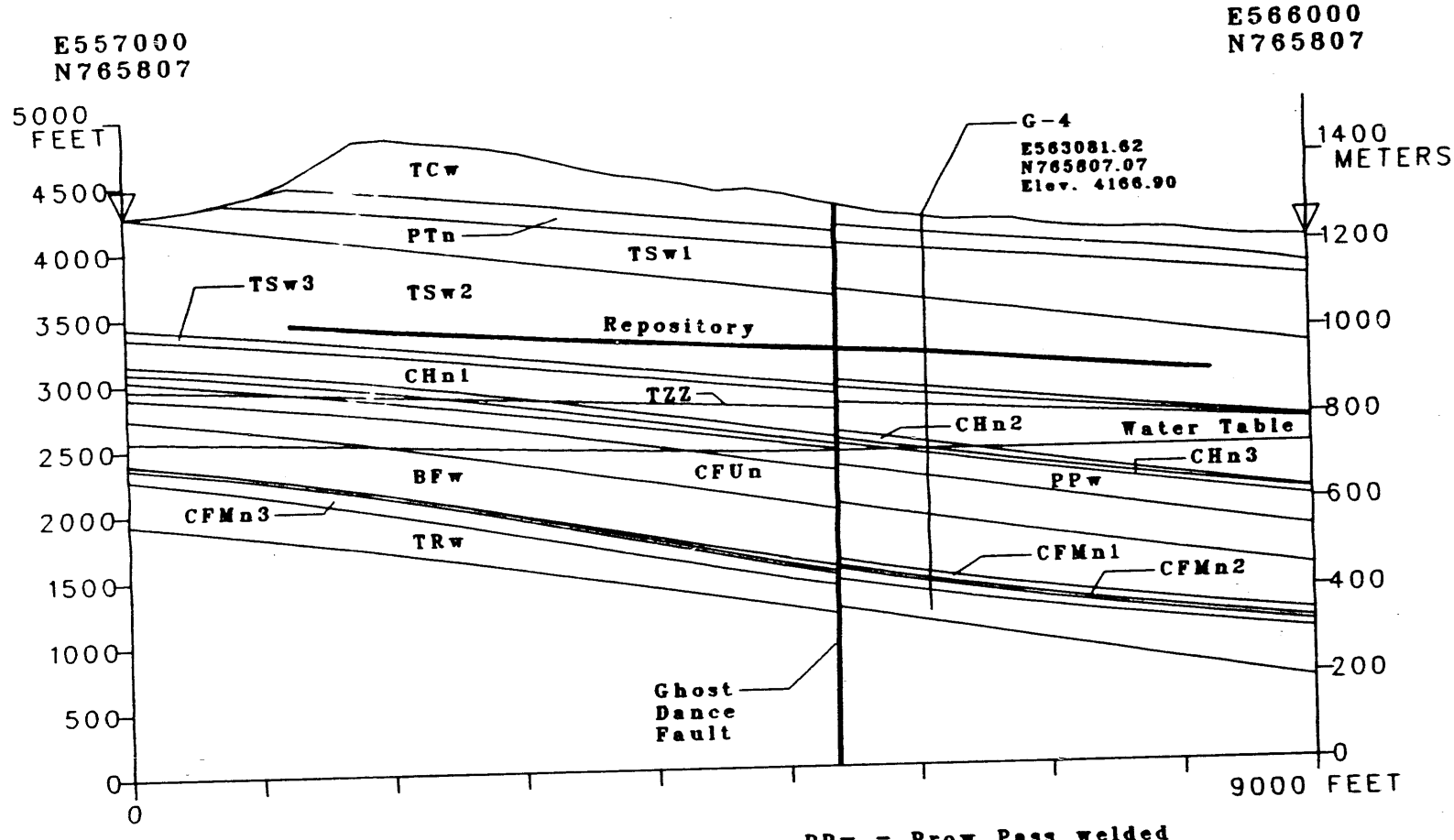

TCw = Tiva Canyon welded
PTn = Paintbrush Tuff nonwelded
TSw1 = Topopah Spring welded #1
TSw2 = Topopah Spring welded #2
TSw3 = Topopah Spring welded #3
CHn1 = Calico Hills nonwelded #1
CHn2 = Calico Hills nonwelded #2
CHn3 = Calico Hills nonwelded #3

PPw = Prow Pass welded
CFUn = Upper Crater Flat nonwelded
BFw = Bullfrog welded
CFMn1 = Middle Crater Flat nonwelded #1
CFMn2 = Middle Crater Flat nonwelded #2
CFMn3 = Middle Crater Flat nonwelded #3
TRw = Tram welded
TZZ = Top of Zeolitized Zone

West-East Section Through Drillhole USW G-4

Figure 1: West-East section of Yucca Mountain
through borehole USW G-4

reach specified locations. TOSPAC has been used extensively in the Yucca Mountain Site Characterization Project to solve problems involving flow through porous, fractured, layered, unsaturated media and for GWTT calculations [Peters 1988]. In addition, TOSPAC has met the requirements of SNL's implementation of the YMP's criteria for software quality assurance. For these reasons, TOSPAC was chosen to perform the one-dimensional calculations.

The pulse of water entering the mountain is imposed by placing a hypothetical pond onto the surface of a one dimensional column as depicted in Figure 2. When the pond is drained, the 0.01 mm/yr uniform infiltration rate is imposed on the top of the column and the calculation is continued until the mountain is again at a steady state. The calculational mesh used for these calculations is shown in Figure 3.

4.1.1 Assumptions

The hydrogeological conceptual model used for these calculations is depicted in Figure 2. The hydrogeological layers shown in the figure are those defined by Ortiz et al. [1985]. The material within each of the layers is assumed to be homogeneous and isotropic. The stratigraphy was obtained from the RIB, and corresponds to that for borehole USW G-4. The data from borehole USW G-4 was chosen because of its location within the repository block. Because material hydrologic property data in the RIB corresponding to this stratigraphy are incomplete,[3] the material hydrologic properties were not obtained from the RIB. Instead, the best data available at the initiation of these calculations were used. Data for all stratigraphic units except the alluvium are taken from USW G-4 and USW GU-3 data; these data were considered to be representative of Yucca Mountain by Peters et al. [1984]. No published hydrological properties data for alluvium currently exists; therefore, the material properties used for the alluvium layer were those values estimated by Alan Flint of the U.S. Geological Survey (personal communication, July 19, 1989). These data are contained in Appendix A.

A steady-state saturation profile produced by TOSPAC, with an infiltration rate of 0.01 mm/yr imposed on the top surface, is shown in Figure 4. This saturation profile agrees very well with RIB data for saturation except at the vitric Paintbrush Tuff layer (PTn) and the vitric Calico Hills layer (CHnlv). The RIB values for porosity and saturation throughout the stratigraphy were taken primarily from boreholes USW G-1 and USW H-1. In those values, the porosity value given for PTn is 45%±15%, and the saturation value given is 61%±15%. The porosity value used for this analysis, which was determined to be a mean value from the measurements from USW G-4 and USW GU-3, was 40% [Peters, et. al., 1984]. Using 40% porosity and a steady-state infiltration of 0.01 mm/yr, a saturation value of 10% was calculated for PTn. It is known that there is a significant qualitative difference in PTn at different locations. At some places, PTn has been compacted more and mixed with the neighboring layers to some degree; at other locations, the layers have not been compacted as much and are distinctly different. Because of the large amount of water that can be held by PTn, as indicated by the porosity used

---

3. Only saturated matrix hydraulic conductivity and porosity data for drill hole USW G-4 presently reside in the RIB.

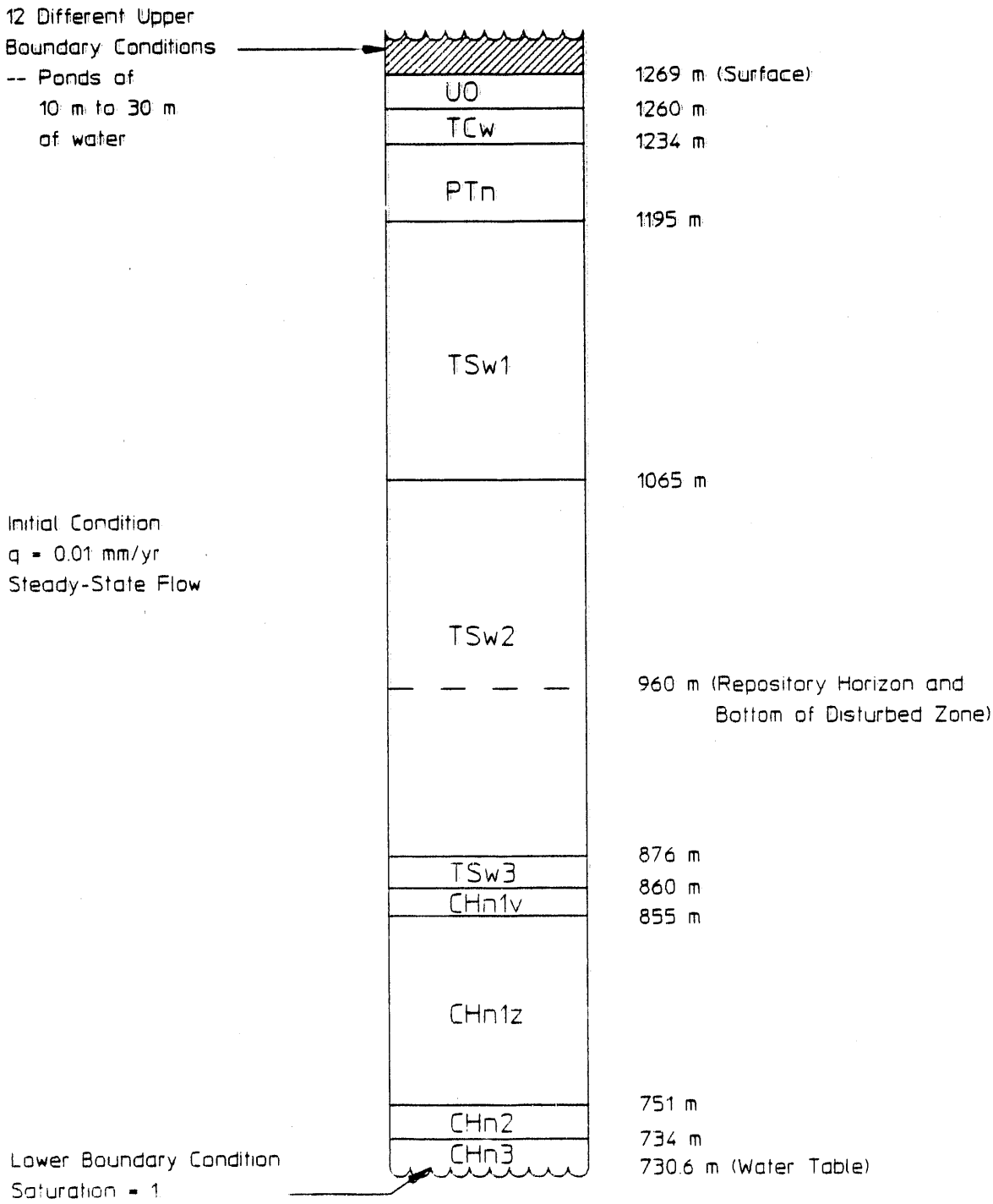

Figure 2: Conceptualization of the one-dimensional problem
(refer to Figure 1 for definition of stratigraphic layers)

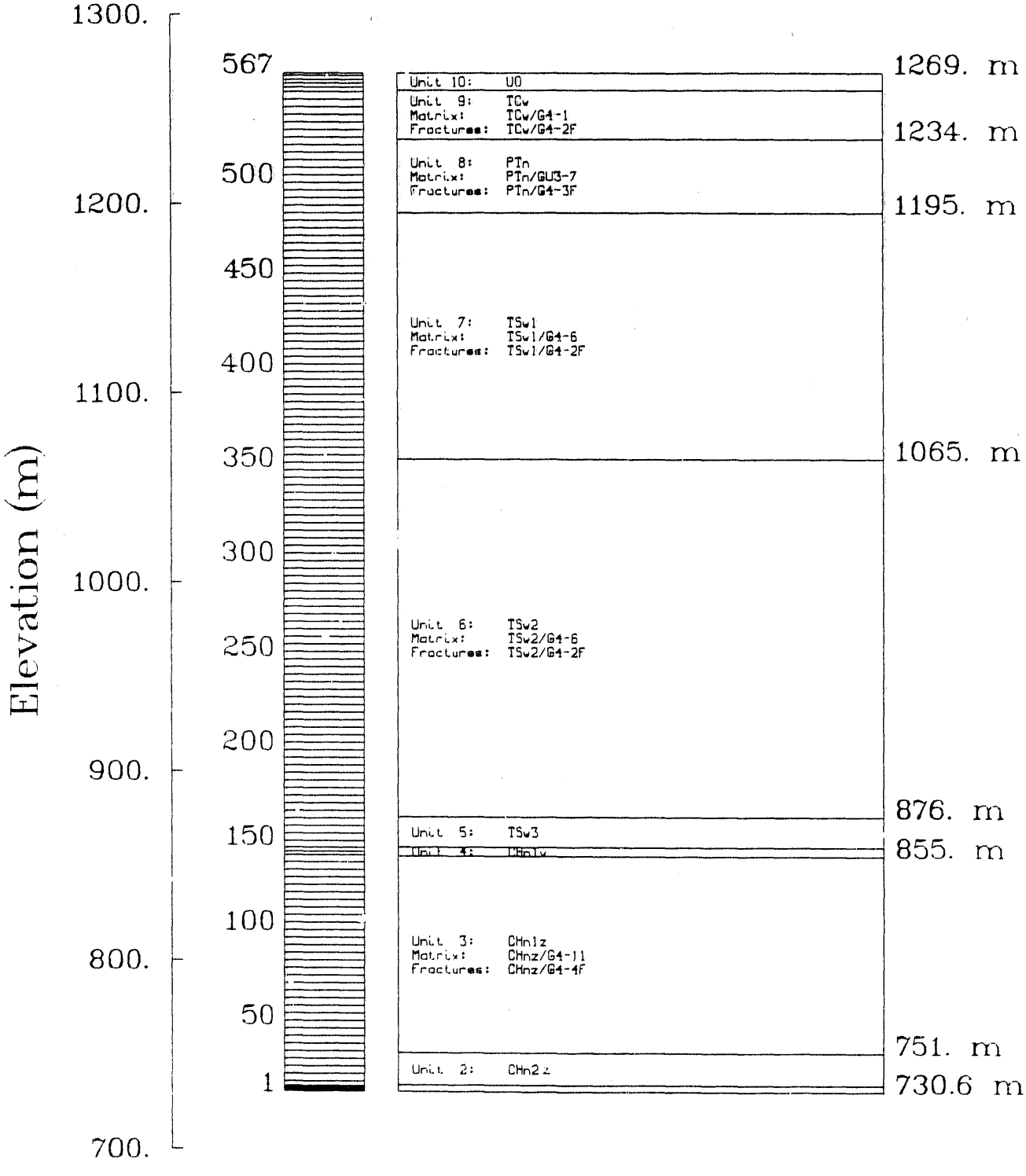

Figure 3: One-dimensional calculational grid

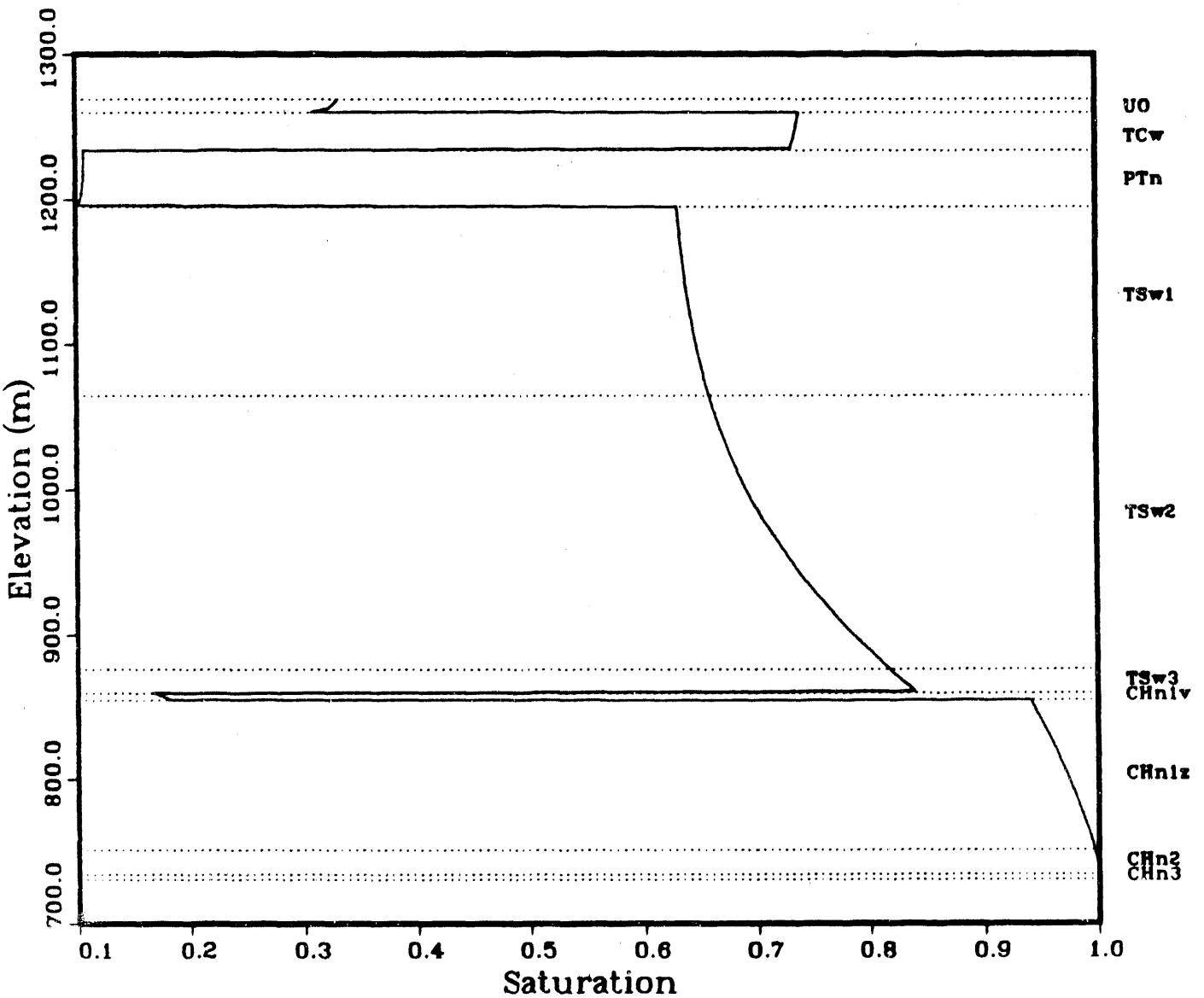

Figure 4: Steady-state saturation profile - 1-D calculation

here, the amount of allowable surface water is quite sensitive to variation in that porosity in PTn. It may also be sensitive to variation in the van Genuchten parameters for conductivity, especially β, which represents the change in saturation as a function of pressure head. For CHnlv, the value for in-situ saturation given in the RIB is 90%; this value is based on only one sample. The value calculated for in-situ saturation in CHnlv using the steady-state infiltration of 0.01 mm/yr was approximately 18%. This discrepancy for the in-situ saturation of the vitric Calico Hills layer had no impact on these calculations.

The bottom and top surfaces of the model coincide with the water table and the upper surface of the mountain, respectively. The initial conditions in the model were the steady-state conditions calculated by TOSPAC corresponding to a uniform surface flux of 0.01 mm/yr, represented in Figure 4. The boundary condition used at the bottom surface was complete saturation (i.e., total pressure was set equal to the elevation head, with the pressure head equal to zero). A total head of water was imposed on the upper boundary at "time zero." This water was allowed to infiltrate the surface with no time constraint. It was reasoned that the time required for the water to infiltrate the mountain in this manner is negligible compared to the 10,000-year period of concern. Subsequent to all of the water entering the mountain, the steady-state infiltration rate of 0.01 mm/yr was re-imposed on the top surface.

4.1.2 Discussion

One-dimensional calculations were made for 12 values of the initial pond depth, i.e., the amount of water that infiltrates the mountain. Table 1 contains a summary of these calculations, giving the water added to the mountain (initial pond depth), the time required for the water to enter the mountain (drain time), the computer time required (CPU time), and restart basis for each calculation. Calculations 1 and 6 were made by starting from in-situ conditions while the other calculations were started from the results of previous calculations. These calculations were started by imposing an increased pond depth onto the solution for a shallower pond at the time when the shallower pond becomes fully drained. This method is acceptable because the effects of the pond drain time on repository performance are negligible. This procedure greatly reduces the computer time required for the analyses, as can be seen from Table 1. The start numbers in Table 1 indicate the calculation that was used to start each calculation. To illustrate, calculation 2 was performed by imposing a 5 m pond onto the calculation 1 solution at 30.535 years.

Calculations of GWTT were made by releasing particles at an elevation of 960 m, assumed to be the bottom of the repository disturbed zone, and removing particles at 730.6 m elevation (water table). The depth of the water table was assumed to be constant. In these calculations, no consideration is made for the GWTT through the saturated zone to the accessible environment; consequently, these calculations are expected to result in conservative values of the pre-emplacement GWTT from the disturbed zone to the accessible environment. Because it cannot be determined beforehand which water particle will have the minimum travel time, particles have to be released before, during, and after an infiltration event. Two methods were used to calculate

TABLE 1: SUMMARY OF THE ONE-DIMENSIONAL CALCULATIONS

Cal. No.	Pond§ Depth (m)	Drain Time (yrs)	CPU* Time (h:m)	Start Cal. No.
1	10	30.535	1:25	---
2	15	50.981	0:52	1
3	16	54.754	1:32	1
4	17	58.467	2:36	1
5	18	66.651	3:12	1
6	20	90.859	5:14	---
7	22	132.98	2:42	6
8	23	155.29	3:03	6
9	25	199.58	3:59	6
10	28	266.46	2:52	9
11	29	286.89	5:26	6
12	30	308.47	7:33	6

§ Initial
* VAX 8700.

GWTT: the composite and the average-fastest-particle methods. The composite method uses the area-weighted average of the velocity of water in the matrix and in the fractures ($V_{composite} = V_m A_m/A_t + V_f A_f/A_t$, where V ≡ velocity, m ≡ matrix, f ≡ fracture, and t = total), and gives results that correspond to travel times for a nonsorbing tracer when there is a strong coupling between the matrix and fractures. The water particle, by random chance or Brownian motion, spends part of its time in the matrix water and part in the fracture water. The average-fastest-particle method uses, as the particle velocity, the faster of the water velocity in the matrix or the water velocity in the fractures, provided the flow in that regime is at least one percent of the total flow. Because the average-fastest-particle method assumes a water particle can instantaneously, and with preference, migrate to the faster regime, this method is expected to under-predict the GWTT when the fracture and matrix flows are strongly coupled.

Preliminary calculations were used to determine appropriate times for solution output and to release particles for GWTT calculations. These predetermined times, snapshots, are given in Table 2. Solution output is automatically provided at each snapshot time and when the pond becomes fully drained. Each calculation begins before water is placed on the column (negative problem time) so that GWTT calculations can be made. At the 13th snapshot, "time zero", a pond is placed on top of the column and begins draining. The time snapshots are spaced so as to capture flow variations.

TABLE 2: RELATIONSHIP BETWEEN SNAPSHOTS AND PROBLEM TIME

Snapshot Number	Time	Snapshot Number	Time
1	-6,000,000 years	17	1 year
2	-5,000,000 years	18	10 years
3	-4,000,000 years	19	50 years
4	-3,000,000 years	20	100 years
5	-2,000,000 years	21	200 years
6	-1,000,000 years	22	500 years
7	-100,000 years	23	1000 years
8	-50,000 years	24	5000 years
9	-20,000 years	25	10,000 years
10	-10,000 years	26	20,000 years
11	-1000 years	27	50,000 years
12	-100 years	28	100,000 years
13	0	29	200,000 years
14	1 day	30	300,000 years
15	1 week	31	1,000,000 years
16	1 month	32	10,000,000 years

A Crank-Nicolson implicitness factor of unity[4] and the table-interpolation method for determining the saturations and hydraulic conductivities were used in all calculations. Accuracy was determined primarily by mass balances, which indicate that for all calculations, approximately 12 cm of water was created at the top of the column during pond infiltration. This amount represents less than a two percent error. The mesh spacing is approximately 1 m between mesh points, which is adequate for tracking the relaxation of water within the column,[5] but is inadequate for tracking the influx of the pond.[6] The accuracy of the pond influx was estimated by monitoring the change in the void space in the column. During pond draining, the void space decrease in the column was within two percent of the amount of water which had entered the mountain. This error is consistent with the results of the mass balances.

4.1.3 Results

The results of the one-dimensional calculations are presented in Figures 5 through 18. Figures 5 and 6 present GWTT and saturation at the repository horizon (960 m elevation), respectively, as functions of the amount of water added to the mountain. Figures 7-18 are saturation profiles in the mountain

4. See Dudley et al. [1988], or Crank, J. [1975], Mathematics of Diffusion, Oxford University Press, Oxford.

5. Dudley et al. [1988] contains formulas for determining adequate mesh-point spacing.

6. The length scale for the pond influx is less than a few millimeters.

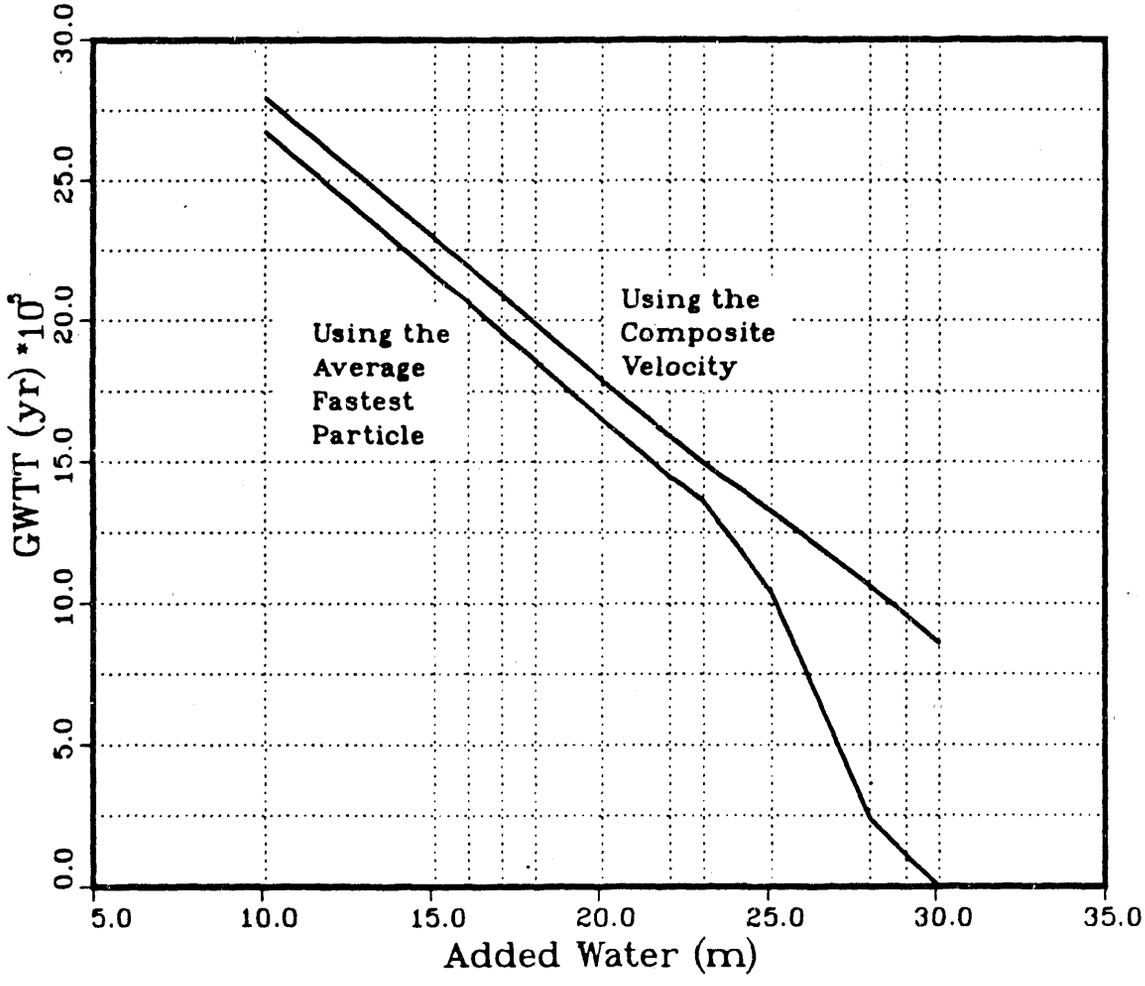

Figure 5: Groundwater travel time from 960 m elevation to the water table as a function of surficial water added to Yucca Mountain

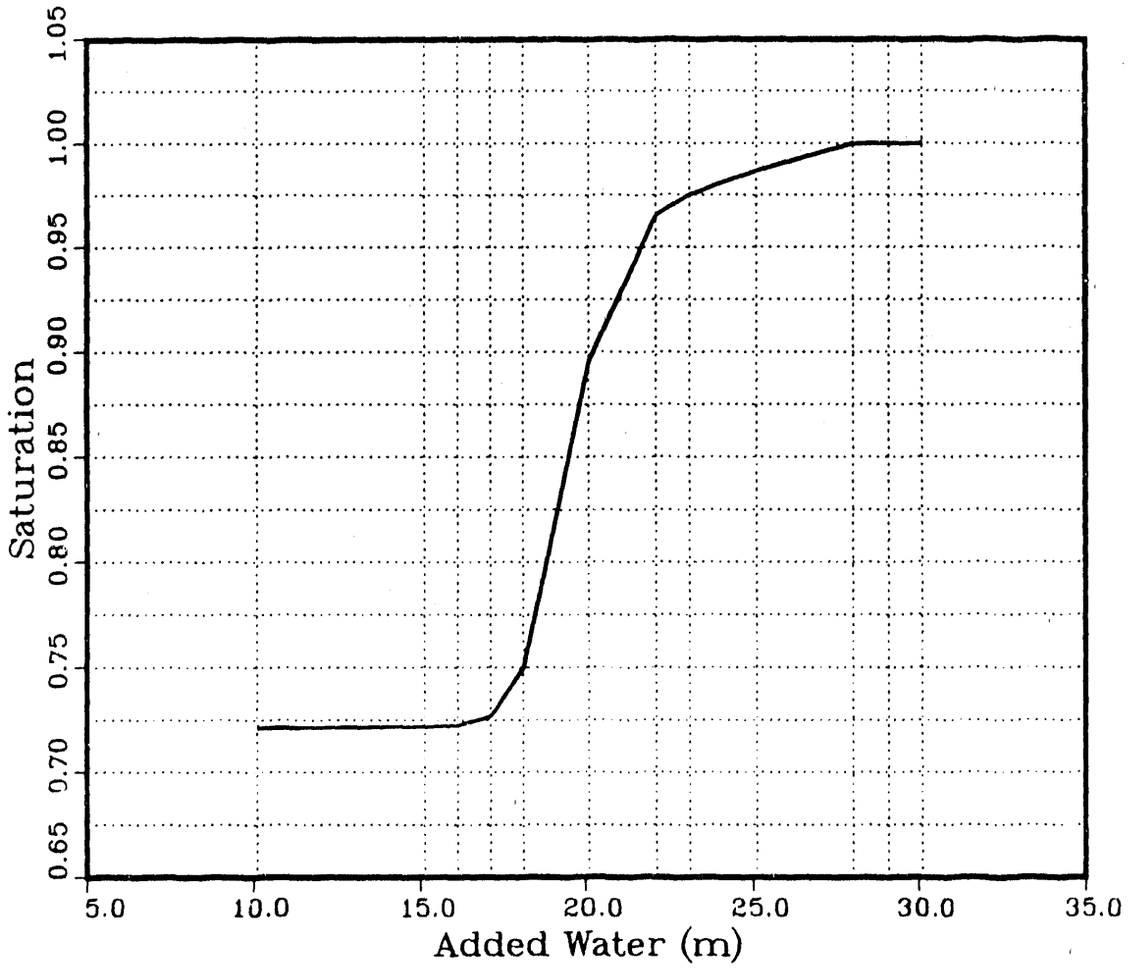

Figure 6: Maximum saturation at repository horizon during 10,000 years

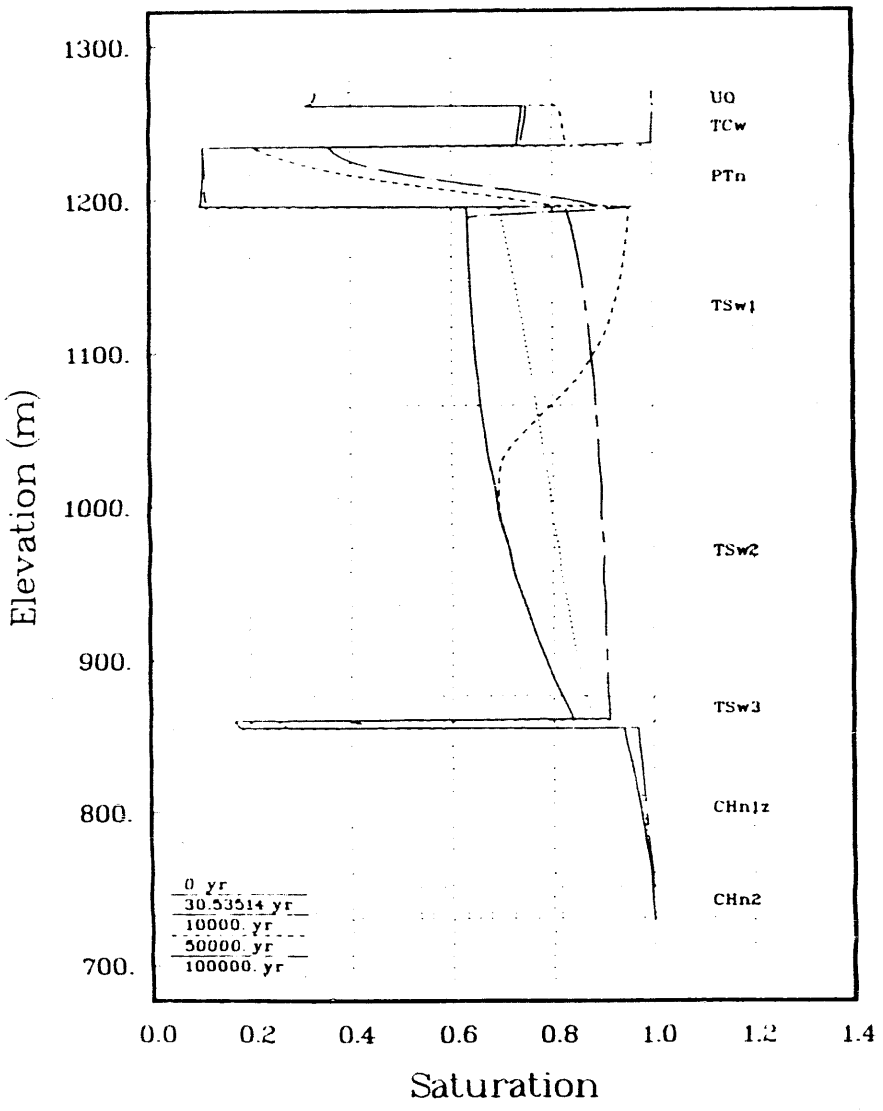

Figure 7: 10m of surficial water

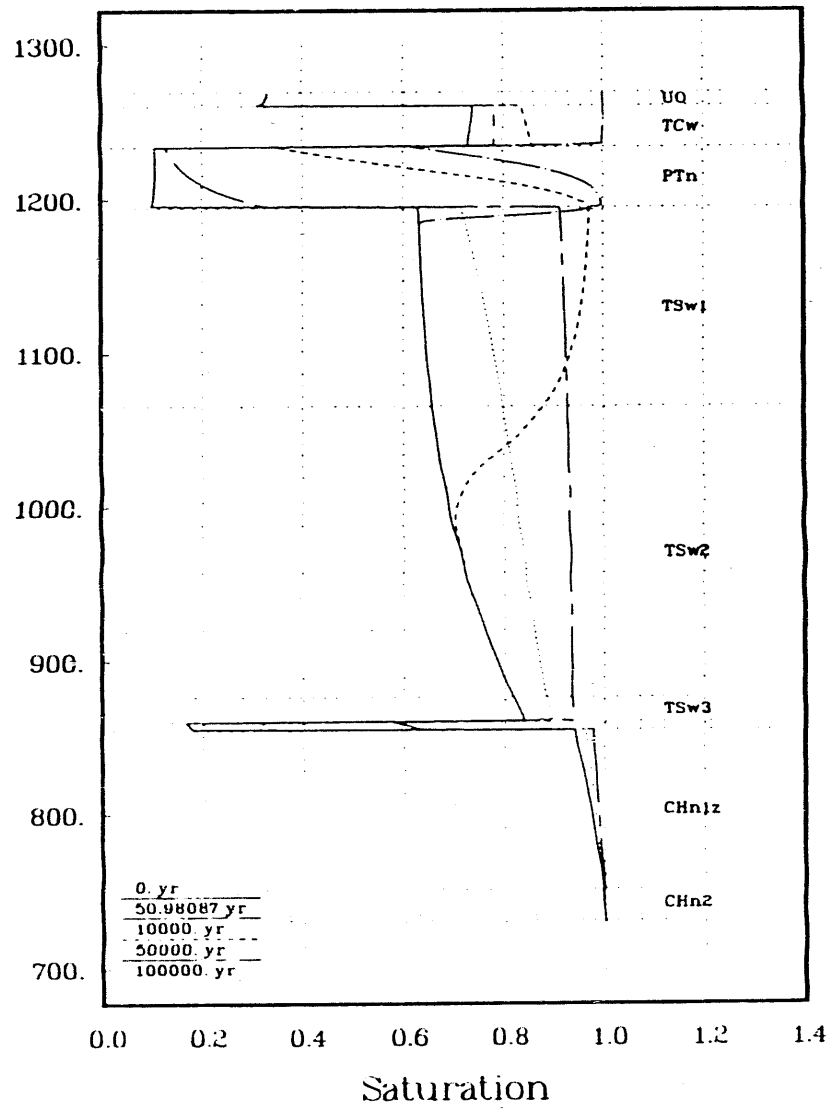

Figure 8: 15m of surficial water

Saturation profiles at selected times from 1-D calculations

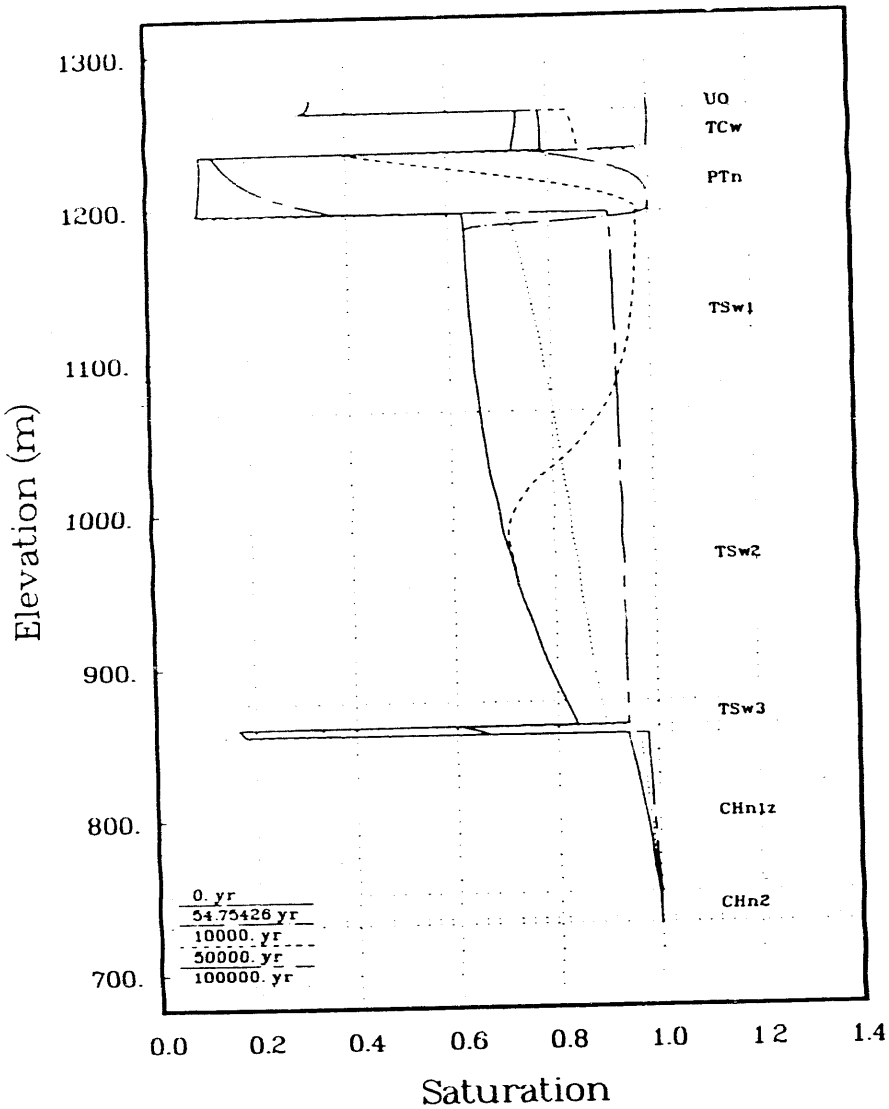

Figure 9: 16m of surficial water

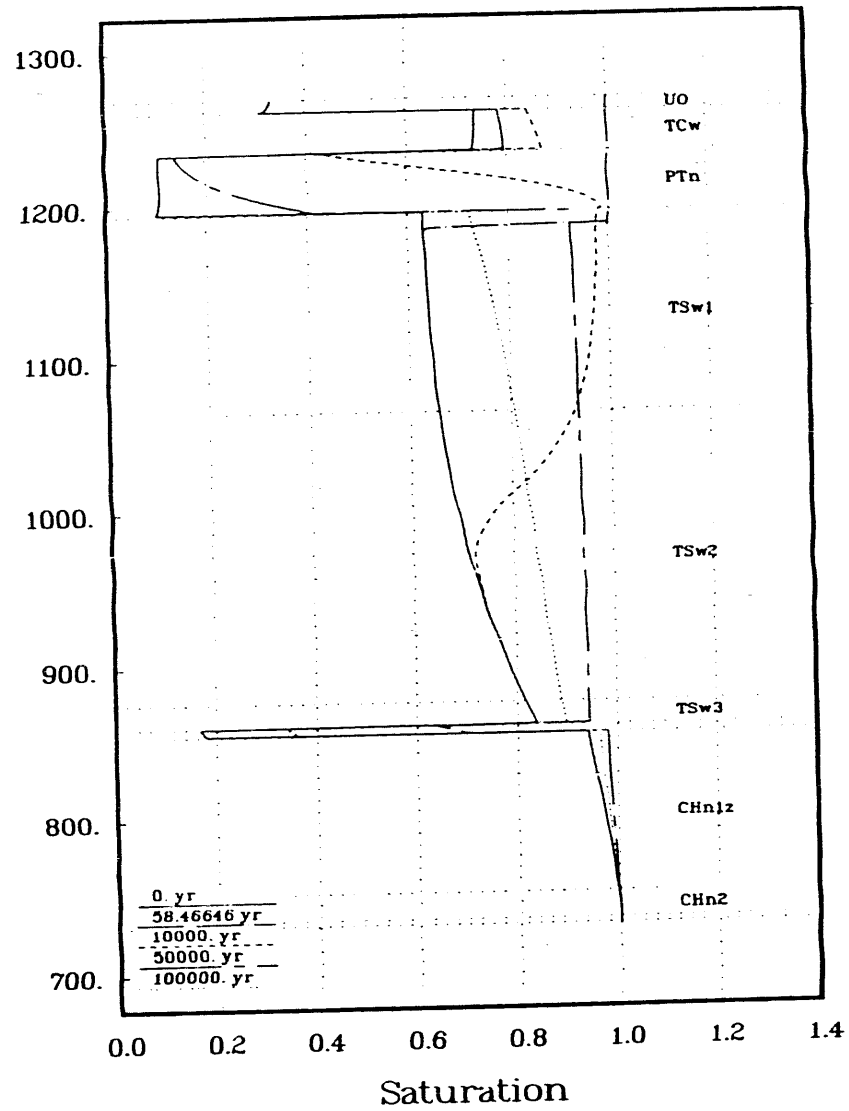

Figure 10: 17m of surficial water

Saturation profiles at selected times from 1-D calculations

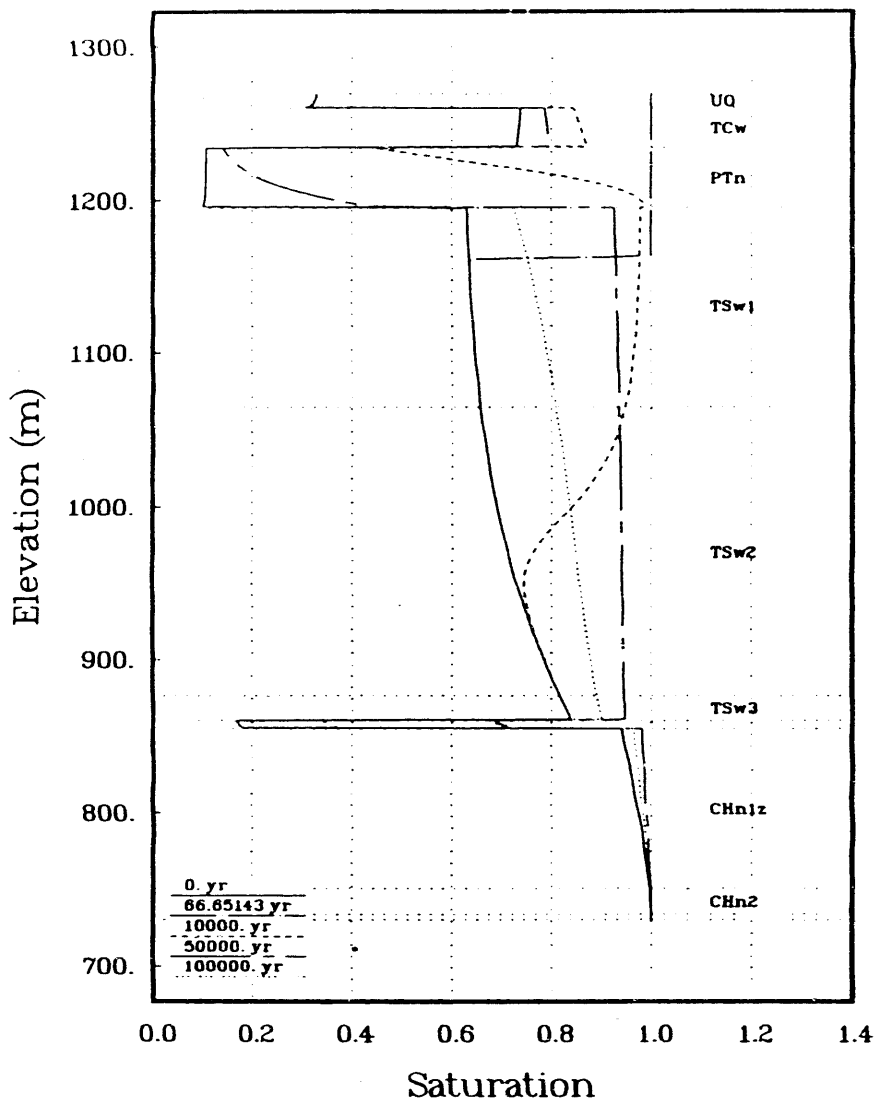

Figure 11: 18m of surficial water

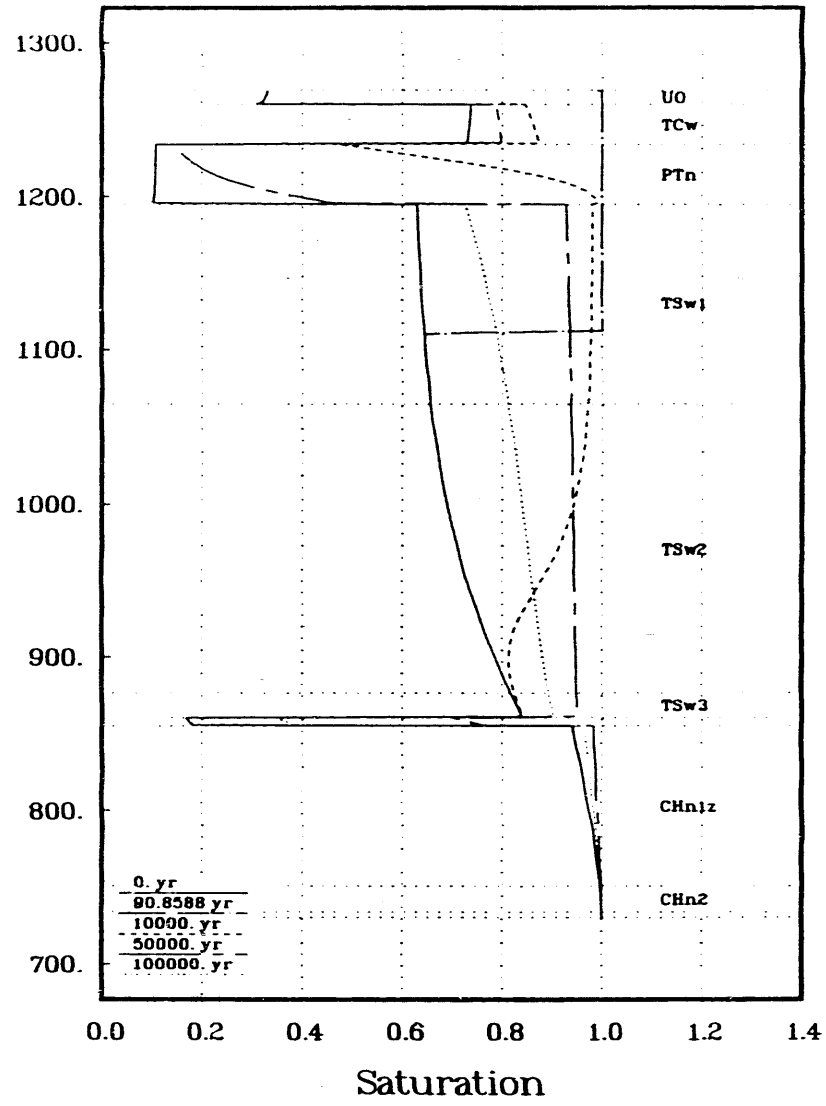

Figure 12: 20m of surficial water

Saturation profiles at selected times from 1-D calculations

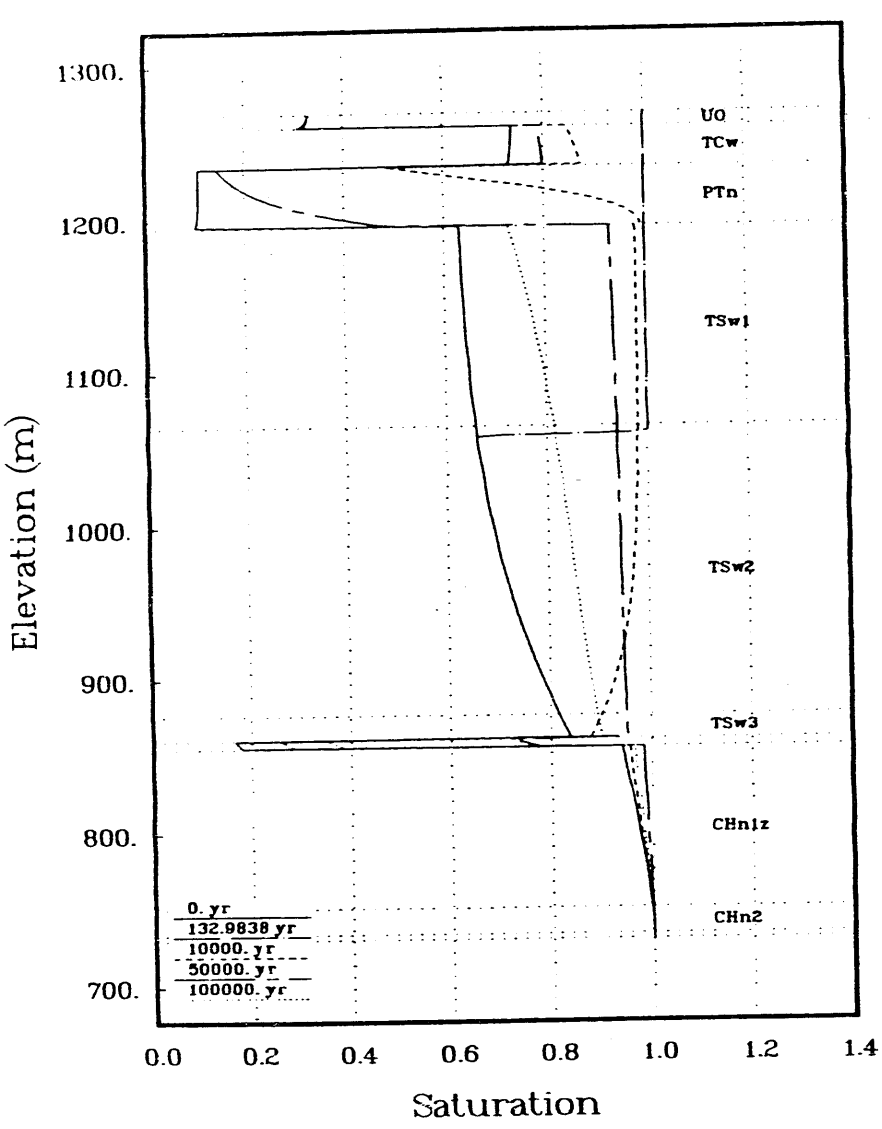

Figure 13: 22m of surficial water

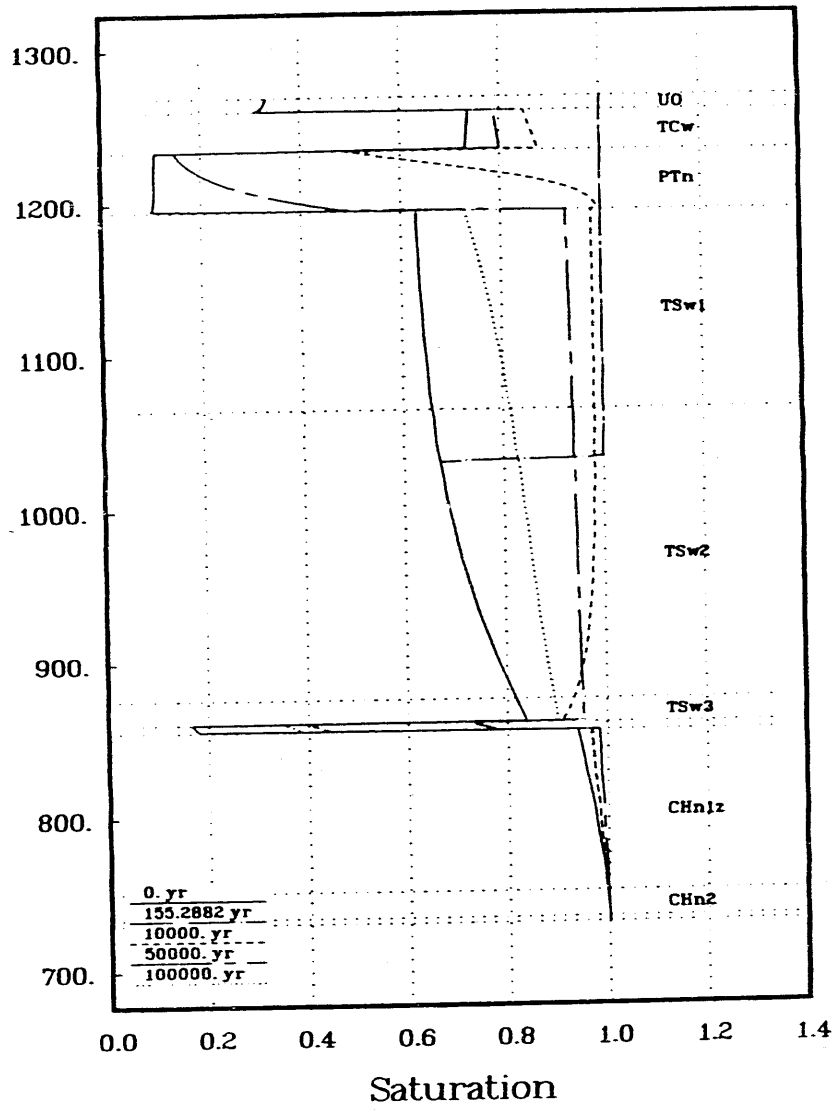

Figure 14: 23m of surficial water

Saturation profiles at selected times from 1-D calculations

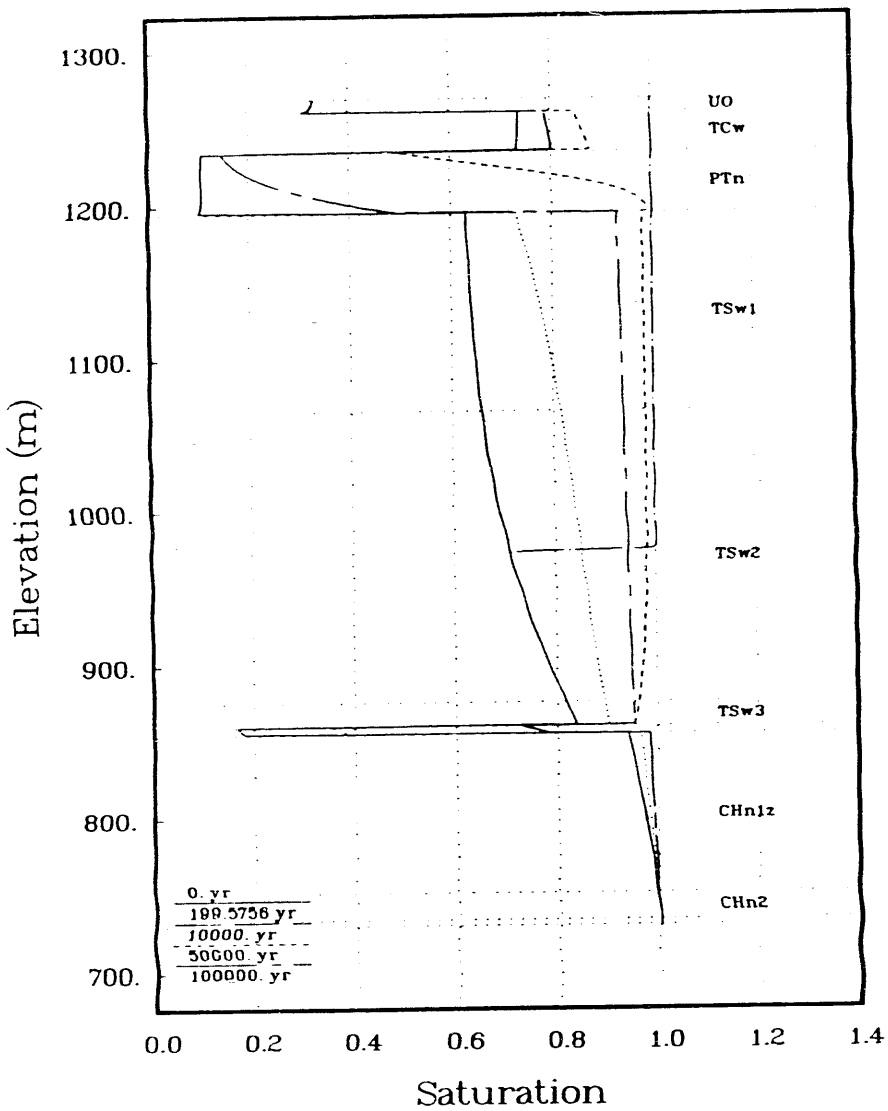

Figure 15: 25m of surficial water

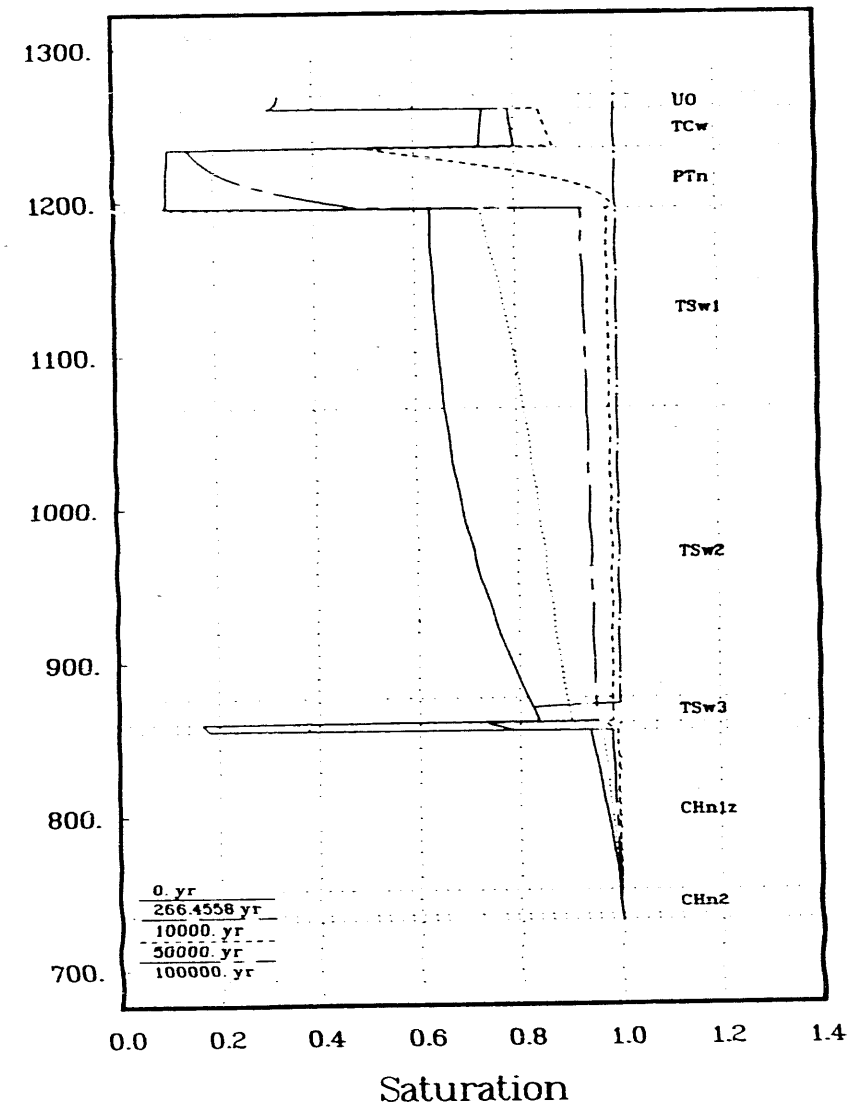

Figure 16: 28m of surficial water

Saturation profiles at selected times from 1-D calculations

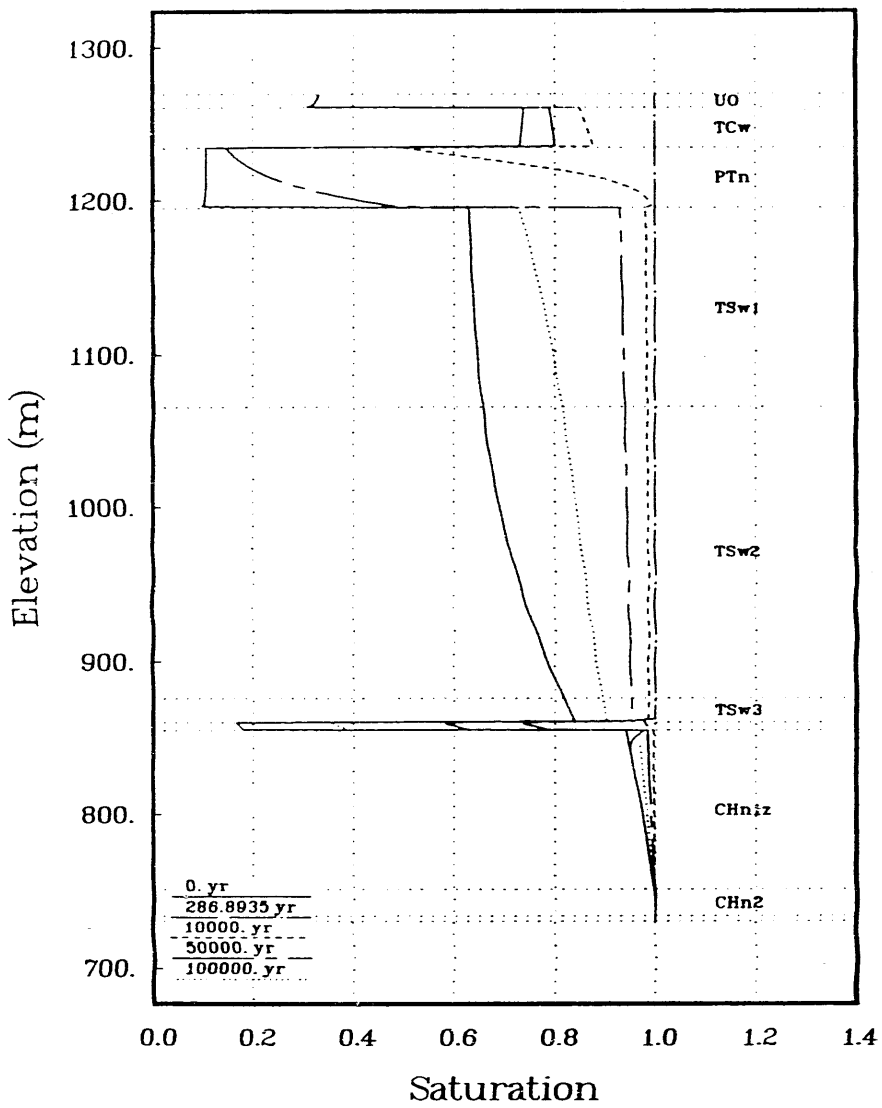

Figure 17: 29m of surficial water

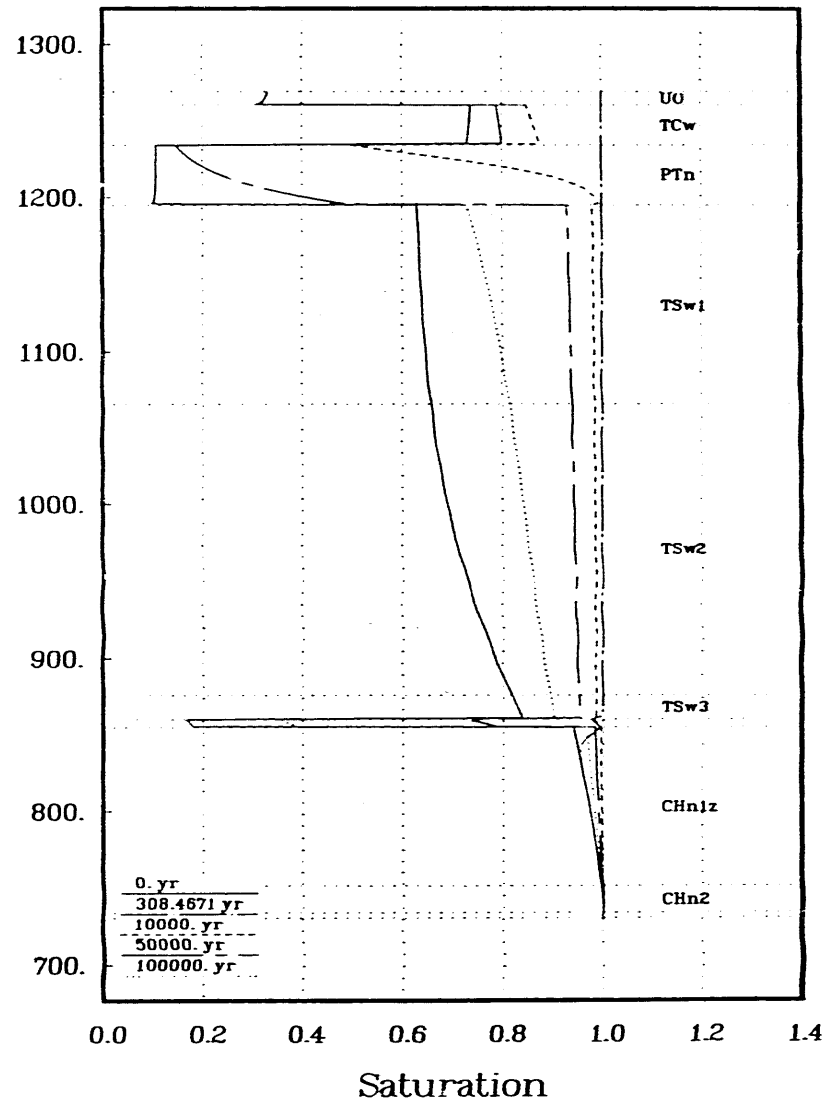

Saturation profiles at selected times from 1-D calculations

Figure 18: 30m of surficial water

as functions of time for each of the 12 calculations listed in Table 1. Figures 5 and 6 display the results so that performance degradation, as measured by the criteria discussed in Section 3, is apparent, while Figures 7 through 18 provide the saturation state in the mountain as functions of time.

The GWTT calculated by both the composite and the average-fastest-particle methods is plotted in Figure 5. The GWTT calculated by both methods decreases with increasing water addition, but only the GWTT calculated by the average-fastest-particle method shows performance degradation. Because the GWTT calculated by the average-fastest-particle method is expected to under-predict the actual GWTT, the results of the average-fastest-particle method are a conservative measure of performance degradation. The average-fastest-particle GWTT falls below 1000 years somewhere between 29 and 30 m of water and a precipitous change in GWTT occurs at about 23 m of water addition.

Figure 6 presents the maximum saturation attained at the repository horizon during the 10,000-year period following the initiation of the infiltration pulse, plotted as a function of the amount of water in the infiltration pulse. From Figure 6, it can be seen that the saturation at the repository horizon remains at the in-situ saturation value for up to 16 m of added water. At slightly higher values of added water, the saturation at the repository horizon abruptly increases and repository performance is degraded according to the metric discussed in Section 3. Thus, 16 m of water is a conservative measure for the greatest amount of water that can be put into the mountain without degrading repository performance.

Figures 7 through 18 present saturation profiles in the mountain at five times for each of the 12 one-dimensional calculations listed in Table 1. In each of these figures, the zero-year profile is the in-situ (steady-state) profile prior to addition of water, and the profile at the next later time is the saturation when all of the water has entered the mountain; this profile delineates the water pulse. The remaining three profiles are at 10,000, 50,000, and 100,000 years after the water starts to enter the mountain.

These profiles show the distribution of the water in the mountain for each case. In the relatively porous PTn unit, the pulse of water is dispersed until sufficient water is added to saturate that unit. This occurs with the addition of between 16 and 17 meters of water (Figures 9 and 10). At this point, a simple check of the calculation can be made. In one dimension, the amount of water required to saturate a geologic unit is the product of the change in the moisture content (the product of the porosity and the change in saturation) and the height of the unit:

$$\text{amount} = \sum_{\text{units}} (\theta_{sat} - \theta_{init})\Delta z$$

$$= n_{UO}(S_{sat,UO} - S_{init,UO})\Delta z_{UO} + n_{TCw}(S_{sat,TCw} - S_{init,TCw})\Delta z_{TCw} + n_{PTn}(S_{sat,PTn} - S_{init,PTn})\Delta z_{PTn}$$

$$\approx 0.32 \times (1.-0.3) \times 9.\text{m} + 0.08 \times (1.-0.7) \times 26.\text{m} + 0.40 \times (1.-0.1) \times 39.\text{m}$$

$$\approx 16.7 \text{ m}$$

where θ_{sat} is the saturated moisture content, θ_{init} is the initial moisture content, n is the porosity, S_{sat} is complete saturation, and S_{init} is initial saturation (taken from the figures). The estimate of 16.7 m of water to saturate the upper three geologic units is consistent with Figure 9, which shows that 16 m is insufficient to saturate these units, and Figure 10, which shows that 17 m is sufficient. From this exercise, it is apparent that PTn holds a disproportionate share of the water (approximately 14 m). Consequently, the results of this analysis are sensitive to the choice of hydrologic parameters used to characterize PTn.

When sufficient water is added to saturate PTn, the pulse moves through the Topopah Spring units (TSw1, TSw2, and TSw3 units) as a shock.[7] Behind the shock, the entire mountain is saturated, while ahead of the shock the mountain is at in-situ conditions. This shock extends down to the relatively porous CHnlv unit after 28 meters of water is added.

The 10,000, 50,000, and 100,000-year profiles indicate the redistribution of the pulse as it drains through the mountain. Figures 9 and 10 show that this draining process is sufficient to increase the saturation at the repository horizon (960 m elevation) when between 16 and 17 meters of water are added. Comparing Figure 5 with Figures 14 through 18 indicates that the precipitous change in the GWTT calculated by the average-fastest-particle method occurs when the shock front passes the repository horizon. The GWTT calculated by this method falls below 1000 years when the CHnlv unit becomes fully saturated (Figure 18). Figure 19 is an extraction of Figure 9, the saturation profile at 10,000 years after the addition of 16 m of surficial water.

4.2 Two-Dimensional Analysis

PDM 72-29 describes the two-dimensional flow analysis. The computer program NORIA-SP [Hopkins et al., 1990] was used to perform the two-dimensional calculations. NORIA [Bixler, 1985], a finite element code, numerically solves the two-dimensional Richards' equation for the transient flow of water in layered, fractured, unsaturated porous media. NORIA has been used extensively in such analyses in the YMP. NORIA does not simulate radionuclide transport and does not perform GWTT calculations. NORIA-SP is a single phase (liquid water) version of NORIA. Because the mathematical model for single phase flow in NORIA-SP is much simpler than the two-phase model implemented in NORIA, single phase calculations are more economical. NORIA-SP has met the requirements of SNL's implementation of the YMP's criteria for software quality assurance. For these reasons, NORIA-SP was chosen to perform the two-dimensional calculations.

From the results of the one-dimensional analysis, it was determined that an infiltration of 16 cubic meters of water per square meter of disturbed surface area into the mountain would result in a negligible, yet perceptible change in saturation at the repository horizon, 10,000 years after ESF construction. Of the three indicators described above, this indicator resulted in the most

---

7. Dudley et al. [1988] contains a discussion of why an infiltration pulse appears to disperse through some geologic units, e.g., PTn, while it forms a shock front in others, e.g., TSw.

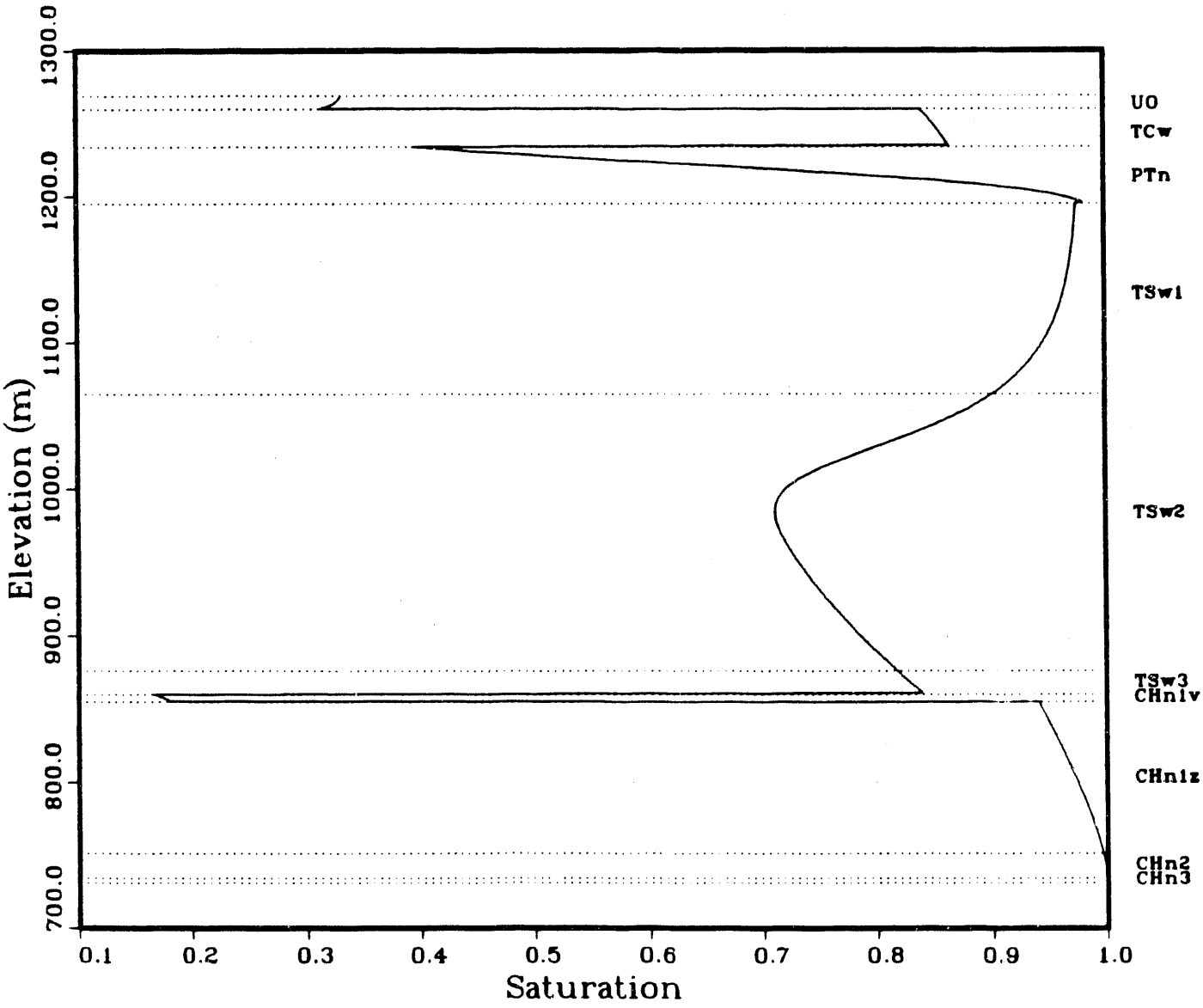

Figure 19: Saturation profile at 10,000 years with 16m of surficial water - 1-D calculation

conservative value for the maximum allowable water infiltration. The goals of the two-dimensional analysis were the following:

- Corroborate the results of the one-dimensional analysis concerning saturation at the repository horizon, using boundary conditions that would force the 16 meters of water into the mountain in five years.

- Using the same calculations, determine the lateral movement of the water within the mountain. This lateral movement will indicate the potential effects on experiments to be conducted in the ESF, and set guidelines for locations of experiments.

4.2.1 Assumptions

A pulse containing 16 meters of water is put into the mountain over a five-year period (the expected ESF construction period) at the constant rate 3.2 m/yr. The water enters uniformly through an area of 392,091 m^2, which is equal to the combined areas of roads and pads above the repository.[8] The calculation is simplified to two dimensions by assuming that the shape of the water entry area is circular and the stratigraphic layers are horizontal and parallel. Results of two-dimensional cartesian calculations, COVE2A [Hopkins, 1990] and HYDROCOIN [Prindle and Hopkins, 1990], show that the downdip of the TSw1 unit acts as a shed which diverts water from the repository block. Thus, the no-downdip assumption is conservative if the individual layers of the mountain are indeed homogeneous and isotropic as assumed in the hydrogeological models used in COVE2A and HYDROCOIN, and in these calculations. With these simplifications, the two-dimensional problem is defined as the axisymmetric model depicted in Figure 20. For convenience, the radius of the water infiltration area was rounded to the nearest meter.

The following assumptions and conditions were used in setting up the two-dimensional analysis:

- The problem domain was defined as two-dimensional and axisymmetric, with stratigraphic layers that are horizontal and parallel (no downdip).

- As for the one-dimensional case, borehole USW G-4 from the RIB[9] was used for the stratigraphy. The thermomechanical properties were the current best available from holes USW G-4 and USW GU-3 [Peters et

---

8. Values for the area of the exploratory shaft pad and roads and emplacement exhaust pads were obtained from Case B3 of the ESF Alternative Study [Stevens and Costin, 1991] and the Yucca Mountain Site Characterization Plan [SNL, 1987].

9. The stratigraphy used for the two-dimensional analysis (shown in Appendix A and in Figure 20) was taken from a 1987 version of the RIB. This stratigraphy differs slightly from the one taken from the 1991 version of the RIB and used for the one-dimensional analysis (see Figure 2). This discrepancy was inadvertent, but because the difference between the two stratigraphies is so small, its effects on the results of these analyses are negligible.

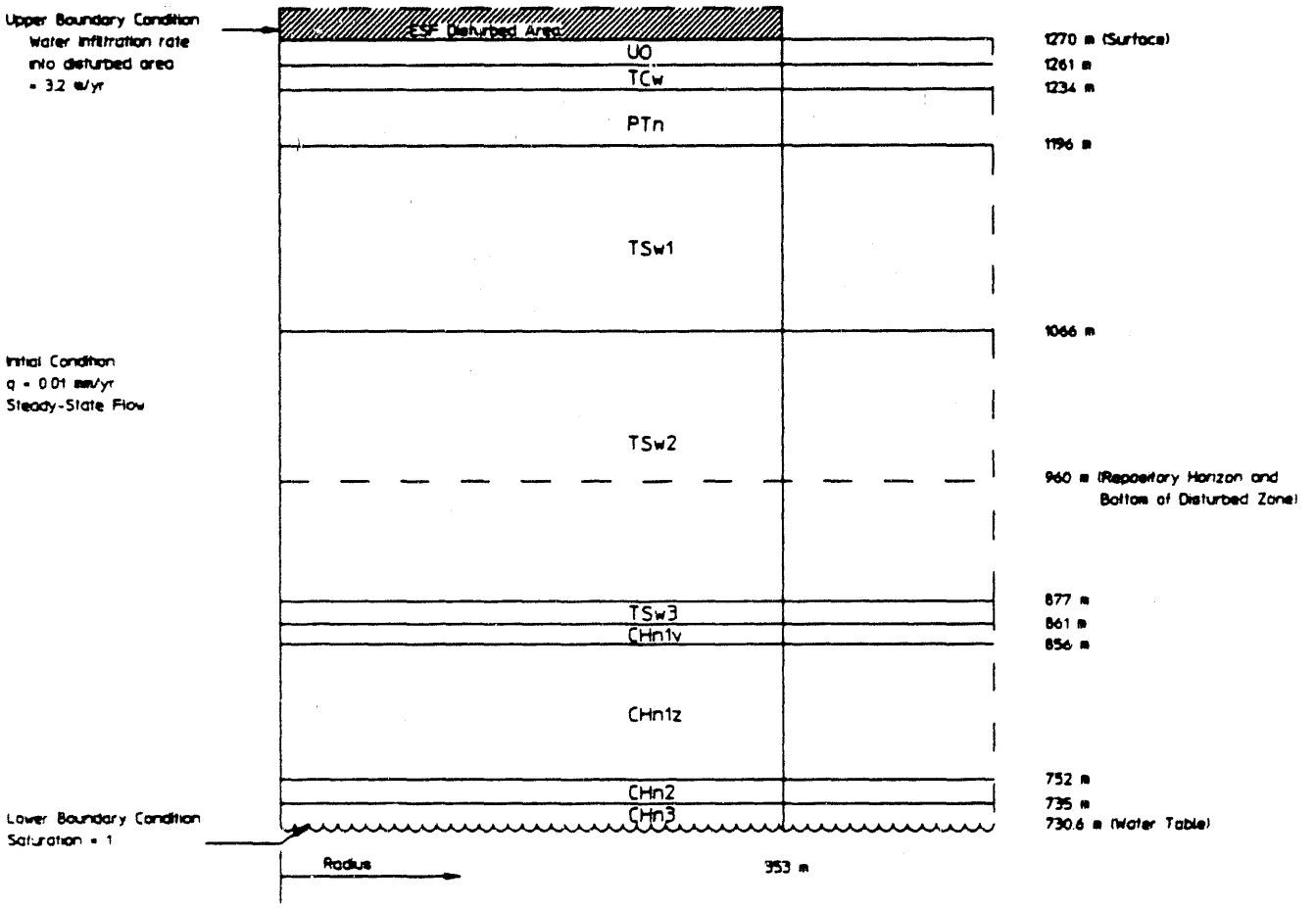

Figure 20: Conceptualization of the two-dimensional problem

al., 1984]. The material properties used for the alluvium layer at the surface were those values estimated by Alan Flint of the U.S. Geological Survey (personal communication, July 19, 1989). The thermomechanical properties in each layer were assumed to be homogeneous and isotropic throughout that layer.

- A steady-state infiltration rate of 0.01 mm/yr was imposed on the top surface of the mountain.

- The bottom and top surfaces of the model correspond to the water table and the upper surface of the alluvium on top of the mountain, respectively. Saturated conditions were imposed along the bottom surface. One vertical boundary is the axis of symmetry. No-flux boundary conditions were imposed on both vertical boundaries of the model. Along the top surface, an infiltration of 3.2 m/yr (16 m over 5 years) was imposed onto the disturbed area for five years. After five years, a 0.01 mm/yr infiltration rate was imposed. Elsewhere on the upper surface, a 0.01 mm/yr infiltration rate was imposed at all times.

4.2.2 Discussion

The two-dimensional analysis was performed in four steps: calculation of initial conditions; calculation of water dispersion during the five-year ESF construction period; extrapolation of calculational results at two years to an estimation at five years; and calculation from five years to 10,000 years. In all but the third step, NORIA-SP was used to perform the calculations.

4.2.2.1 Initial Conditions -- The first step of the analysis used NORIA-SP to determine the steady-state conditions throughout a computational domain of 539.4 m height and 600 m radius. A 0.01 mm/yr infiltration boundary condition was imposed on the top surface. The boundary conditions on the other surfaces are those discussed in the previous section. The computational grid consisted of 880 finite elements formed by dividing the height into 44 rows and the radius into 20 columns (see Figure 21). The first nine columns in the top row correspond to the disturbed area. These steady-state conditions were used as the initial conditions for the perturbed flow calculations described in the following sections. Figure 22 displays the NORIA-SP steady-state saturation profile along the axis of the grid. This profile is almost identical to the one-dimensional results from TOSPAC (Figure 4).

4.2.2.2 Dispersion of Water During Five-Year Construction Period -- The second step of the analysis was the calculation of the changes in the saturation and pressure levels throughout the stratigraphy due to the perturbation of water added through the top surface during the five-year construction period. The infiltration rate into the disturbed areas during the five-year construction period was 3.2 m/yr. Because of the expected difficulty of the calculations, a subset of the computational grid used in the first step was used to minimize computing time. The domain of the grid was 600 m radius by 74 m in height, consisting of the alluvium (elevation 1261-1270 meters), Tiva Canyon (TCw, 1234-1261 m), and PTn (1196-1234 m) hydrologic layers (i.e., the top 11 rows of elements from the original grid, as shown in Figure 23). The initial constant pressure conditions at the PTn-TSw1 interface from the in-situ calculations was imposed on the lower boundary of

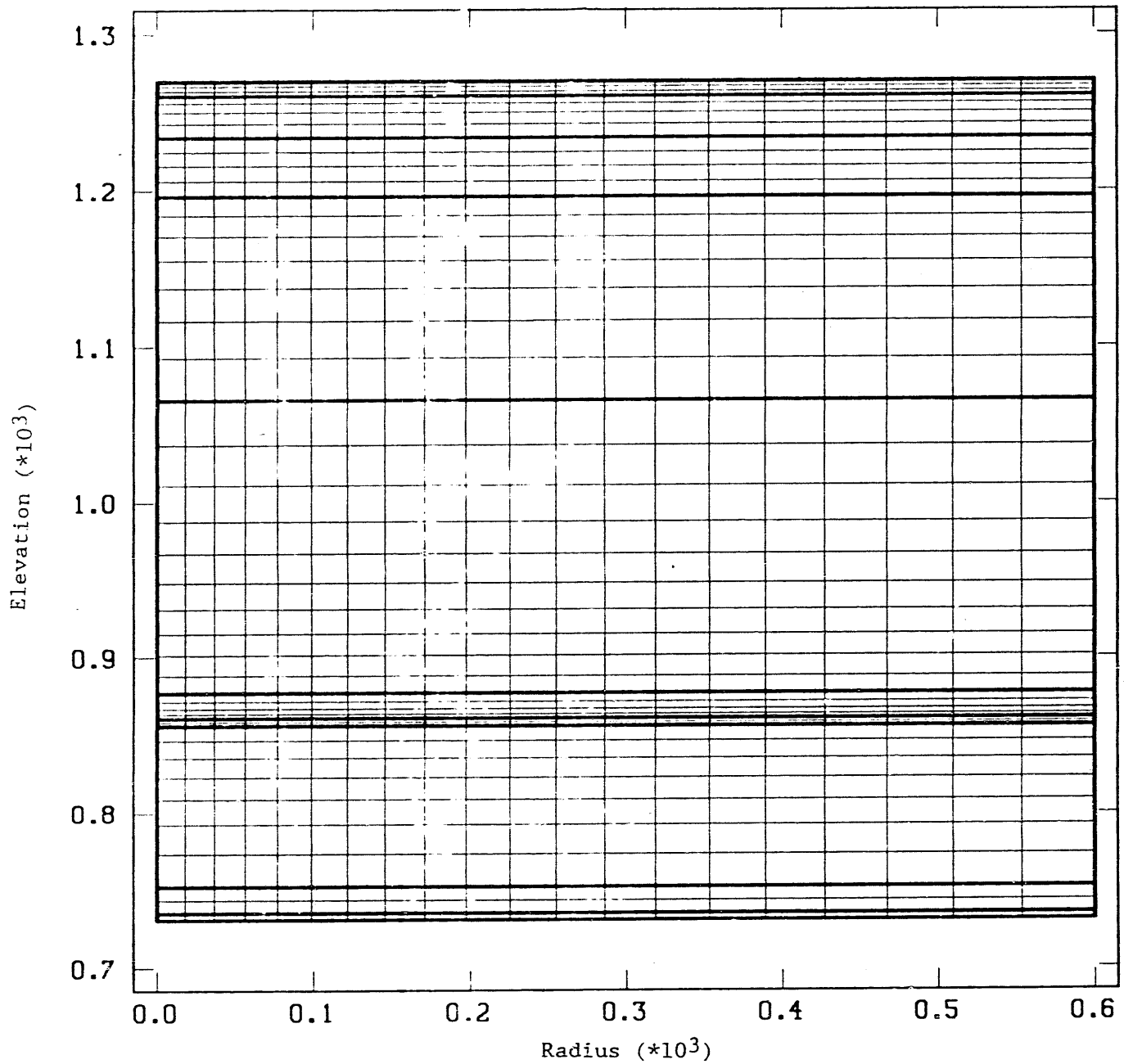

Figure 21: Two-dimensional computational grid for steady-state calculations

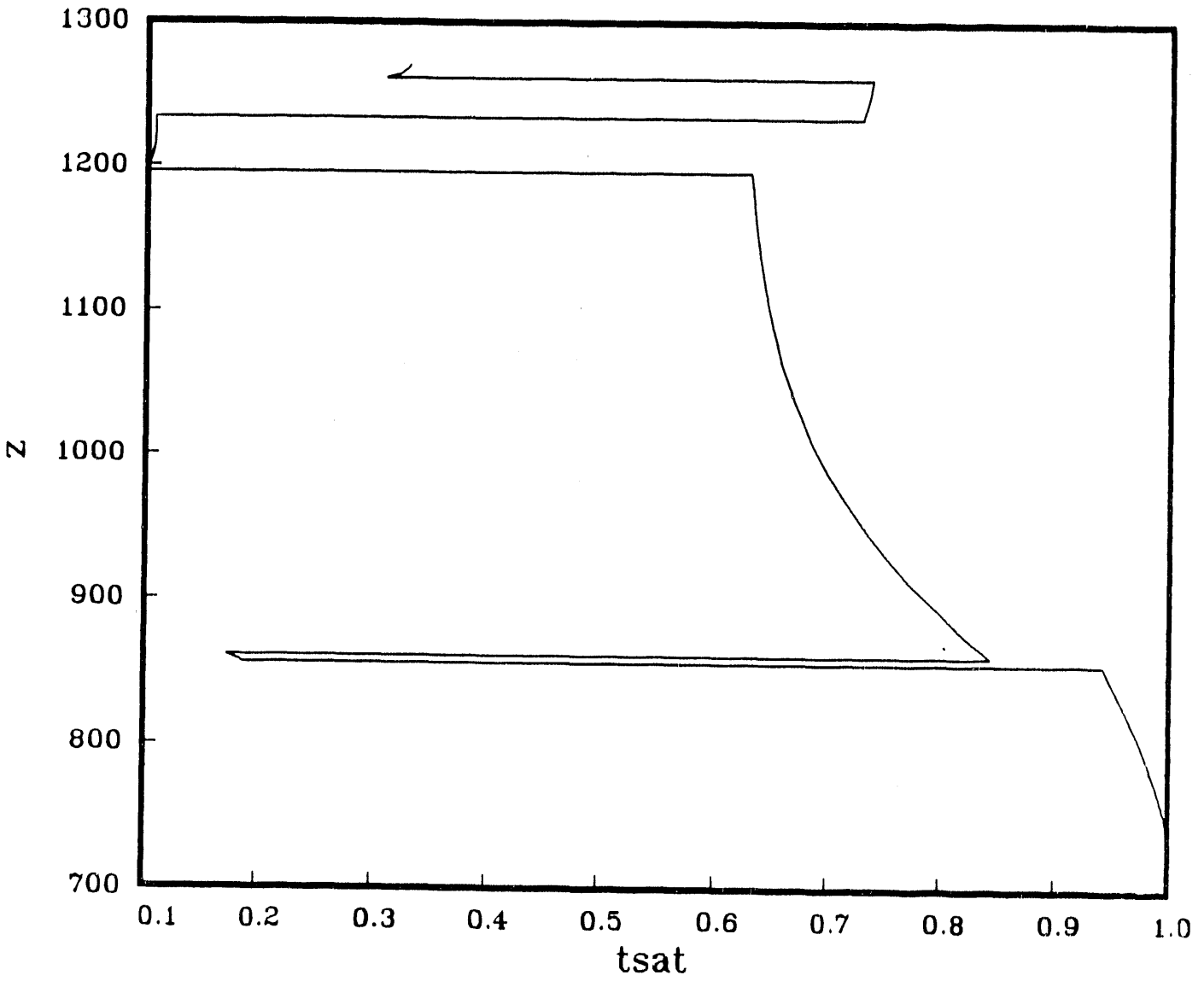

Figure 22: Steady-state saturation profile - 2-D calculation
(tsat=Total saturation; z=elevation)

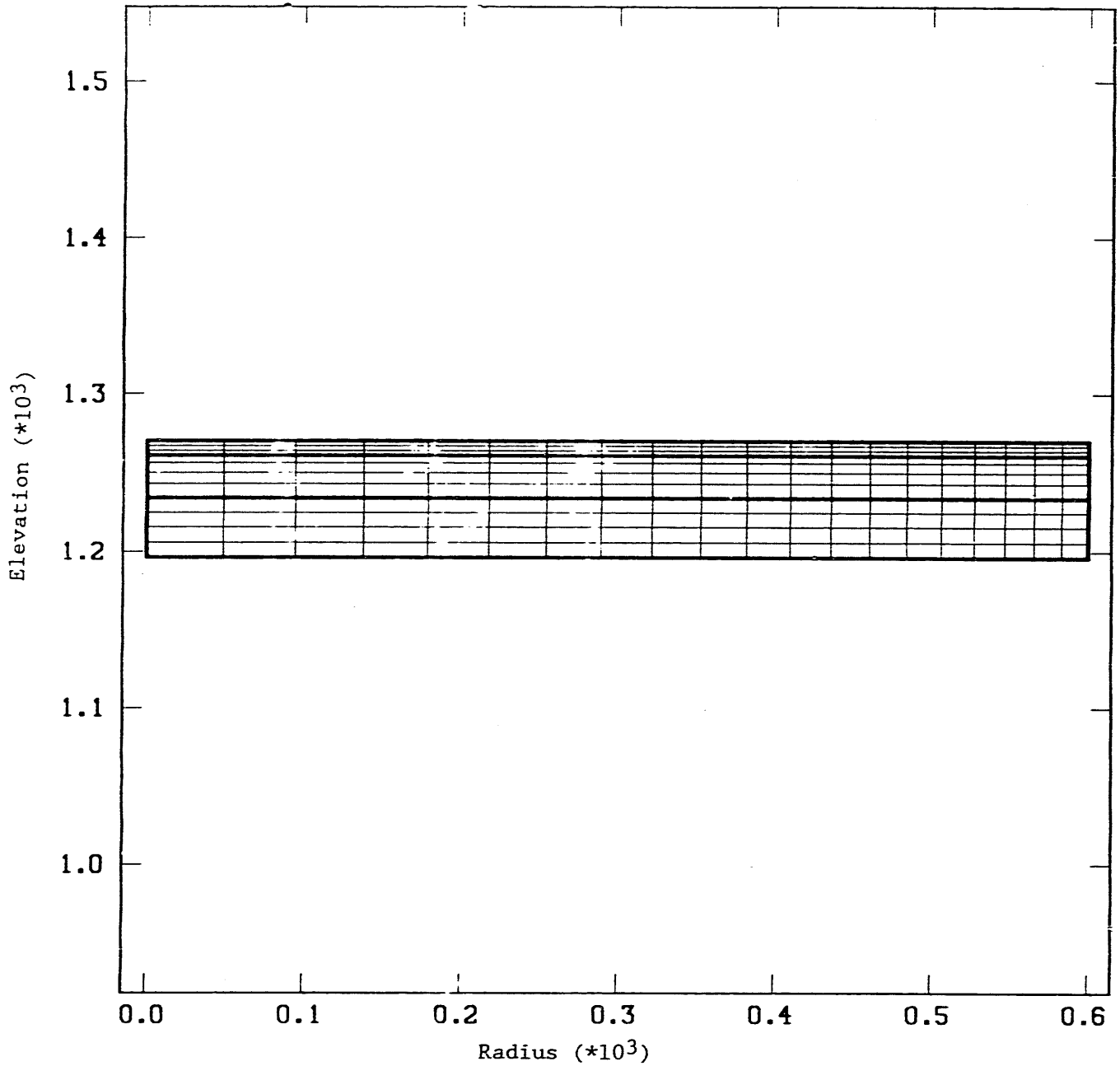

Figure 23: Two-dimensional computational grid
for 0 through 2.26 years

this grid, and the solutions were monitored to ensure that the water pulse did not reach the bottom of the grid.

The NORIA-SP solution encountered stability problems from about six months to two years. According to the NORIA-SP calculations, a water pressure equivalent to a pond of a depth of 460 meters (roughly equal to the maximum depth of Lake Superior) is required to build and maintain an infiltration rate through the given materials of 3.2 m/yr (Comparable results were exhibited in the one-dimensional calculations by TOSPAC when a similar boundary condition was applied.). Figure 24 shows the saturation profile along the axis of this disturbed area as a function of elevation (altitude), and Figure 25 shows a two-dimensional contour plot of saturation, in the top three layers of the stratigraphy, after 1 year of surface water application. Figures 26 and 27 display the same results, respectively, after 2 years. Because of the very large pressure gradients created by the high pressures at the surface, the pulse of water flowing through the alluvium appeared as a shock wave. The "shock" occurs in the regions of high saturation gradient from fully saturated (saturation=1.0) to the initial condition. Pressure values at the secondary nodes of the finite elements containing the shock (especially those elements in the alluvium layer) fluctuated wildly before stabilizing near expected levels. This instability resulted in very small computational timesteps, which required nearly 40 hours of CPU time on the Cray Y-MP to obtain the solution at 2 years.

4.2.2.3 Extrapolation of the NORIA-SP 2-Year Solution to Five Years -- The third step of the two-dimensional analysis was the calculation of the water distribution at five years. Due to the large expense of obtaining the NORIA-SP solution at two years, and to the behavior of the water dispersion during the two years, it was decided to extrapolate the NORIA-SP solution at two years to an estimated solution at five years. In the 2-year solution, there was significant radial dispersion of the water in the alluvium and TCw, and both layers were almost entirely saturated out to a radius of 400-450 m (the lower number being at the bottom of TCw, the higher at the surface). There was also a significant amount of water that had entered PTn, although saturation was not reached anywhere. Therefore, both radial and downward dispersion of water were significant. For this step of the analysis, the following assumptions and calculations were made.

- Distribution of water in the top three hydrologic levels. The water stored above steady-state levels in the top three stratigraphic layers (alluvium, TCw, PTn), the sum of the water stored in these layers, and the cumulative perturbed infiltration as functions of time are shown in Figure 28. The values shown for times ranging from 0 through 2.26 years correspond to those calculated by NORIA-SP; those values from 3 through 5 years are estimated values based on the NORIA-SP runs. A linear extrapolation based on the values at 1 year and 2 years was chosen for three reasons: (1), the relationship between the volume of additional water and time for each layer appeared to be roughly linear; (2), as a number of other assumptions were made to bring the calculation to this point, it was decided that any extra accuracy gained by curve-fitting with a more sophisticated method would be "lost in the noise"; and (3), the linear-extrapolation method would continue the trend of lateral water dispersion that had already been displayed by NORIA-SP, so the effects of a two-dimensional flow would be further evaluated. It should not be

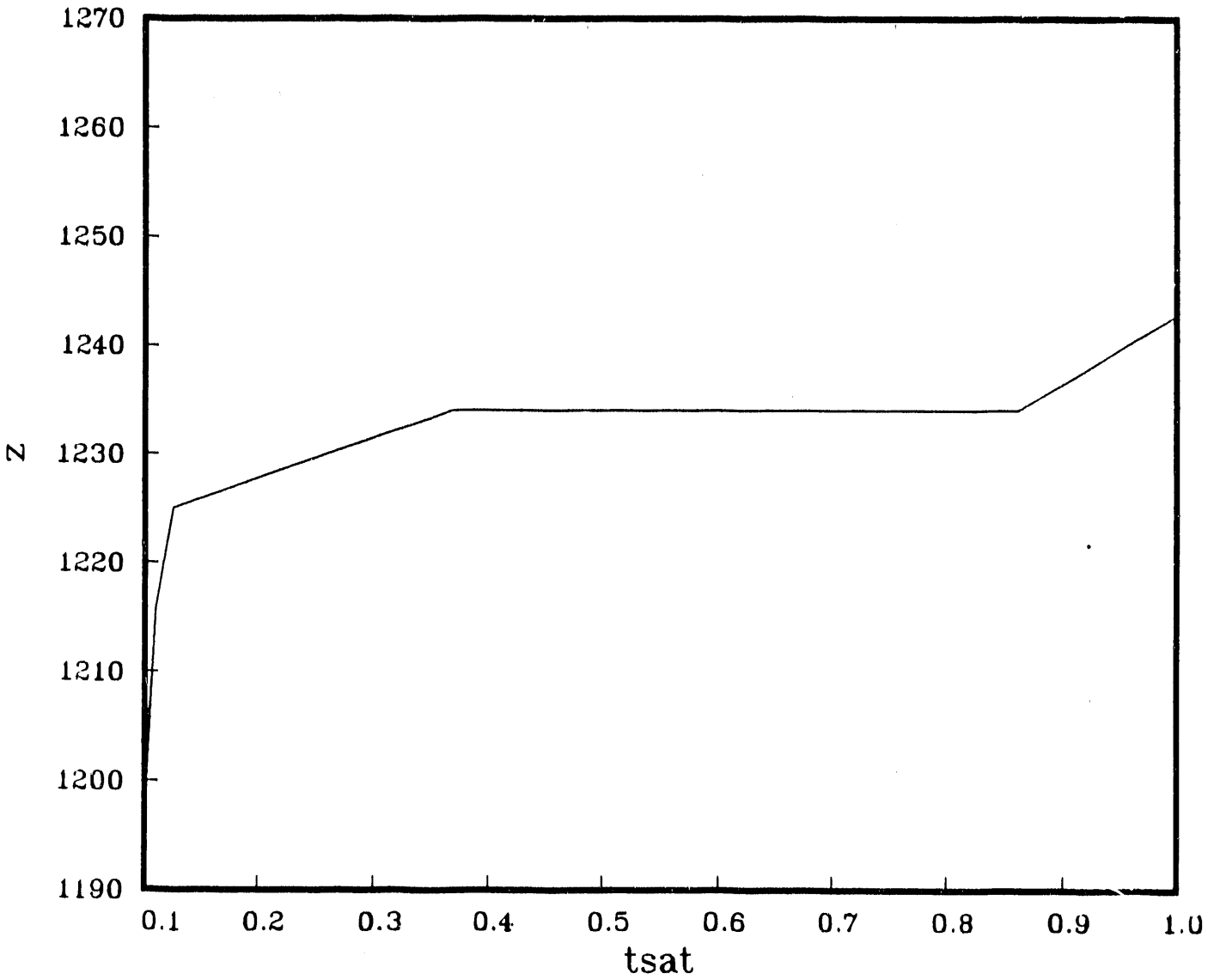

Figure 24: Saturation profile along axis of disturbed surface area after 1 year of surficial water at 3.2m/yr - 2-D calculation (tsat=Total saturation; z=elevation)

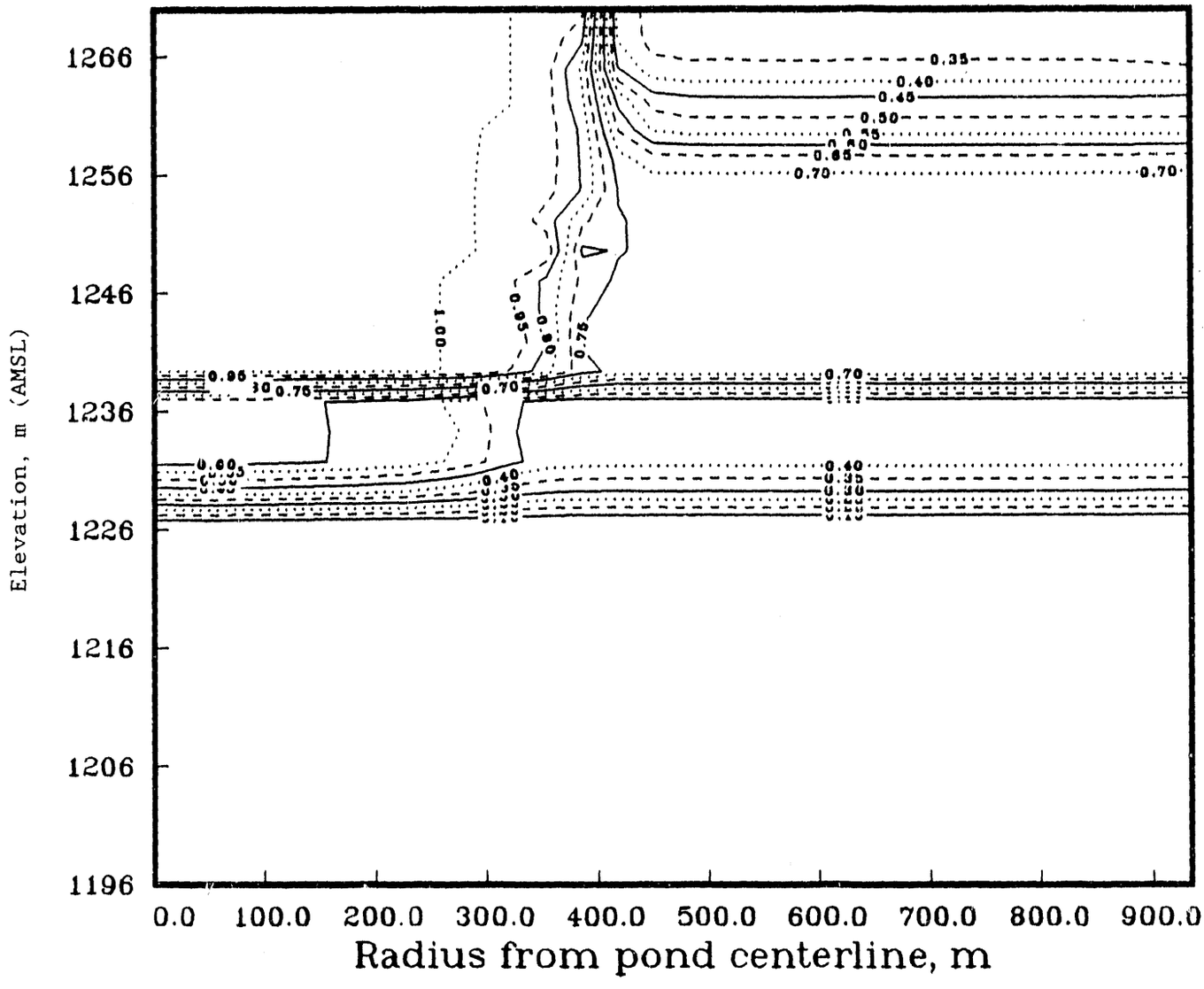

Figure 25: Two-dimensional saturation profile after 1 year of surficial water addition at 3.2 m/yr

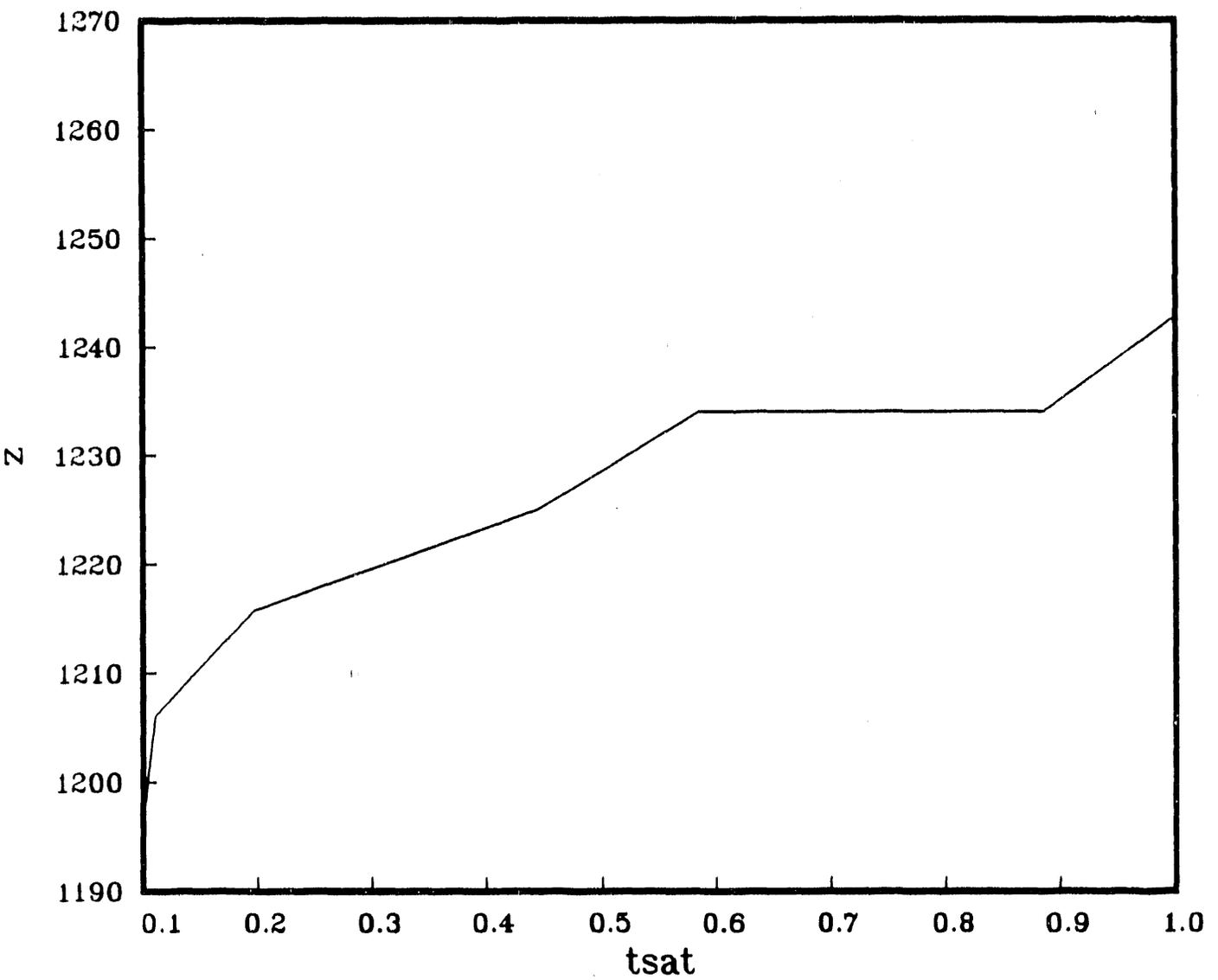

Figure 26: Saturation profile along axis of disturbed surface area after 2 years of surficial water at 3.2 m/yr - 2-D calculation (tsat=Total saturation; z=elevation)

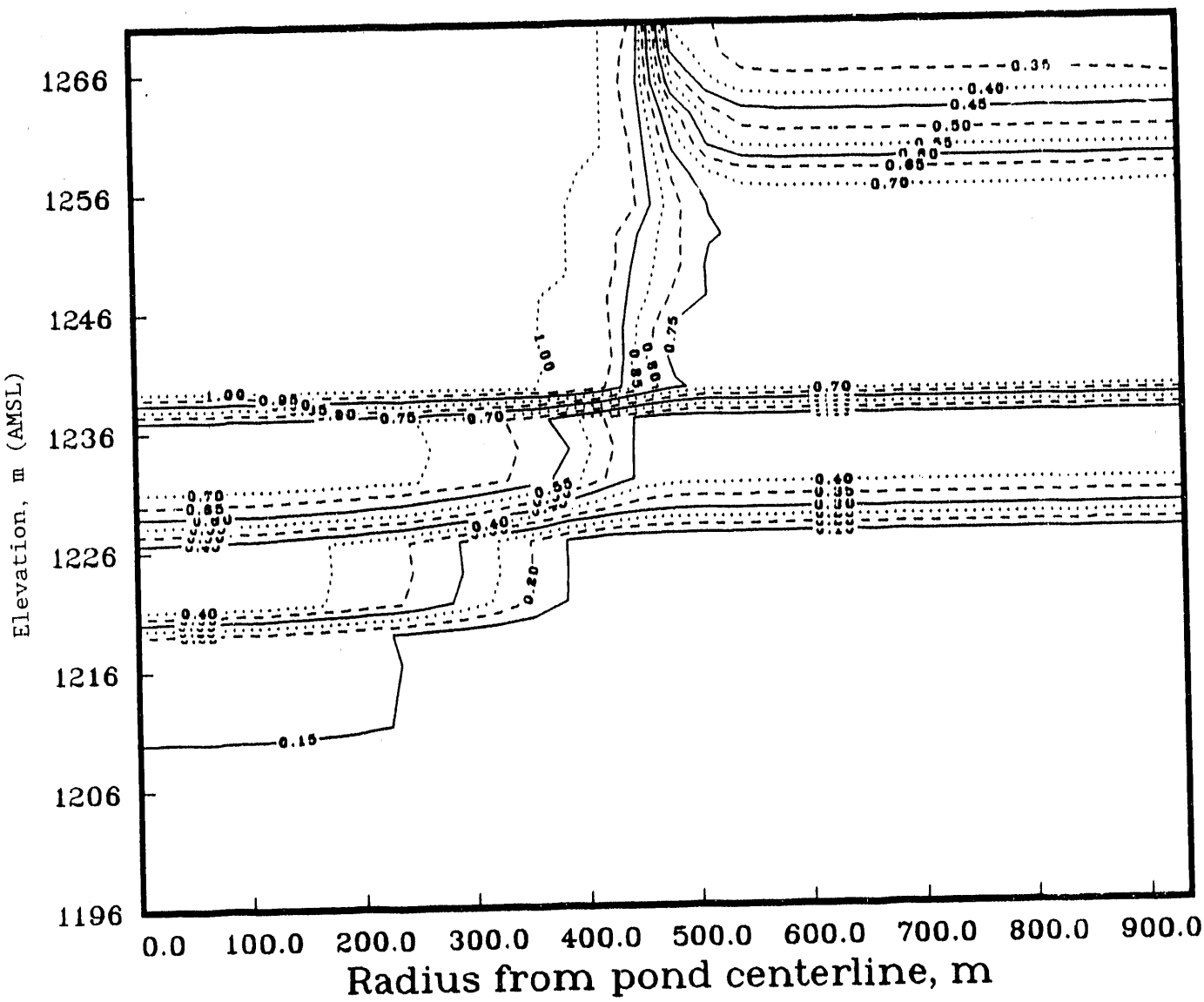

Figure 27: Two-dimensional saturation profile at 2 years of surficial water addition at 3.2 m/yr

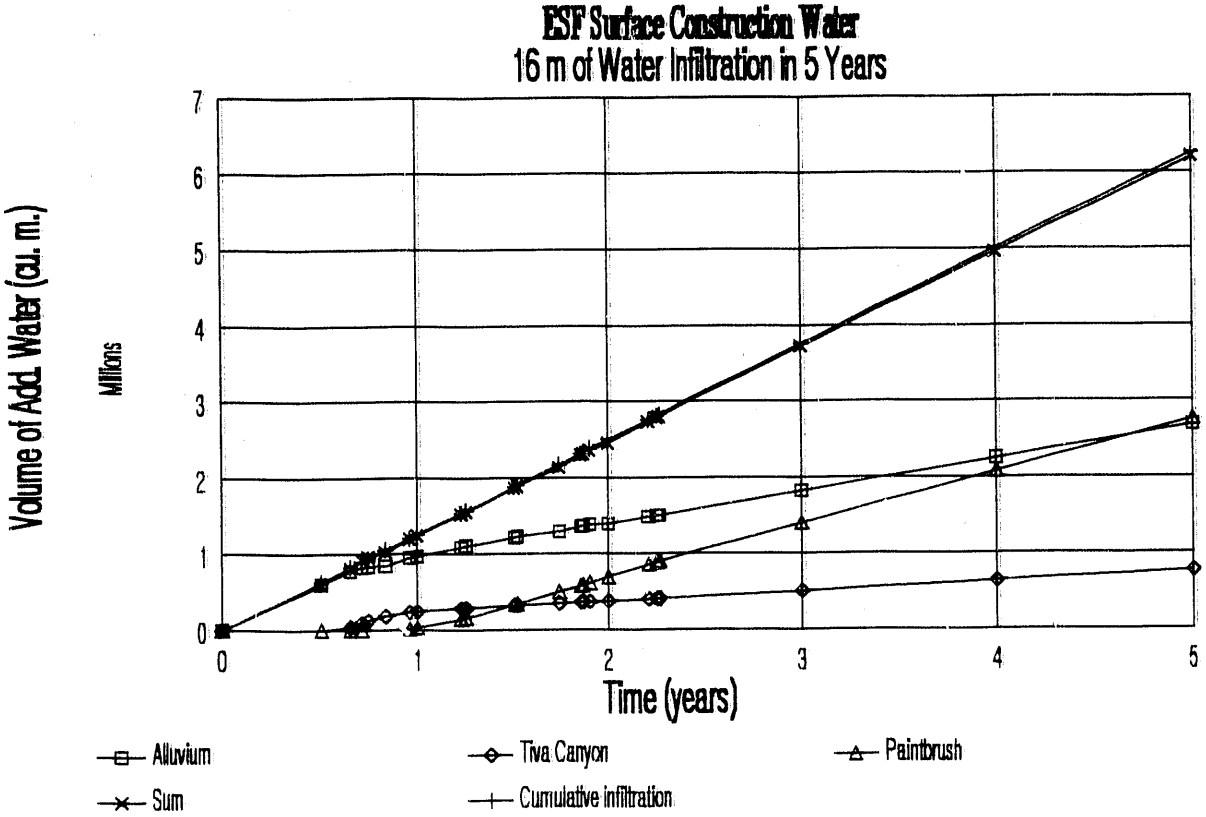

Figure 28: Storage of surficial water at 3.2 m/yr in the top three hydrological layers

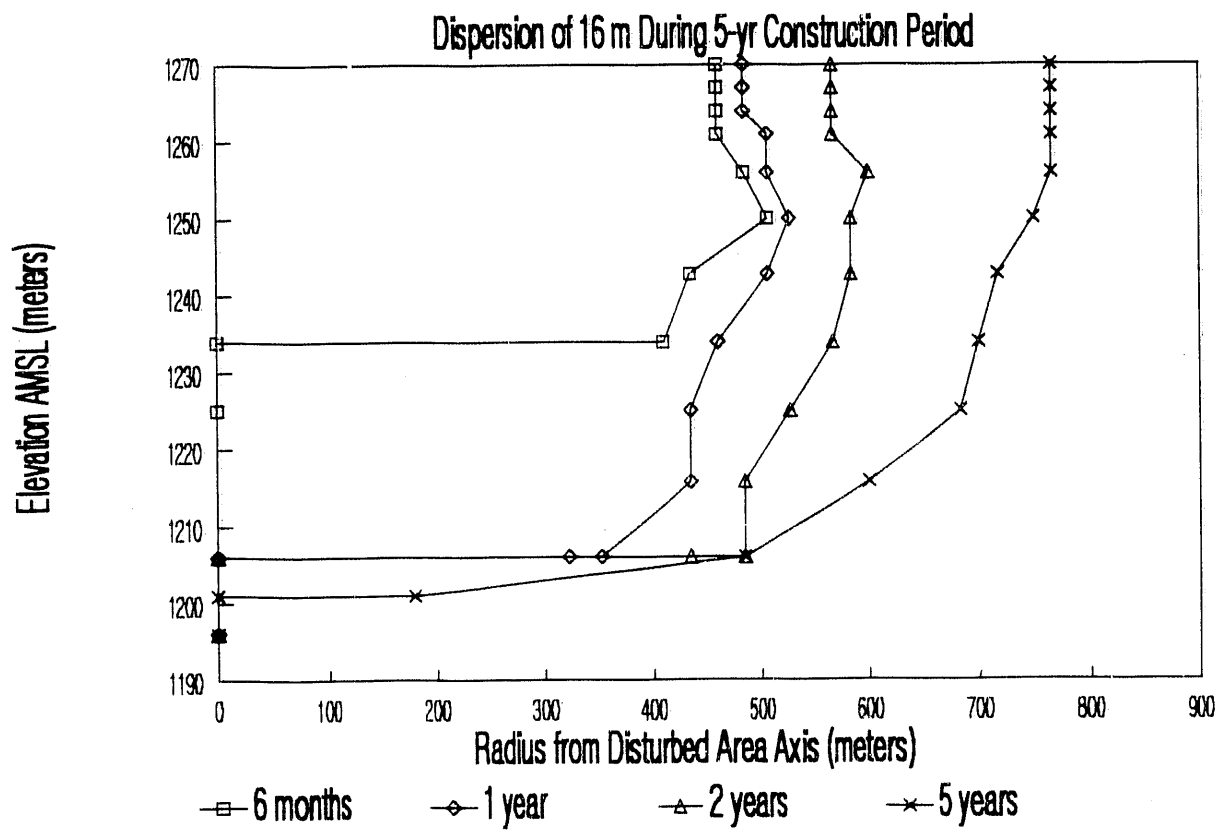

Figure 29: Maximum extent of surficial water movement at 6 months, 1, 2, and 5 years

assumed that linear extrapolation is conservative. NORIA-SP calculations were advanced to obtain solutions at 2.20, 2.24 and 2.26 years to test the "accuracy" of the linear-extrapolation method. The largest discrepancy in the value for added water in a stratigraphic layer was 0.7% in PTn at 2.26 years. Figure 28 indicates that the sum of the water added to the three layers differs only slightly from the cumulative perturbed infiltration. The water storage in each of these layers at five years was adjusted so that the sum of the water stored in the three layers agreed with the cumulative infiltration.

- Total pressure in the alluvium and TCw layers. Based on the results at and through two years, an equivalent saturated radius was calculated for each horizontal grid layer in the alluvium and TCw hydrologic layers at five years. This equivalent saturated radius was based on the volume of additional water contained in each of the horizontal grid layers. It was assumed that the volumetric distribution of the additional water throughout the top seven grid layers (three horizontal layers in alluvium, four in TCw) would maintain the same relative ratios at five years as they had at two years. The amount of water assigned to each grid layer was then partitioned into two constituent volumes: the central volume, which was completely saturated; and the peripheral volume, in which the saturation level decreased from saturation to the steady-state condition. The relative ratios of these volumes at two years were used to calculate the corresponding constituent volumes at five years. The radial pressure gradient in the peripheral volume in each grid layer at five years was assumed to be identical to the corresponding radial pressure gradient at two years, with slight adjustments made to preserve continuity. Pressure values at the interface between the alluvium and TCw layers were determined by applying pressure continuity across the interface; this implies a saturation jump across hydrogeological interfaces. Values for total pressure at the grid points on the surface and below that had reached saturation were set to the saturated value for pressure (i.e., after five years, any surficial "pond" was removed).

- Total pressure in PTn. The assumption was made that no water enters the Topopah Spring layer (TSw1) during the first five years. This assumption was made for two reasons: the combination of the high porosity and low initial saturation of PTn, which effectively provides for the storage and dispersion of the infiltration pulse; and the results of the one-dimensional analysis. The one-dimensional results indicate that PTn saturates after a surficial water infiltration of slightly more than 16 meters and before water migrates to TSw1. Therefore, the total pressure at the base of PTn remained unchanged from the steady-state value for this step of the calculation. The values for total pressure at the other grid points in PTn were calculated by imposing a pressure gradient that conserved the additional mass of water onto the values for pressure at the TCw and TSw1 interfaces.

Using this method, the solution at five years was obtained and applied to an expanded computational grid. The grid was expanded due to the extent of the radial dispersion of the water. This grid is described in the next section. Figure 29 shows the maximum lateral movement of surface water at 6 months, 1 year, 2 year, and 5 years. The maximum extent of water movement was

determined by a 0.001 change in saturation at a grid point relative to its initial condition.

4.2.2.4 Calculation from 5 Years to 10,000 Years -- The fourth step of the two-dimensional analysis was to advance the solution, using NORIA-SP, from 5 years to 10,000 years, using the estimated 5-year solution and an expanded computational grid. The horizontal size of the new grid was increased to 934 m radius, and the grid height was returned to the full USW G-4 stratigraphy height of 539.4 m. The grid comprised 44 rows and 40 columns (see Figure 30). The steady-state infiltration rate of 0.01 mm/yr was imposed as the boundary condition for the entire upper surface. The solution from 5 years to 10,000 years consumed 22 hours of CPU time on the Cray Y-MP. Approximately half of this CPU time was used to "smooth out" the extrapolated solution at 5 years to a solution at 5 years plus 5 days. This "smoothed-out" solution shows the beginning of water migration into the Topopah Spring layer. Figure 31 shows the extent of water movement at 5 years plus 5 days, and at 5 years plus 6 months, while Figure 32 displays the extent of water movement through 10,000 years.

4.2.3 Results

Saturation profiles along the axis of the disturbed areas are plotted in Figures 33 through 38 for the solutions at 5 years (the extrapolated solution), 5 years and 5 days (the "smoothed-out" solution), and 10, 100, 1000, and 10,000 years. One of the results of the two-dimensional analysis, as shown in Figure 38, is the substantiation of the results of the one-dimensional analysis: 16 cubic meters of water per square meter of disturbed surface area can enter the mountain before increasing the saturation at the repository horizon within 10,000 years. An important conclusion from a comparison of Figure 38 and Figure 19 is that the accumulated amount of infiltrated water is more important to repository performance than the rate of the infiltration. Figures 39 through 43 show two-dimensional contour plots of saturation at 5, 10, 100, 1000, and 10,000 years.[10] These plots show that the lateral extent of the water is confined to an area four times larger than the disturbed surface area, and is primarily confined to the TCw and PTn hydrologic layers.

5. LIMITATIONS AND ASSUMPTIONS

The validity of the results of this analysis depend on the assumptions underlying the conceptual model of flow. This section contains a list of the assumptions and a discussion of the potential errors in the calculations if these assumptions are incorrect. Omitted is the fundamental question of the applicability of Darcy's law and Richards' equation -- capillary-bundle theory

---

10. The contour plots were produced by the DISSPLA plotting package. The very high gradients in saturation at the interfaces between hydrologic layers at some places, and the diffusion of the "gradient" at other places such that apparent values of saturation are less than the in-situ values, are due to the authors' inability to use the plotting package to handle discontinuities in a variable (as would occur for saturation at a boundary between two different rock types)

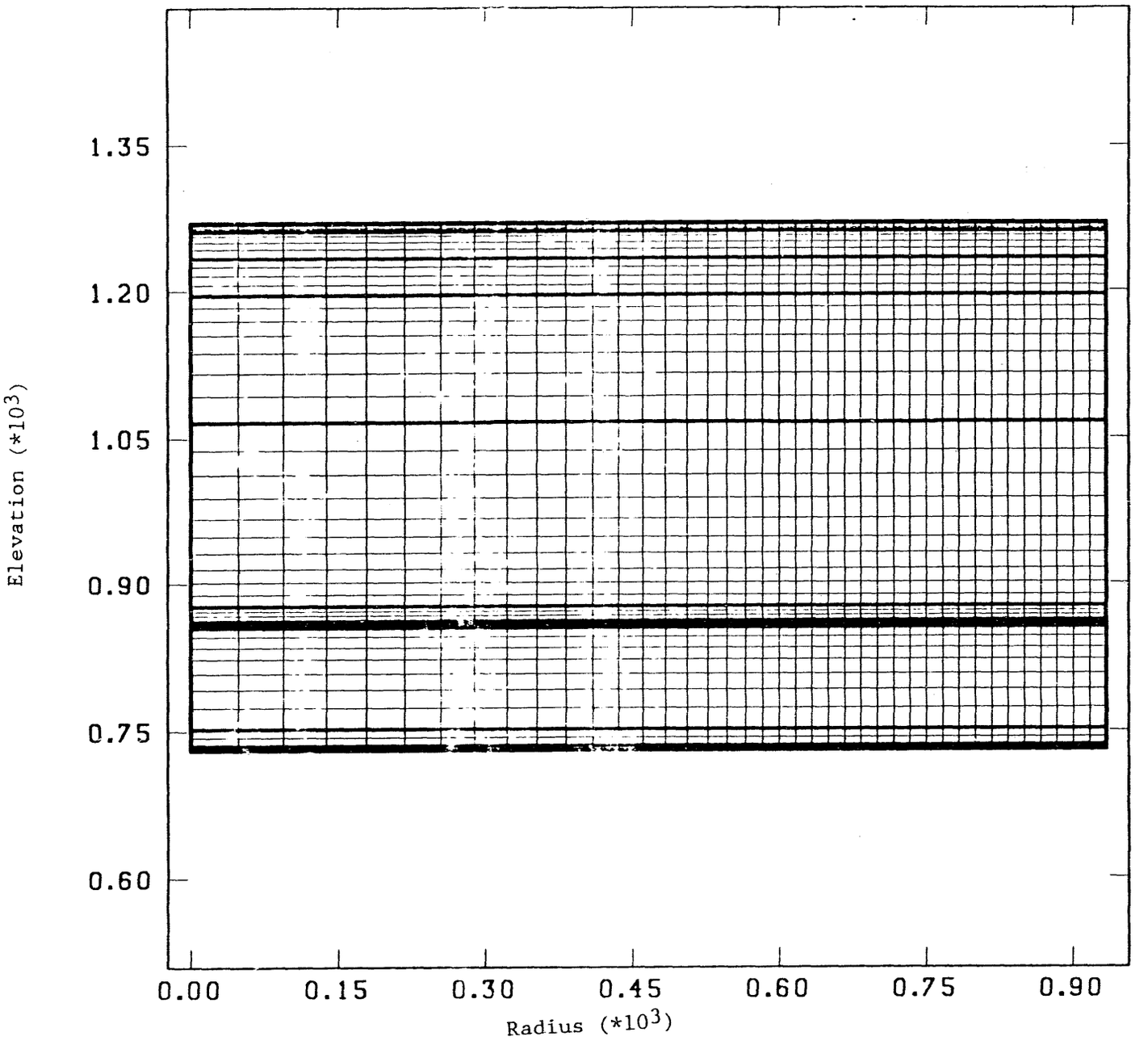

Figure 30: Two-dimensional computational grid
for 5 through 10,000 years

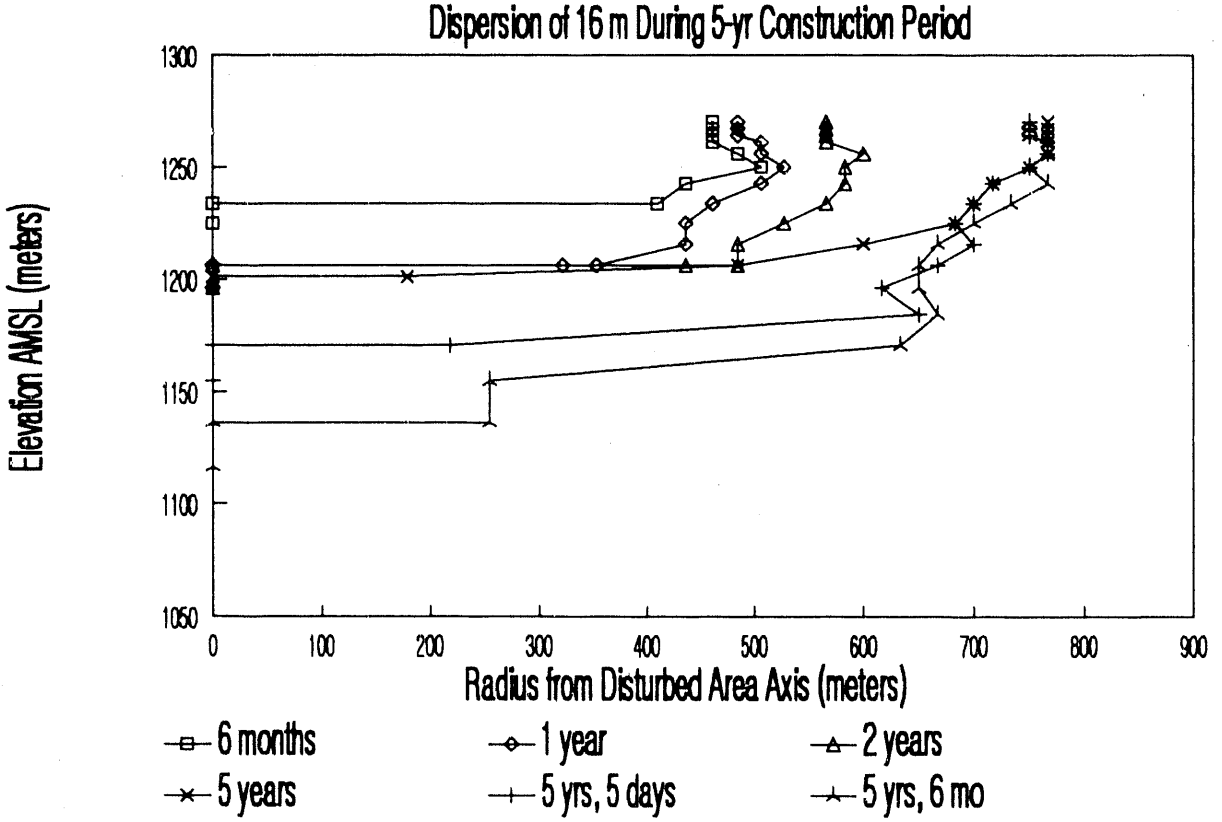

Figure 31: Maximum extent of surficial water movement through 5½ years

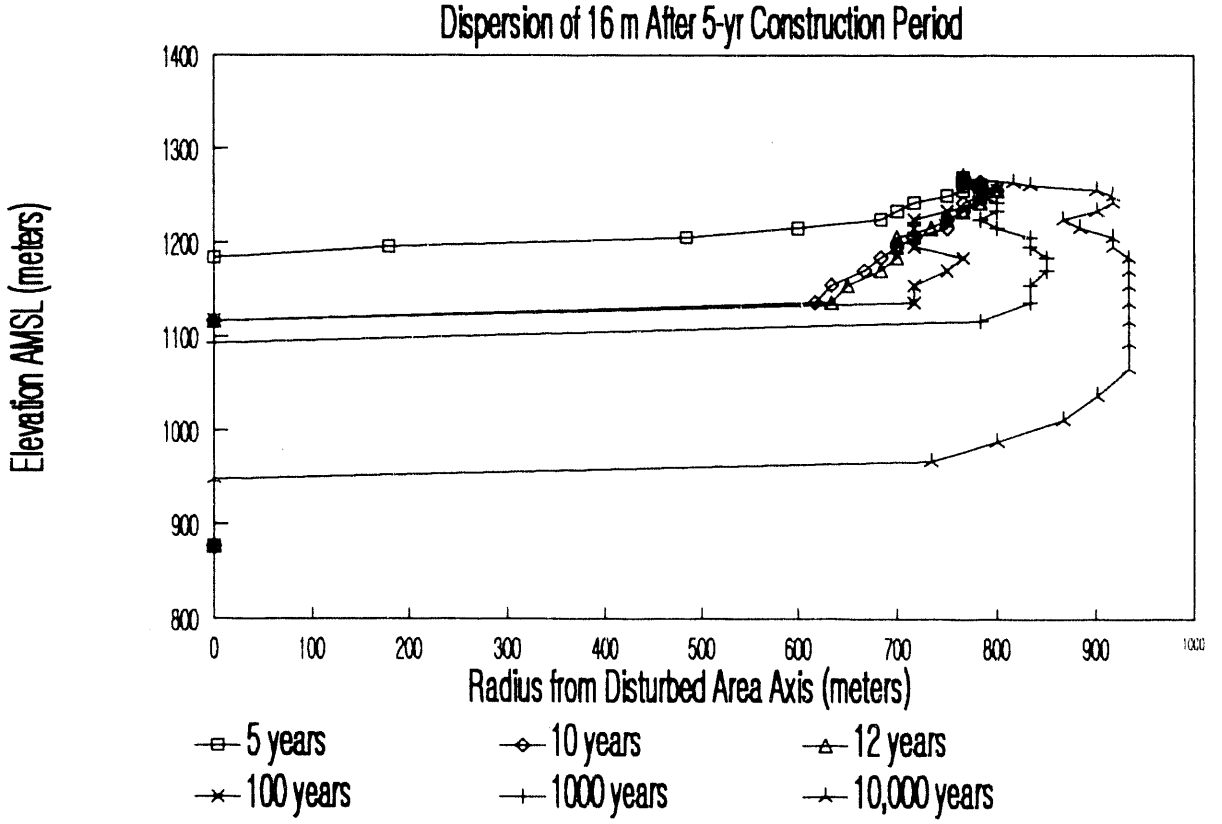

Figure 32: Maximum extent of surficial water movement at 5, 10, 12, 100, 1000, and 10,000 years

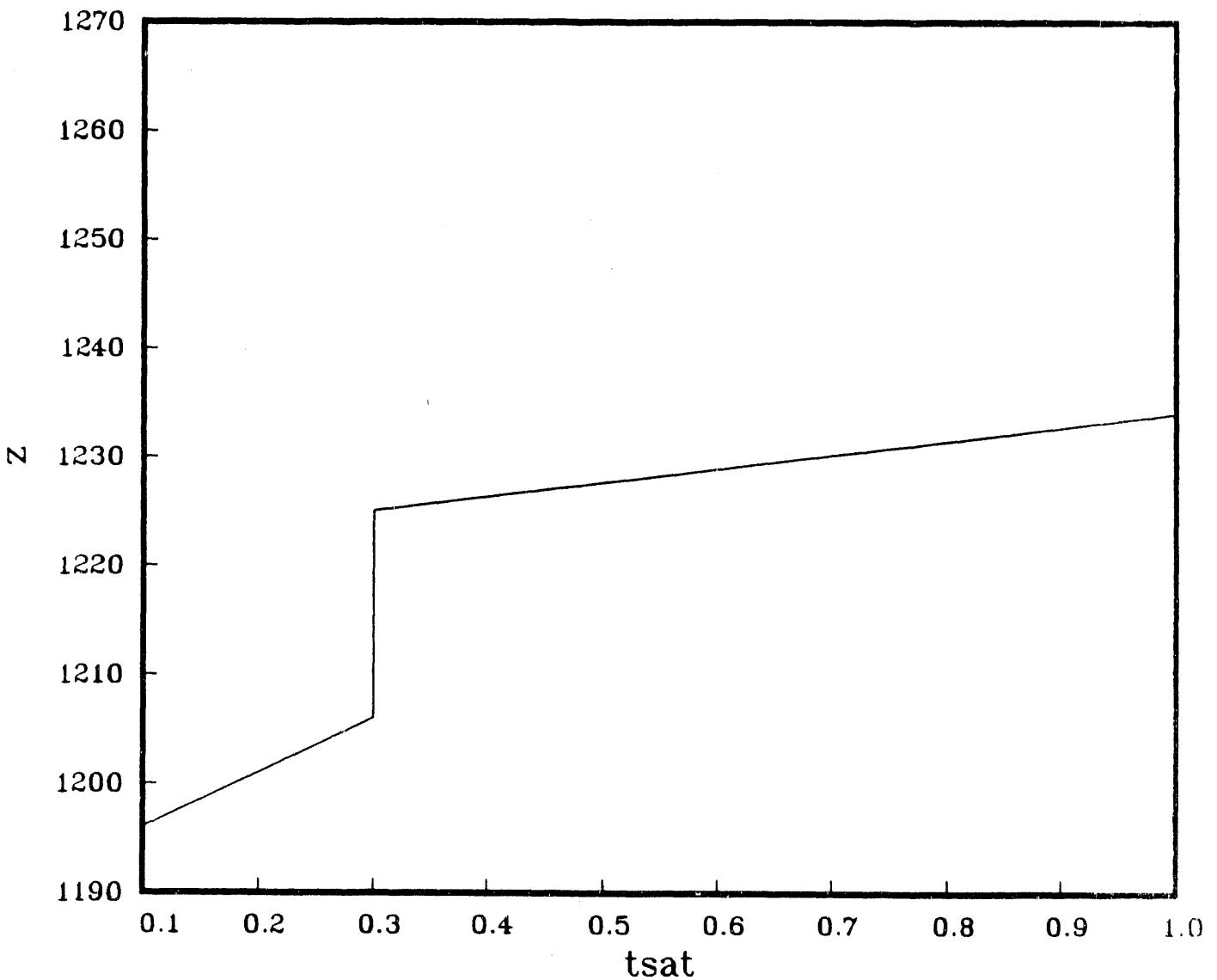

Figure 33: Saturation profile along axis of disturbed surface area after 5 years - extrapolated solution - 2-D calculation (tsat≡Total saturation; z≡elevation)

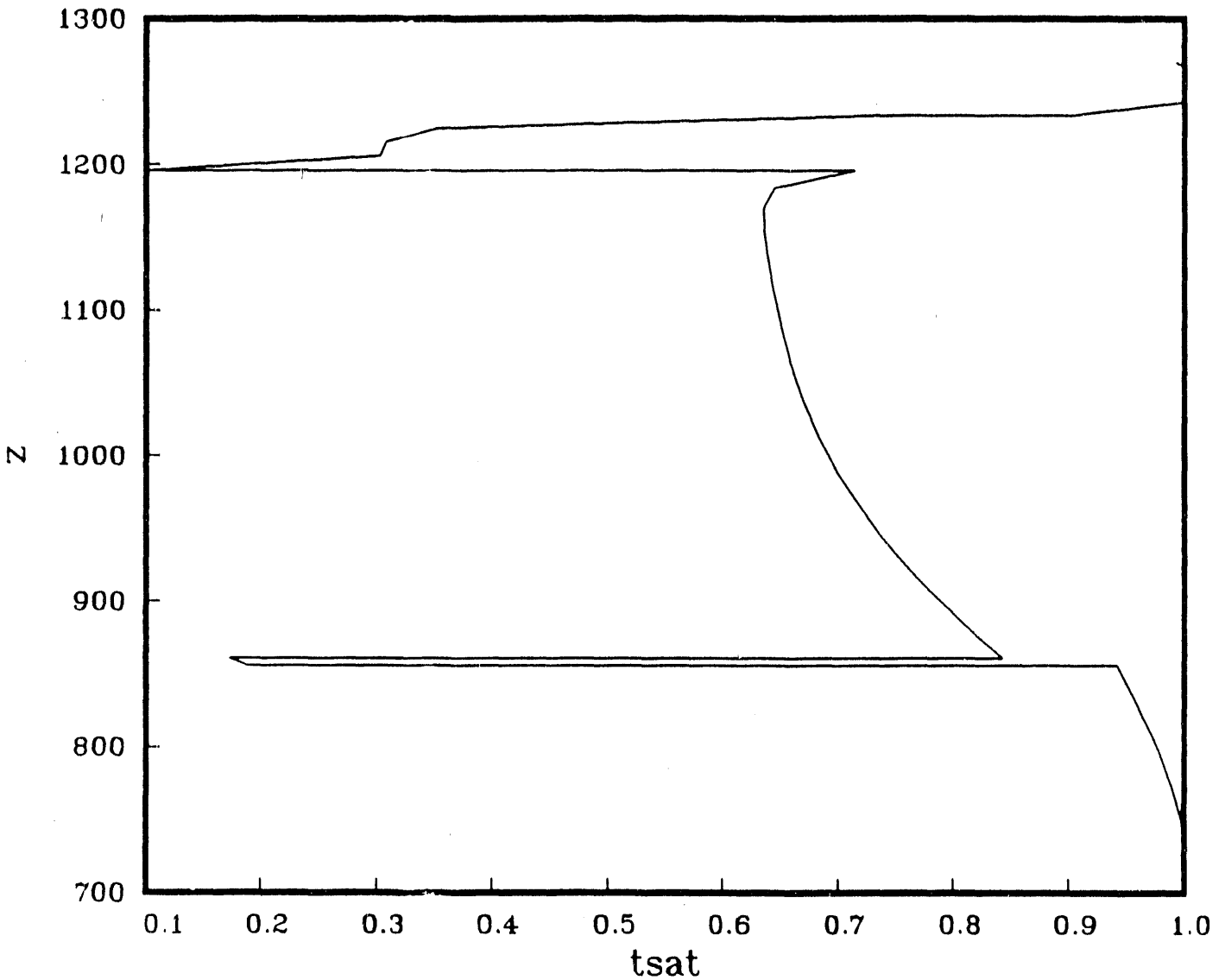

Figure 34: Saturation profile along axis of disturbed surface area after 5 years and 5 days - "smoothed-out" solution - 2-D calculation (tsat=Total saturation; z=elevation)

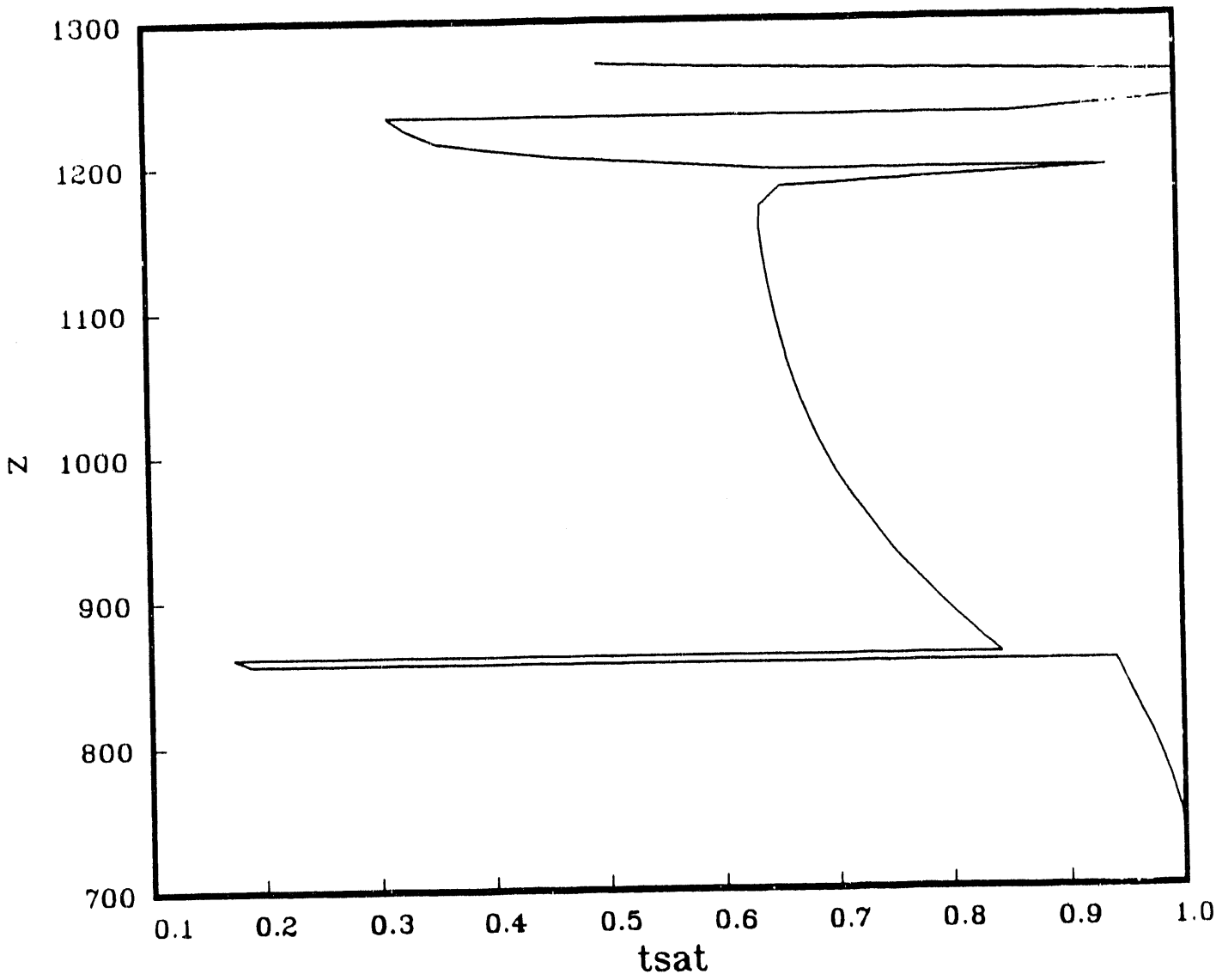

Figure 35: Saturation profile along axis of disturbed surface area at 10 years - 2-D calculation
(tsat=Total saturation; z=elevation)

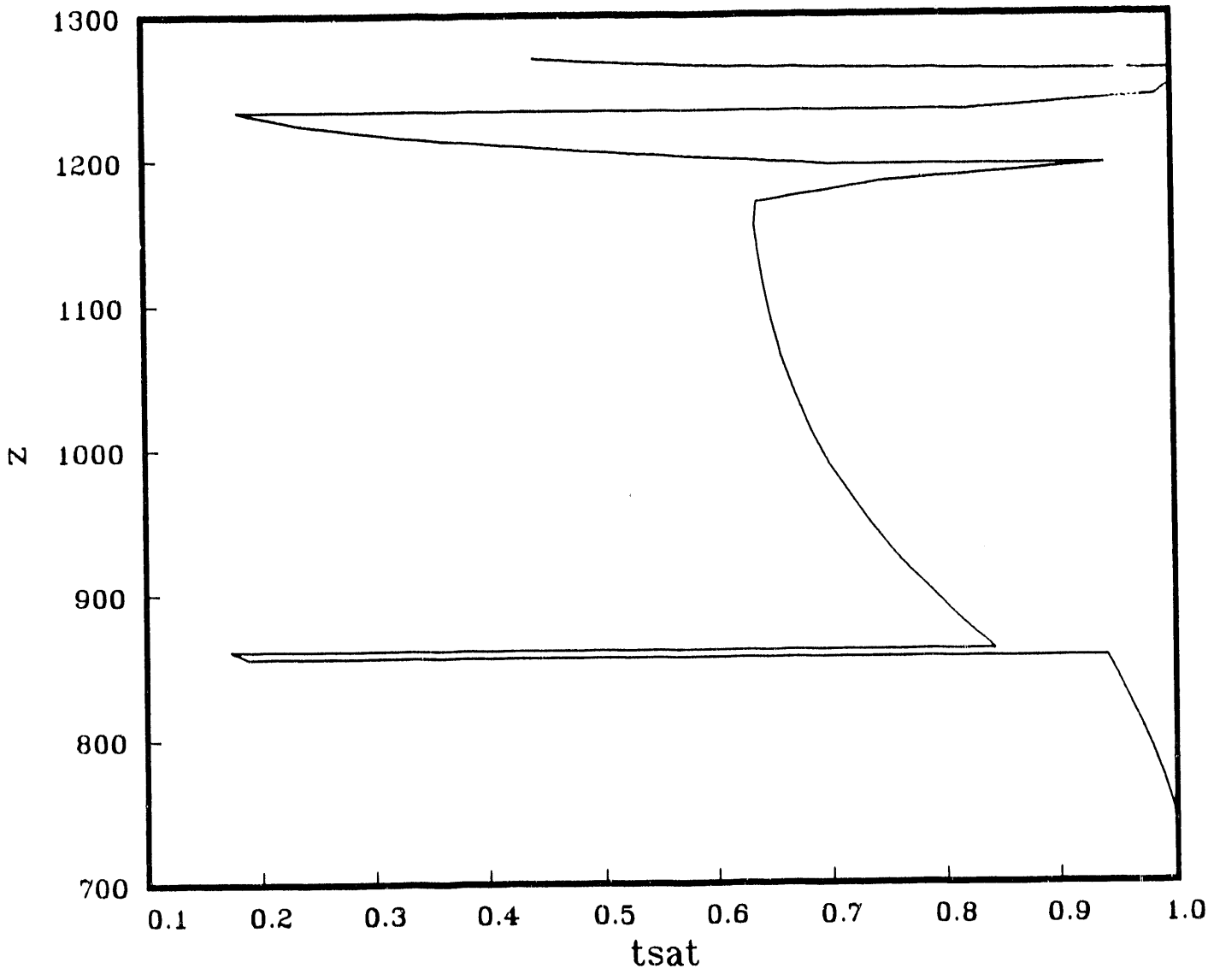

Figure 36: Saturation profile along axis of disturbed surface area at 100 years - 2-D calculation
(tsat=Total saturation; z=elevation)

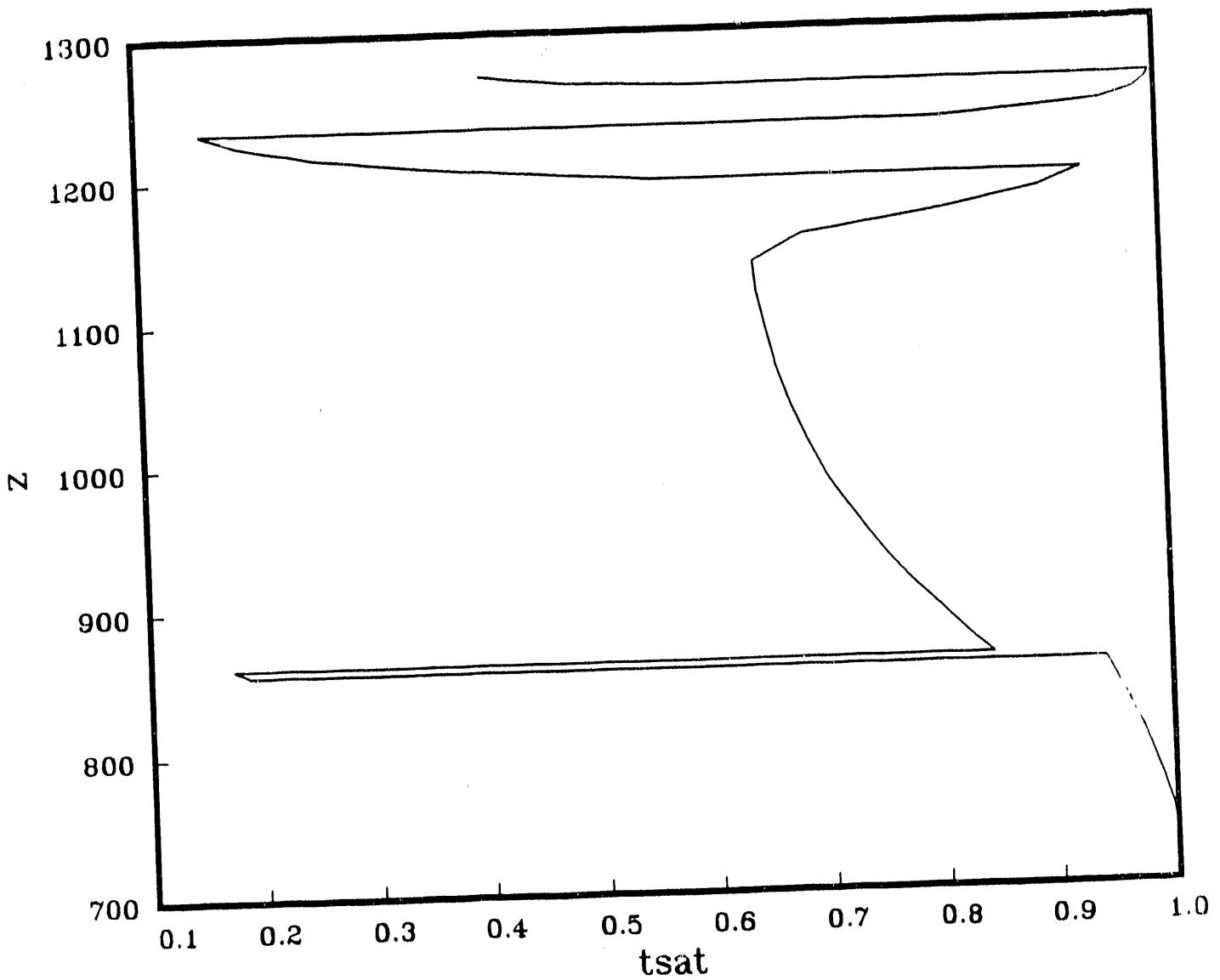

Figure 37: Saturation profile along axis of disturbed surface area at 1000 years - 2-D calculation
(tsat=Total saturation; z=elevation)

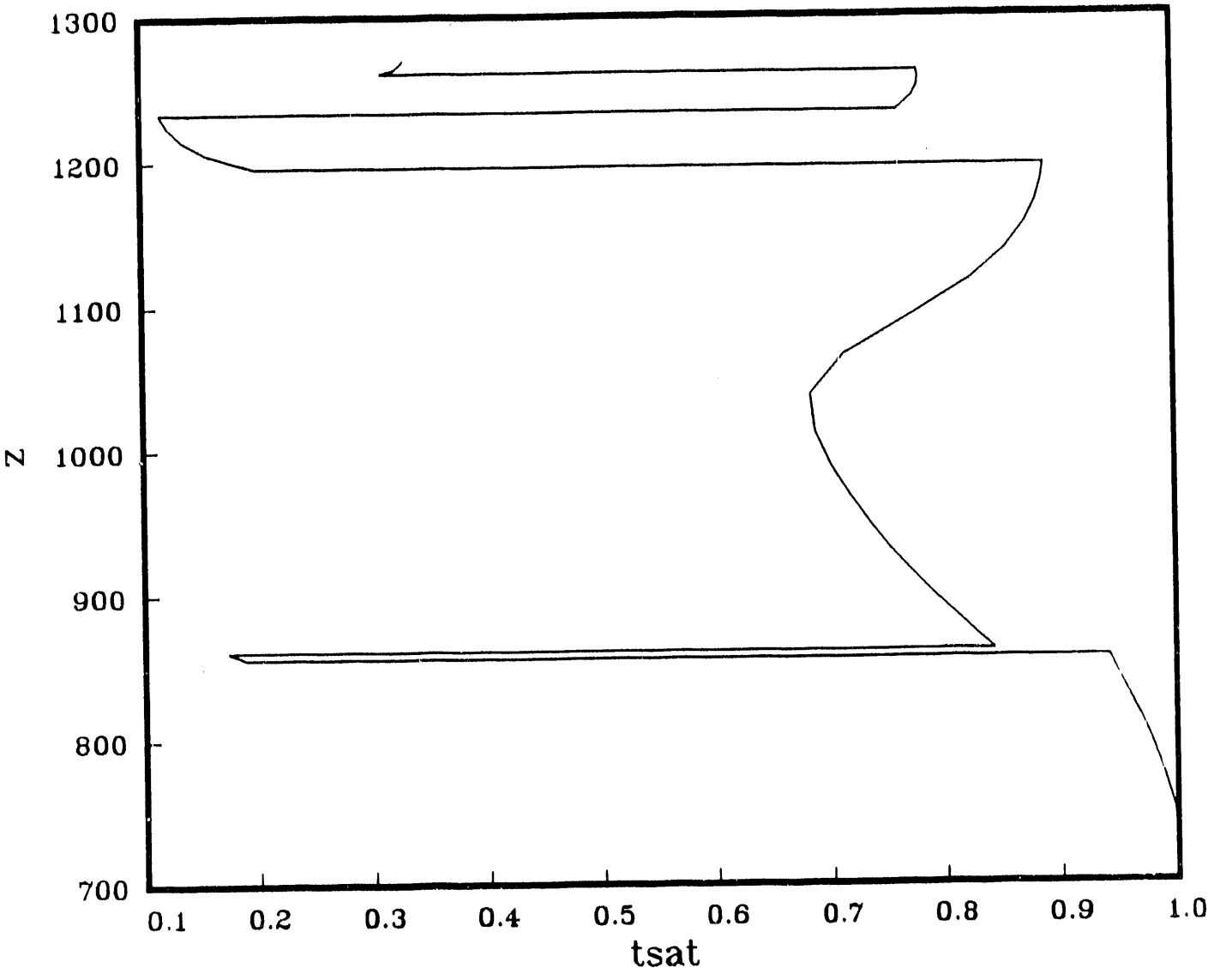

Figure 38: Saturation profile along axis of disturbed surface area at 10,000 years - 2-D calculation
(tsat=Total saturation; z=elevation)

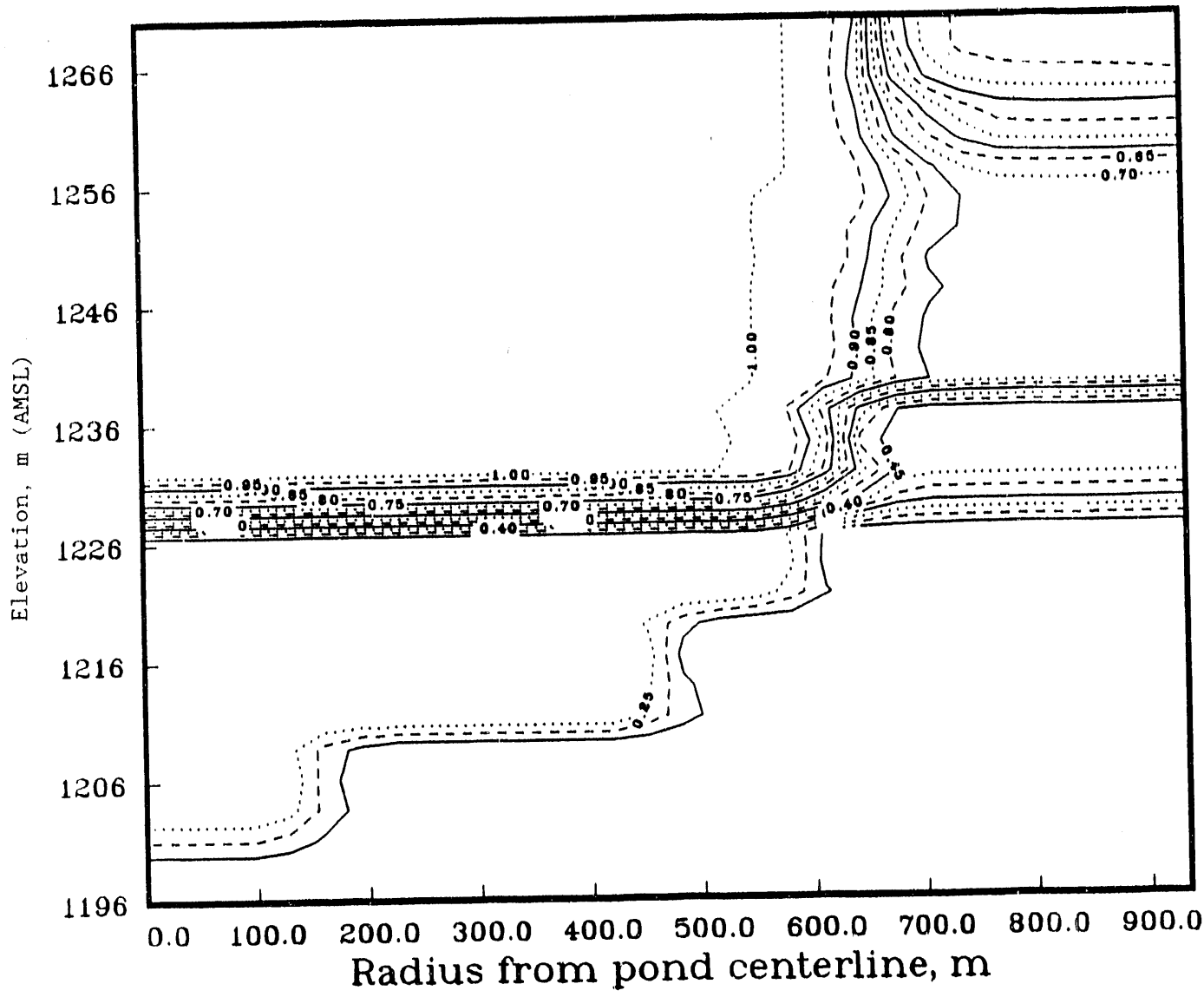

Figure 39: Two-dimensional saturation profile at 5 years

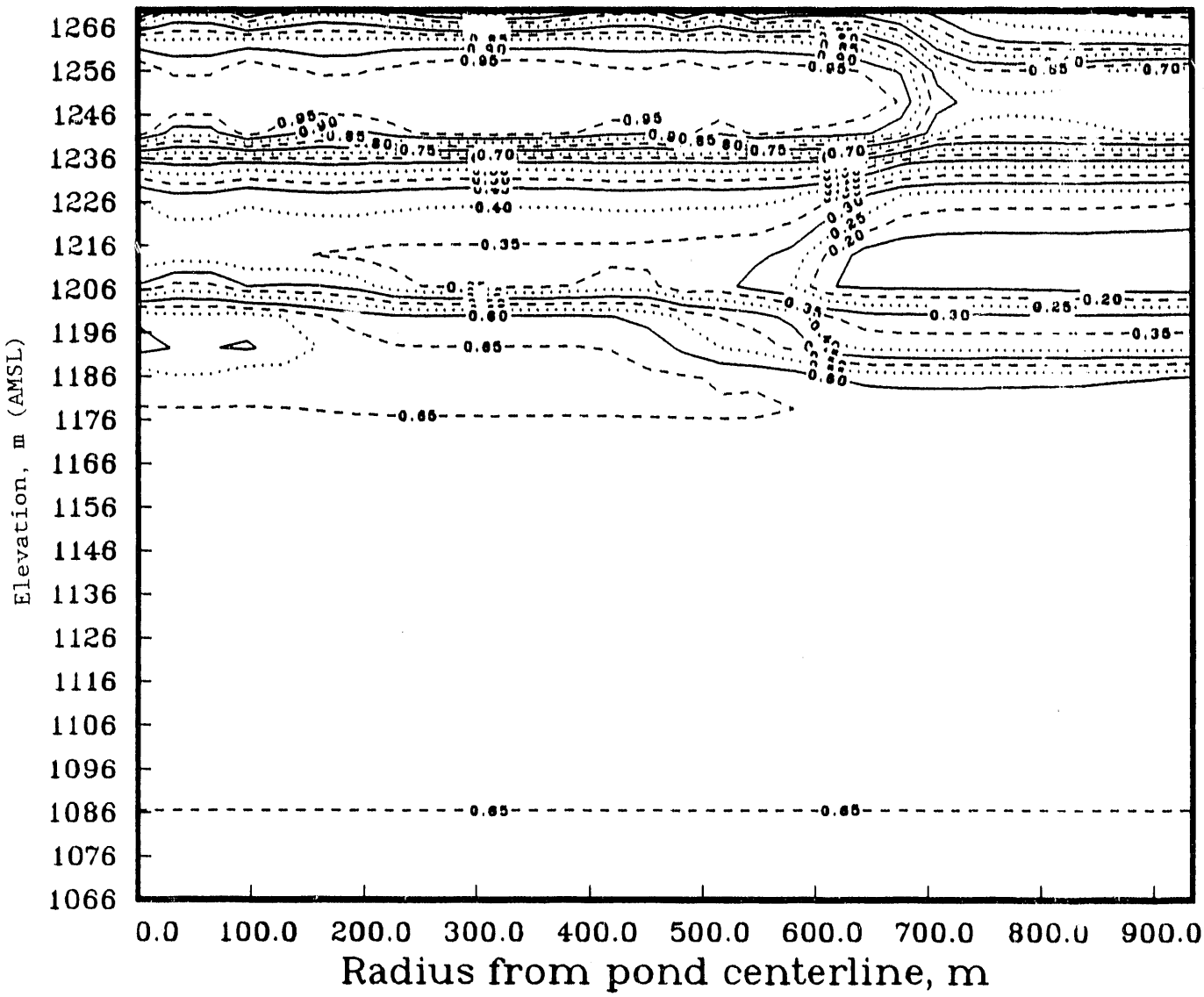

Figure 40: Two-dimensional saturation profile at 10 years

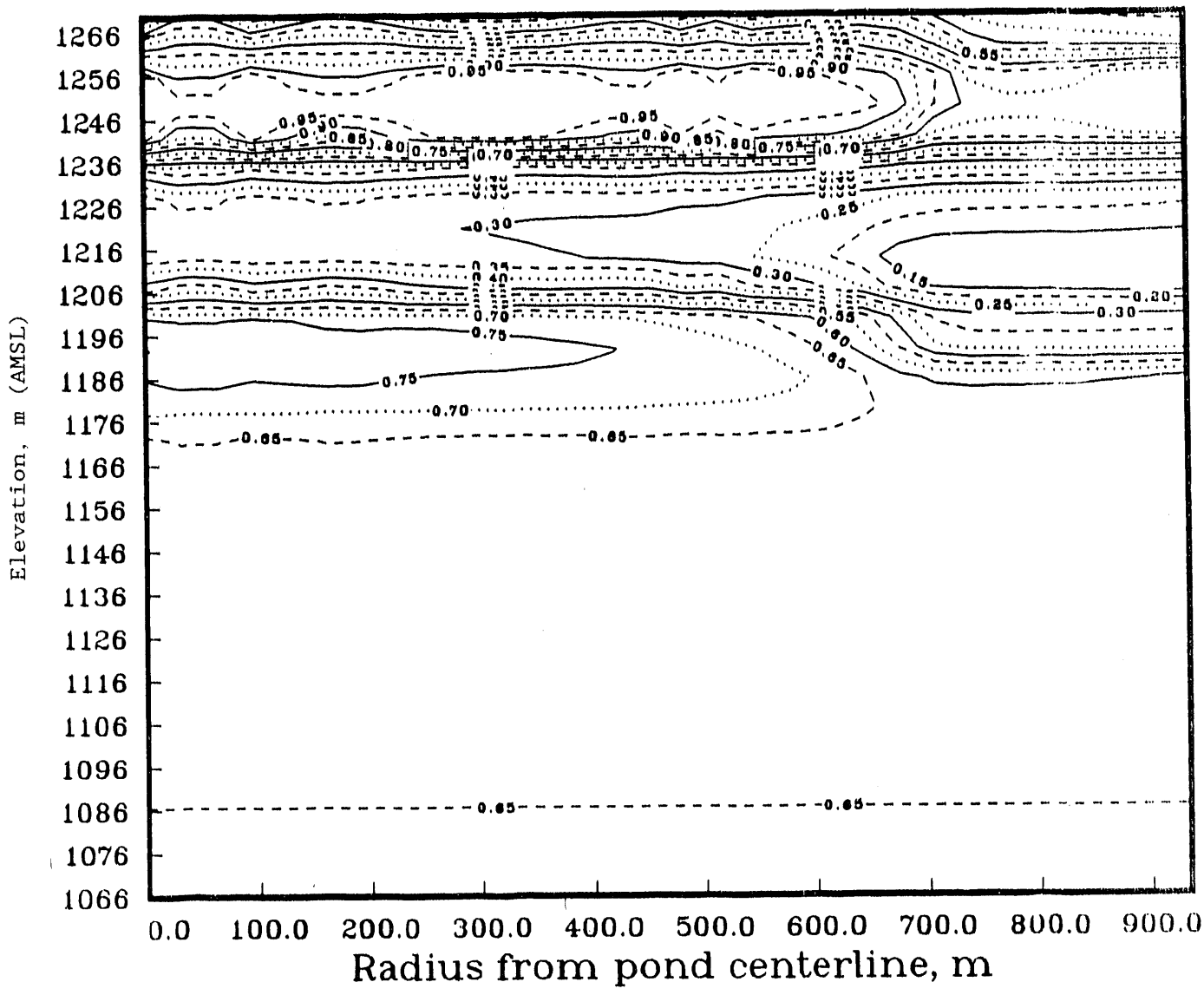

Figure 41 Two-dimensional saturation profile at 100 years

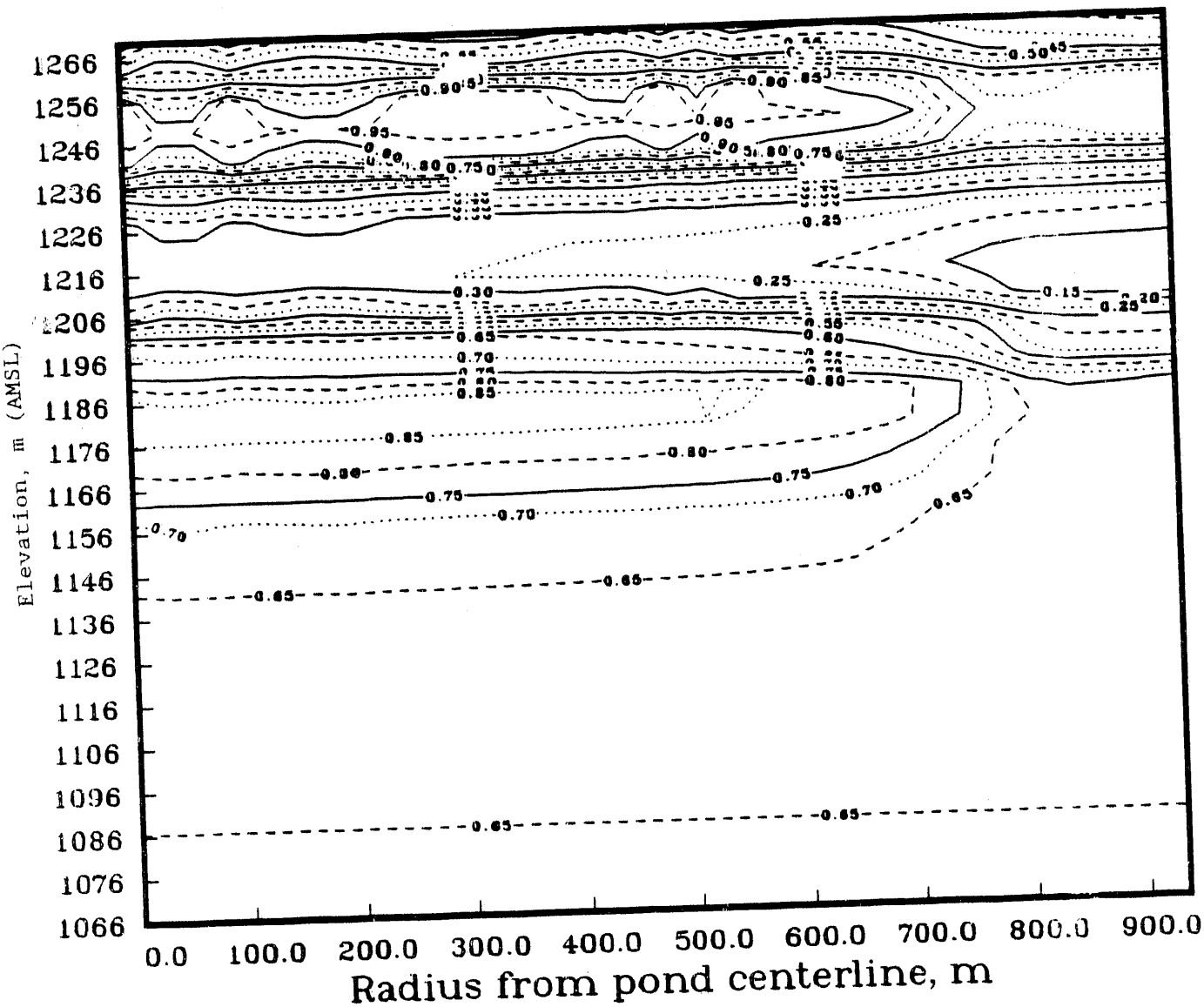

Figure 42: Two-dimensional saturation profile at 1000 years

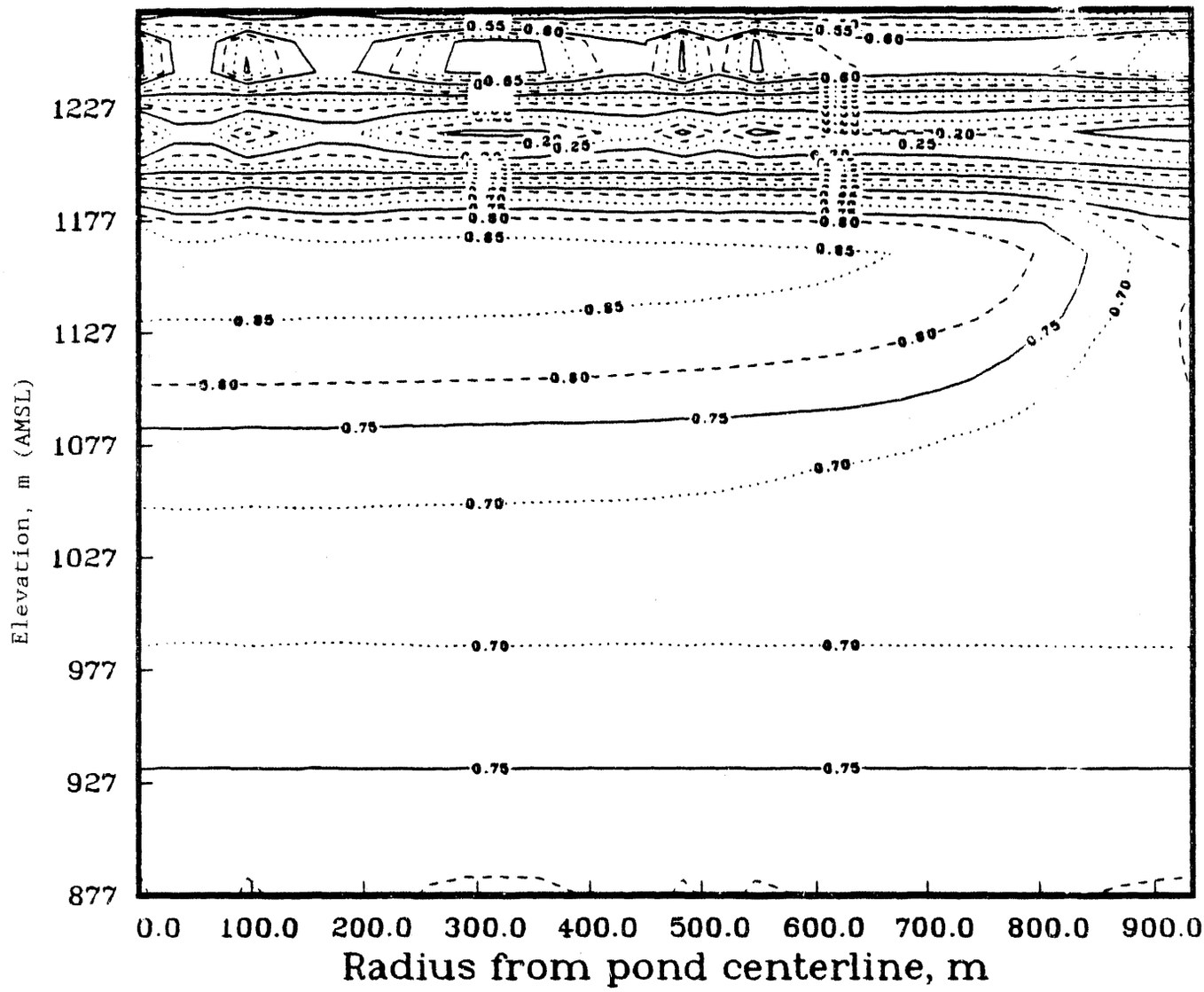

Figure 43. Two-dimensional saturation profile at 10,000 years

in general -- to the modeling of unsaturated flow through relatively impermeable rock.

5.1 Code Limitations

The code NORIA-SP was chosen for this analysis for the reasons stated in Section 4.2. This code, and its predecessor NORIA, have been used extensively and successfully for many types of flow problems. The conduct of this analysis demonstrated a limitation of NORIA-SP, in that the code encounters stability problems when high pressure gradients are imposed on the problem. These stability problems were demonstrated in two places: at the advancing infiltration pulse, especially in the alluvium layer; and at the PTn-TSw1 interface for calculations starting with the extrapolated solution at 5 years (requiring the "smoothing-out" discussed earlier). Though it seems that reasonable solutions can still be achieved even while encountering these stability problems, the cost of running NORIA-SP to get these solutions can become quite high.

An additional limitation on the validity of this analysis is the way in which the surface infiltration is modelled. For NORIA-SP, an infiltration rate equal to 3.2 m/yr was imposed on the disturbed surface. NORIA-SP then determined the necessary pressure at the surface to enforce the infiltration boundary condition. This stipulation produced the unrealistic "Lake Superior" over the disturbed area. A better understanding is required of surface infiltration processes, including fracture flow at the surface and evapotranspiration, and consequently should be appropriately modelled in NORIA-SP and other two-dimensional flow codes.

5.2 Material Properties Used for PTn

The results of the calculations are sensitive to the material properties used. As mentioned in Section 4.1.3, 14 m of the critical 16-m value is from water imbibed by the highly porous, highly conductive PTn unit. Data reported from the RIB and data given by Weeks and Wilson (1984) suggest that PTn is more saturated than the initial condition given for these calculations. (Greater initial saturation reduces the amount of space available to store the incoming surface water. Greater initial saturation also calls into question the choice of the characteristic curve.) The material hydrologic properties used in the calculations for PTn come from a core sample taken at drill hole USW GU-3, not USW G-4. However, the properties for the USW GU-3 sample are near the average of values reported for USW G-4 samples [Peters et al., 1984]. A different porosity value or a different characteristic curve for PTn could significantly change the amount of water which perturbs the saturation at the repository horizon and the GWTT.

5.3 One-dimensional Flow

It is reasonable to expect that with an increase in spatial dimensionality, the prospects of water finding a fast-flow path increases. (A fast-flow path could be a fault zone, which would form a weep or seep with the additional water.) Thus, a one-dimensional simulation would overestimate GWTT. The effect on the saturation at the repository horizon is not known.

It is also reasonable to expect that with an increase in spatial dimensionality, the prospects of water finding more circuitous routes also increases. Specifically, water could be diverted laterally through highly conductive strata (e.g., the surficial alluvium, Paintbrush, the vitric Calico Hills layers). If this lateral diversion occurs, water added to the surface of Yucca Mountain could be diverted entirely from the repository region. Another possibility is that the water could be diverted to such an extent that any pulse would be dispersed over a large area. In this case the effective amount of applied water would be greatly reduced. This type of lateral movement is suggested by comparing Figure 9, for the one-dimensional calculation with 16 meters of surface water, to Figures 33 through 38, the results from the two-dimensional calculation. If the additional effect of the dip of the hydrogeologic layers is considered, the flow is truly three-dimensional, and the dip may increase the lateral diversion of the surface water. Thus, a one-dimensional simulation would underestimate GWTT, and overestimate the change in saturation at the repository horizon.

5.4 Homogeneity of Geologic Units

Geologic units, e.g., the Tiva Canyon welded tuffs, are modelled as a single matrix material and a single fracture material. It is known that hydrologic properties from samples within a geologic unit can vary greatly [Peters et al., 1984]. It is unknown what effect this variation would have on flow. For these particular analyses, variations in hydrologic properties in highly conductive and porous regions, such as the surficial alluvium and PTn, may have large effects on the vertical and horizontal dispersion of water. If highly conductive regions are vertically connected, GWTT could be shortened. If highly conductive regions are horizontally connected, lateral dispersion of flow could be enhanced.

5.5 Composite-porosity Model

The composite-porosity model treats the matrix and the fractures as an equivalent porous medium. The pressure head in the matrix and the fractures at any given location are assumed equal. Different flow models have been proposed for Yucca Mountain.

For example, the weeps-and-seeps model holds that flow is primarily in limited regions down connected fracture networks. Water to sustain these weeps and seeps comes from diversion of large areas of surface water into these limited regions. Water in a weep travels at much higher velocity than water in an equivalent porous medium. If the weeps-and-seeps model is applicable to flow at Yucca Mountain, the result would be that a great deal of the surface water could flow directly to the water table within a few years. Such short travel times imply that surface water would not affect the repository: first, the matrix would have little time to saturate, and second, the water would be gone before the repository would be sealed.

5.6 Fracture Apertures

Fracture apertures used in these calculations were taken from laboratory measurements [Peters et al., 1984]. Actual fractures within Yucca Mountain could have much different apertures. Smaller apertures would tend to favor more flow through the matrix, decreasing GWTT, but increasing saturations.

Larger apertures would have the opposite effect. Larger apertures could also favor a mechanism of flow different from that modelled by the composite-porosity model. Presence of extremely large apertures (fault zones) could increase the chance of a weeps-and-seeps mechanism that would short circuit flow directly to the water table.

5.7 Hysteresis

Typically, water imbibes into a material at a higher pressure head than it drains from the material. This hysteretic effect can be attributed to the entrapment of air in the material. From a modeling viewpoint, hysteresis can be represented by characteristic curves that vary depending on whether the material is filling or draining. In this analysis, only characteristic curves derived from measurements involving draining materials are used--i.e., hysteretic effects caused by wetting are not included. The net effect is that in a given time period less water would enter the matrix and more would run down the fractures. By not considering hysteresis, this analysis could be underestimating the GWTT, while overestimating the increase in saturation at the repository horizon.

6. CONCLUSIONS

Both one- and two-dimensional calculations were conducted to determine the maximum amount of water that can enter through the top surface of Yucca Mountain without degrading the performance of a nuclear waste repository in the mountain. The following amounts of water were found to meet the conditions set by the three indicators described in Section 3, with the figure number referring to the saturation profile at 10,000 years for that case:

- 30 meters of water (GWTT $\leq$ 1000 years - see Figure 18);
- 23 meters of water (Precipitous change in GWTT - see Figure 14);
- 16 meters of water (Change in saturation at the repository horizon in 10,000 years - see Figure 9).

Therefore, using the most conservative measure of performance degradation, it is recommended that up to 16 cubic meters of water per square meter of disturbed surface area may be allowed for surface application at Yucca Mountain without degrading repository performance. This value for allowable surface water is considered to be ultra-conservative because of the assumptions used for this analysis: using the most conservative measure of performance degradation; neglecting surface phenomena such as runoff, evapotranspiration, and abnormal rainfall; and combining all the various road and pad areas into one large wetted area. This value was determined by one-dimensional calculations, and corroborated by two-dimensional calculations. It should be emphasized that, for developing a water budget for surface application of water, the results of these analyses indicate that the total quantity of water used is the most important parameter; of lesser importance are the rate and the time span of distribution of the water.

To illustrate how the value of 16 meters of surficial water may be used to construct a water budget, a simple example is provided here. For this example, there are 250,000 m2 of road area, and 150,000 m2 of pad and facilities areas, all above the potential repository. The maximum amount of water that may be used for all activities on the roads is (16m)X(250,000 m2) =

4.0 X 106 m3, or 1.06 X 109 gallons. For this example, the only expected water application on the roads will be for dust control; therefore, all of the 1.06 billion gallons may be used for road watering for dust control. It is re-emphasized here that the rate at which the water is applied, and the length of time over which the roads are watered are not important; what is important is that the total accumulated water applied to the roads over the duration of ESF/repository activities does not exceed 1.06 X 109 gallons. Similarly, the maximum amount of water that may be used at the pads is (16m)X(150,000 m2) = 2.4 X 106 m3, or 634 X 106 gallons. There are a number of activities at the pads that require water (construction, experiments, etc.); it will be up to the project engineers charged with ESF design, testing, and operation to portion the water to the various activities.

It is possible that the project engineers will determine that more water is needed for various activities than the limit of 16 m will allow. Because this value is based on an ultra-conservative analysis, additional analyses would be required to provide a more realistic surface water constraint. It is expected that 16 m is a very strict constraint which could be relaxed considerably with a more detailed analysis.

The results of the two-dimensional calculations, which predict the maximum extent of water movement, provide guidance for the location of experiments in the ESF. These figures show that below the top few meters of the Topopah Spring lithophysae layer, TSw1, surficial water will have no effects on experiments; above this elevation, the effects are confined within an area four times the wetted surface area.

These calculations are based on available data and on the present conceptual understanding of the processes and mechanisms perceived active at Yucca Mountain, and may be refined as better understanding evolves through site characterization and through additional analyses. Some of the effects of the limitations and assumptions used in performing these analyses were discussed in Section 5 of this report.

7. REFERENCES

Bixler, N. E., 1985. NORIA-- A Finite Element Computer Program for Analyzing Water, Vapor, Air, and Energy Transport in Porous Media, SAND84-2057, Sandia National Laboratories, Albuquerque, New Mexico. (NNA.870721.0002)

DOE (U.S. Department of Energy), "General Guidelines for the Recommendation of Sites for Nuclear Waste Repositories," Code of Federal Regulations, Energy, Title 10, Part 960 (10 CFR 960), U.S. Government Printing Office, Washington, D.C., 1987. (HQS.880517.2924)

Dudley, A. L., R. R. Peters, M. S. Tierney, E. A. Klavetter, J. H. Gauthier, and M. L. Wilson, 1988. Total System Performance Assessment Code (TOSPAC) Volume 1: Physical and Mathematical Bases, SAND85-0002, Sandia National Laboratories, Albuquerque, New Mexico. (NNA.881202.0211)

Hopkins, P. L., 1990. COVE 2A Benchmarking Calculation Using LLUVIA, SAND88-2511, Sandia National Laboratories, Albuquerque, New Mexico. (NNA.900314.0236)

Hopkins, P. L., N. E. Bixler, and R. R. Eaton, 1991. NORIA-SP - A Finite Element Computer Program for Analyzing Liquid Water Transport in Porous Media, SAND90-2542, Sandia National Laboratories, Albuquerque, New Mexico. (NNA.911202.0031)

Montazer, P., and W. E. Wilson, 1984. Conceptual Hydrologic Model of Flow in the Unsaturated Zone, Yucca Mountain, Nevada, WRIR 84-4345, U.S. Geologic Survey, Lakewood, Colorado. (NNA.890327.0051)

NRC (U.S. Nuclear Regulatory Commission), "Disposal of High-Level Radioactive Wastes in Geologic Repositories," Code of Federal Regulations, Energy, Title 10, Part 60 (10 CFR 60), U.S. Government Printing Office, Washington, D.C., 1987. (HQS.880517.2923)

Ortiz, T. S., R. L. Williams, F. B. Nimick, B. C. Whittet, and D. L. South, 1985. A Three-Dimensional Model of Reference Thermal/Mechanical and Hydrological Stratigraphy at Yucca Mountain, Southern Nevada, SAND84-1076, Sandia National Laboratories, Albuquerque, New Mexico. (NNA.890315.0013)

Peters, R. R., 1988. Hydrological Technical Correspondence in Support of the Site Characterization Plan, SAND88-2784, Sandia National Laboratories, Albuquerque, New Mexico. (NNA.881202.0204)

Peters, R. R., E. A. Klavetter, I. J. Hall, S. C. Blair, P. R. Heller, and G. W. Gee, 1984. Fracture and Matrix Hydrologic Characteristics of Tuffaceous Materials from Yucca Mountain, Nye County, Nevada, SAND84-1471, Sandia National Laboratories, Albuquerque, New Mexico. (NNA.870407.0036)

Peters, R.R. and E. A. Klavetter, 1988. "A Continuum Model for Water Movement in an Unsaturated Fractured Rock Mass", Water Resources Research, Vol. 24, No. 3, pages 416-430, March 1988. (NNA.890523.0139)

Peterson, A. C., R. R. Eaton, A. J. Russo, and J. A. Lewin, 1988. Technical Correspondence in Support of an Evaluation of the Hydrologic Effects of Exploratory Shaft Facility Construction at Yucca Mountain, SAND88-2936, Sandia National Laboratories, Albuquerque, New Mexico. (NNA.881202.0206)

Prindle, R. W., and P. L. Hopkins, 1990. On Conditions and Parameters Important to Model Sensitivity for Unsaturated Flow Through Layered, Fractured Tuff: Results of Analyses for HYDROCOIN Level 3 Case 2, SAND89-0652, Sandia National Laboratories, Albuquerque, New Mexico. (NNA.900523.0211)

Problem Definition Memo, "ESF SDRD Analysis #1 - Calculation of Maximum Surface Water Use Above the Repository," PDM No. 72-28, Sandia National Laboratories, Albuquerque, New Mexico, December 1990. (NNA.910301.0074)

Problem Definition Memo, "ESF SDRD Analysis #1 - Effects of Surface Water on Experiments in the ESF," PDM No. 72-29, Sandia National Laboratories, Albuquerque, New Mexico, December 1990. (NNA.910301.0075)

SNL (Sandia National Laboratories), Site Characterization Plan Conceptual Design Report, SAND84-2641, H. R. MacDougall, L. W. Scully, and J. R. Tillerson, compilers, Albuquerque, New Mexico, September 1987. (NNA.880902.0014-.0019)

Stevens, A. L., and L. S. Costin, 1991. Findings of the ESF Alternatives Study, SAND90-3232, Sandia National Laboratories, Albuquerque, New Mexico. (NNA.910219.0003)

van Genuchten, M., 1980. "A closed-form equation for predicting the hydraulic conductivity of unsaturated soils," Soil Sci. Soc. Am. J., Vol. 44, pp. 892-898, 1980. (NNA.890522.0287)

Weeks, E. P., and W. E. Wilson, 1984. Preliminary Evaluation of Hydrologic Properties of Cores of Unsaturated Tuff, Test Well USW H-1, Yucca Mountain, Nevada, WRIR 84-4193, U.S. Geologic Survey, Lakewood, Colorado. (NNA.870407.0037)

Appendix A

Parameters Used for the Analyses

Description of variable, units	Value	Reference
Geometry		
Area of repository, m^2	5610000	RIB
Area of ES Pad and Roads, m^2	374955	ESF Alt. Study Case B3
Area of Empl. Exhaust Pad, m^2	17136	SCP, p6-130
(Total disturbed surface area, m^2)	392091	
Corresponding radius of disturbed surface area, m	353	
Water Properties		
Density of water, kg/m^3	1000	Standard
Compressibility of water, 1/m	4.30E-06	Standard
Dyn. Viscosity of water, kg/(m*sec)	0.001	Standard @ 68°F
Acceleration of gravity, m/sec^2	9.8	Standard
Steady-st. infil. rate (q), mm/yr	0.01	
m/sec	3.17E-13	Given: Boundary condition on surface

USW G-4 Stratigraphy and Rock Characteristics

Description of variable, units	Value	Reference
Material # 1 - CHn3, Calico Hills (water table is bottom boundary)		
Min. elevation, m	730.6	RIB (water table)
Max. elevation, m	735	RIB
Matrix effective porosity, none	0.28	CHnz/G4-11 SAND84-1471
Matrix sat. hyd. conductivity, m/s	2.00E-11	CHnz/G4-11 SAND84-1471
Matrix van Genuchten parameters		
Saturation value, none	1	CHnz/G4-11 SAND84-1471
Residual saturation, none	0.11	CHnz/G4-11 SAND84-1471
ALPHA coefficient, 1/m	0.00308	CHnz/G4-11 SAND84-1471
BETA coefficient, none	1.602	CHnz/G4-11 SAND84-1471
Fracture effective porosity, none	1	CHnz/G4-4F SAND84-1471
Fract. sat. hyd. conductivity, m/s	2.00E-04	CHnz/G4-4F SAND84-1471
Fracture van Genuchten parameters		
Saturation value, none	1	CHnz/G4-4F SAND84-1471
Residual saturation, none	0.0395	CHnz/G4-4F SAND84-1471
ALPHA coefficient, 1/m	1.2851	CHnz/G4-4F SAND84-1471
BETA coefficient, none	4.23	CHnz/G4-4F SAND84-1471
Fracture porosity, none	4.60E-05	SAND84-1471
Bulk-rock compressibility, 1/m	2.60E-06	SAND84-1471
Fracture compressibility, 1/m	2.80E-08	SAND84-1471

USW G-4 Stratigraphy and Rock Characteristics

Description of variable, units	Value	Reference
Material # 2 - CHn2, Calico Hills		
Min. elevation, m	735	RIB
Max. elevation, m	752	RIB
Matrix effective porosity, none	0.28	CHnz/G4-11 SAND84-1471
Matrix sat. hyd. conductivity, m/s	2.00E-11	CHnz/G4-11 SAND84-1471
Matrix van Genuchten parameters		
Saturation value, none	1	CHnz/G4-11 SAND84-1471
Residual saturation, none	0.11	CHnz/G4-11 SAND84-1471
ALPHA coefficient, 1/m	0.00308	CHnz/G4-11 SAND84-1471
BETA coefficient, none	1.602	CHnz/G4-11 SAND84-1471
Fracture effective porosity, none	1	CHnz/G4-4F SAND84-1471
Fract. sat. hyd. conductivity, m/s	2.00E-04	CHnz/G4-4F SAND84-1471
Fracture van Genuchten parameters		
Saturation value, none	1	CHnz/G4-4F SAND84-1471
Residual saturation, none	0.0395	CHnz/G4-4F SAND84-1471
ALPHA coefficient, 1/m	1.2851	CHnz/G4-4F SAND84-1471
BETA coefficient, none	4.23	CHnz/G4-4F SAND84-1471
Fracture porosity, none	4.60E-05	SAND84-1471
Bulk-rock compressibility, 1/m	2.60E-06	SAND84-1471
Fracture compressibility, 1/m	2.80E-08	SAND84-1471
Material # 3 - CHn1z, Calico Hills		
Min. elevation, m	752	RIB
Max. elevation, m	856	RIB
Matrix effective porosity, none	0.28	CHnz/G4-11 SAND84-1471
Matrix sat. hyd. conductivity, m/s	2.00E-11	CHnz/G4-11 SAND84-1471
Matrix van Genuchten parameters		
Saturation value, none	1	CHnz/G4-11 SAND84-1471
Residual saturation, none	0.11	CHnz/G4-11 SAND84-1471
ALPHA coefficient, 1/m	0.00308	CHnz/G4-11 SAND84-1471
BETA coefficient, none	1.602	CHnz/G4-11 SAND84-1471
Fracture effective porosity, none	1	CHnz/G4-4F SAND84-1471
Fract. sat. hyd. conductivity, m/s	2.00E-04	CHnz/G4-4F SAND84-1471
Fracture van Genuchten parameters		
Saturation value, none	1	CHnz/G4-4F SAND84-1471
Residual saturation, none	0.0395	CHnz/G4-4F SAND84-1471
ALPHA coefficient, 1/m	1.2851	CHnz/G4-4F SAND84-1471
BETA coefficient, none	4.23	CHnz/G4-4F SAND84-1471
Fracture porosity, none	4.60E-05	SAND84-1471
Bulk-rock compressibility, 1/m	2.60E-06	SAND84-1471
Fracture compressibility, 1/m	2.80E-08	SAND84-1471

USW G-4 Stratigraphy and Rock Characteristics

Description of variable, units	Value	Reference
Material # 4 - CHnlv, Calico Hills vitric		
Min. elevation, m	856	RIB
Max. elevation, m	861	RIB
Matrix effective porosity, none	0.46	CHnv/GU3-14 SAND84-1471
Matrix sat. hyd. conductivity, m/s	2.70E-07	CHnv/GU3-14 SAND84-1471
Matrix van Genuchten parameters		
Saturation value, none	1	CHnv/GU3-14 SAND84-1471
Residual saturation, none	0.041	CHnv/GU3-14 SAND84-1471
ALPHA coefficient, 1/m	0.016	CHnv/GU3-14 SAND84-1471
BETA coefficient, none	3.872	CHnv/GU3-14 SAND84-1471
Fracture effective porosity, none	1	CHnv/G4-4F SAND84-1471
Fract. sat. hyd. conductivity, m/s	2.00E-04	CHnv/G4-4F SAND84-1471
Fracture van Genuchten parameters		
Saturation value, none	1	CHnv/G4-4F SAND84-1471
Residual saturation, none	0.0395	CHnv/G4-4F SAND84-1471
ALPHA coefficient, 1/m	1.2851	CHnv/G4-4F SAND84-1471
BETA coefficient, none	4.23	CHnv/G4-4F SAND84-1471
Fracture porosity, none	4.60E-05	SAND84-1471
Bulk-rock compressibility, 1/m	3.90E-06	SAND84-1471
Fracture compressibility, 1/m	2.80E-08	SAND84-1471
Material # 5 - TSw3, Topopah Springs		
Min. elevation, m	861	RIB
Max. elevation, m	877	RIB
Matrix effective porosity, none	0.11	TSw2
Matrix sat. hyd. conductivity, m/s	1.90E-11	TSw2
Matrix van Genuchten parameters		
Saturation value, none	1	TSw2
Residual saturation, none	0.08	TSw2
ALPHA coefficient, 1/m	0.00567	TSw2
BETA coefficient, none	1.798	TSw2
Fracture effective porosity, none	1	TSw2
Fract. sat. hyd. conductivity, m/s	1.75E-05	TSw2
Fracture van Genuchten parameters		
Saturation value, none	1	TSw2
Residual saturation, none	0.0395	TSw2
ALPHA coefficient, 1/m	1.2851	TSw2
BETA coefficient, none	4.23	TSw2
Fracture porosity, none	1.80E-04	TSw2
Bulk-rock compressibility, 1/m	5.80E-07	TSw2
Fracture compressibility, 1/m	1.20E-07	TSw2

USW G-4 Stratigraphy and Rock Characteristics

Description of variable, units	Value	Reference
Material # 6 - TSw2, Topopah Springs (repository horizon)		
Min. elevation, m	877	RIB
Max. elevation, m	1066	RIB
Matrix effective porosity, none	0.11	TSw2/G4-6 SAND84-1471
Matrix sat. hyd. conductivity, m/s	1.90E-11	TSw2/G4-6 SAND84-1471
Matrix van Genuchten parameters		
Saturation value, none	1	TSw2/G4-6 SAND84-1471
Residual saturation, none	0.08	TSw2/G4-6 SAND84-1471
ALPHA coefficient, 1/m	0.00567	TSw2/G4-6 SAND84-1471
BETA coefficient, none	1.798	TSw2/G4-6 SAND84-1471
Fracture effective porosity, none	1	TSw2/G4-2F SAND84-1471
Fract. sat. hyd. conductivity, m/s	1.75E-05	TSw2/G4-2F SAND84-1471
Fracture van Genuchten parameters		
Saturation value, none	1	TSw2/G4-2F SAND84-1471
Residual saturation, none	0.0395	TSw2/G4-2F SAND84-1471
ALPHA coefficient, 1/m	1.2851	TSw2/G4-2F SAND84-1471
BETA coefficient, none	4.23	TSw2/G4-2F SAND84-1471
Fracture porosity, none	1.80E-04	SAND84-1471
Bulk-rock compressibility, 1/m	5.80E-07	SAND84-1471
Fracture compressibility, 1/m	1.20E-07	SAND84-1471
Material # 7 - TSw1, Topopah Springs		
Min. elevation, m	1066	RIB
Max. elevation, m	1196	RIB
Matrix effective porosity, none	0.11	TSw1/G4-6 SAND84-1471
Matrix sat. hyd. conductivity, m/s	1.90E-11	TSw1/G4-6 SAND84-1471
Matrix van Genuchten parameters		
Saturation value, none	1	TSw1/G4-6 SAND84-1471
Residual saturation, none	0.08	TSw1/G4-6 SAND84-1471
ALPHA coefficient, 1/m	0.00567	TSw1/G4-6 SAND84-1471
BETA coefficient, none	1.798	TSw1/G4-6 SAND84-1471
Fracture effective porosity, none	1	TSw1/G4-2F SAND84-1471
Fract. sat. hyd. conductivity, m/s	2.20E-05	TSw1/G4-2F SAND84-1471
Fracture van Genuchten parameters		
Saturation value, none	1	TSw1/G4-2F SAND84-1471
Residual saturation, none	0.0395	TSw1/G4-2F SAND84-1471
ALPHA coefficient, 1/m	1.2851	TSw1/G4-2F SAND84-1471
BETA coefficient, none	4.23	TSw1/G4-2F SAND84-1471
Fracture porosity, none	4.10E-05	SAND84-1471
Bulk-rock compressibility, 1/m	1.20E-06	SAND84-1471
Fracture compressibility, 1/m	5.60E-08	SAND84-1471

USW G-4 Stratigraphy and Rock Characteristics

Description of variable, units	Value	Reference
Material # 8 - PTn, Paintbrush Tuff		
Min. elevation, m	1196	RIB
Max. elevation, m	1234	RIB
Matrix effective porosity, none	0.4	PTn/GU3-7 SAND84-1471
Matrix sat. hyd. conductivity, m/s	3.90E-07	PTn/GU3-7 SAND84-1471
Matrix van Genuchten parameters		
Saturation value, none	1	PTn/GU3-7 SAND84-1471
Residual saturation, none	0.1	PTn/GU3-7 SAND84-1471
ALPHA coefficient, 1/m	0.015	PTn/GU3-7 SAND84-1471
BETA coefficient, none	6.872	PTn/GU3-7 SAND84-1471
Fracture effective porosity, none	1	PTn/G4-3F SAND84-1471
Fract. sat. hyd. conductivity, m/s	6.10E-04	PTn/G4-3F SAND84-1471
Fracture van Genuchten parameters		
Saturation value, none	1	PTn/G4-3F SAND84-1471
Residual saturation, none	0.0395	PTn/G4-3F SAND84-1471
ALPHA coefficient, 1/m	1.2851	PTn/G4-3F SAND84-1471
BETA coefficient, none	4.23	PTn/G4-3F SAND84-1471
Fracture porosity, none	2.70E-05	SAND84-1471
Bulk-rock compressibility, 1/m	8.20E-06	SAND84-1471
Fracture compressibility, 1/m	1.90E-07	SAND84-1471
Material # 9 - TCw, Tiva Canyon		
Min. elevation, m	1234	RIB
Max. elevation, m	1261	RIB
Matrix effective porosity, none	0.08	TCw/G4-1 SAND84-1471
Matrix sat. hyd. conductivity, m/s	9.70E-12	TCw/G4-1 SAND84-1471
Matrix van Genuchten parameters		
Saturation value, none	1	TCw/G4-1 SAND84-1471
Residual saturation, none	0.002	TCw/G4-1 SAND84-1471
ALPHA coefficient, 1/m	0.00821	TCw/G4-1 SAND84-1471
BETA coefficient, none	1.558	TCw/G4-1 SAND84-1471
Fracture effective porosity, none	1	TCw/G4-2F SAND84-1471
Fract. sat. hyd. conductivity, m/s	3.80E-05	TCw/G4-2F SAND84-1471
Fracture van Genuchten parameters		
Saturation value, none	1	TCw/G4-2F SAND84-1471
Residual saturation, none	0.0395	TCw/G4-2F SAND84-1471
ALPHA coefficient, 1/m	1.2851	TCw/G4-2F SAND84-1471
BETA coefficient, none	4.23	TCw/G4-2F SAND84-1471
Fracture porosity, none	1.40E-04	SAND84-1471
Bulk-rock compressibility, 1/m	6.20E-07	SAND84-1471
Fracture compressibility, 1/m	1.32E-06	SAND84-1471

USW G-4 Stratigraphy and Rock Characteristics

Description of variable, units	Value	Reference
Material # 10 - UO (Alluvium) (Top elevation is ground surface)		
Min. elevation, m	1261	RIB
Max. elevation, m	1270	RIB
Matrix effective porosity, none	0.32	Alluvium[a]
Matrix sat. hyd. conductivity, m/s	5.00E-07	Alluvium[a]
Matrix van Genuchten parameters		
Saturation value, none	1	Alluvium[b]
Residual saturation, none	0.3	Alluvium[b]
ALPHA coefficient, 1/m	0.423	Alluvium[b]
BETA coefficient, none	2.06	Alluvium[b]
Fracture effective porosity, none	0.32	Alluvium[a]
Fract. sat. hyd. conductivity, m/s	5.00E-07	Alluvium[a]
Fracture van Genuchten parameters		
Saturation value, none	1	Alluvium[b]
Residual saturation, none	0.3	Alluvium[b]
ALPHA coefficient, 1/m	0.423	Alluvium[b]
BETA coefficient, none	2.06	Alluvium[b]
Fracture porosity, none	0	
Bulk-rock compressibility, 1/m	0	
Fracture compressibility, 1/m	0	

a - From Alan Flint, U. S. Geological Survey

b - van Genuchten, M., "A closed-form equation for predicting the hydraulic conductivity of unsaturated soils," Soil Sci. Soc. Am. J., Vol. 44, pp. 892-898, 1980.

Appendix B

Reference Information Base and Site Engineering Properties Data Base

This report uses information from the Reference Information Base (RIB); see Appendix A for a listing of the values used.

This report contains no information for inclusion in the Reference Information Base (RIB).

This report contains no information for inclusion in the Site Engineering Properties Data Base (SEPDB).

DISTRIBUTION LIST

1 J. W. Bartlett, Director (RW-1)
Office of Civilian Radioactive
Waste Management
U.S. Department of Energy
1000 Independence Avenue, S.W.
Washington, D.C. 20585

1 F. G. Peters, Deputy Director (RW-2)
Office of Civilian Radioactive
Waste Management
U.S. Department of Energy
1000 Independence Avenue, S.W.
Washington, D.C. 20585

1 T. H. Isaacs (RW-4)
Office of Strategic Planning
and International Programs
Office of Civilian Radioactive
Waste Management
U.S. Department of Energy
1000 Independence Avenue, S.W.
Washington, D.C. 20585

1 J. D. Saltzman (RW-5)
Office of External Relations
Office of Civilian Radioactive
Waste Management
U.S. Department of Energy
1000 Independence Avenue, S.W.
Washington, D.C. 20585

1 Samuel Rousso (RW-10)
Office of Program and Resources
Management
Office of Civilian Radioactive
Waste Management
U.S. Department of Energy
1000 Independence Avenue, S.W.
Washington, D.C. 20585

1 J. C. Bresee (RW-10)
Office of Civilian Radioactive
Waste Management
U.S. Department of Energy
1000 Independence Avenue, S.W.
Washington, D.C. 20585

1 C. P. Gertz (RW-20)
Office of Geologic Disposal
Office of Civilian Radioactive
Waste Management
U.S. Department of Energy
1000 Independence Avenue, S.W.
Washington, D.C. 20585

1 S. J. Brocoum (RW-22)
Analysis and Verification Division
Office of Civilian Radioactive
Waste Management
U.S. Department of Energy
1000 Independence Avenue, S.W.
Washington, D.C. 20585

1 D. D. Shelor (RW-30)
Office of Systems and Compliance
Office of Civilian Radioactive
Waste Management
U.S. Department of Energy
1000 Independence Avenue, S.W.
Washington, D.C. 20585

1 J. Roberts (RW-33)
Office of Civilian Radioactive
Waste Management
U.S. Department of Energy
1000 Independence Avenue, S.W.
Washington, D.C. 20585

1 G. J. Parker (RW-332)
Office of Civilian Radioactive
Waste Management
U.S. Department of Energy
1000 Independence Avenue, S.W.
Washington, D.C. 20585

1 Associate Director (RW-40)
Office of Storage and Transportation
Office of Civilian Radioactive
Waste Management
U.S. Department of Energy
1000 Independence Avenue, S.W.
Washington, D.C. 20585

1 Associate Director (RW-50)
Office of Contract Business
Management
Office of Civilian Radioactive
Waste Management
U.S. Department of Energy
1000 Independence Avenue, S.W.
Washington, D.C. 20585

1 C. G. Russomanno (RW-52)
Office of Civilian Radioactive
Waste Management
U.S. Department of Energy
1000 Independence Avenue, S.W.
Washington, D.C. 20585

1 D. U. Deere, Chairman
Nuclear Waste Technical
Review Board
1100 Wilson Blvd. #910
Arlington, VA 22209-2297

1 Dr. John E. Cantlon
Nuclear Waste Technical Review Board
1795 Bramble Dr.
East Lansing, MI 48823

1 Dr. Melvin W. Carter
Nuclear Waste Technical Review Board
4621 Ellisbury Dr., N.E.
Atlanta, GA 30332

1 Dr. Donald Langmuir
Nuclear Waste Technical Review Board
109 So. Lookout Mountain Cr.
Golden, CO 80401

1 Dr. D. Warner North
Nuclear Waste Technical Review Board
Decision Focus, Inc.
4984 El Camino Real
Los Altos, CA 94062

1 Dr. Dennis L. Price
Nuclear Wast Technical Review Board
1011 Evergreen Way
Blacksburg, VA 24060

1 Dr. Ellis D. Verink
Nuclear Waste Technical Review Board
4401 N.W. 18th Place
Gainesville, FL 32605

5 C. P. Gertz, Project Manager
Yucca Mountain Project Office
U.S. Department of Energy
P.O. Box 98608--MS 523
Las Vegas, NV 89193-8608

1 C. L. West, Director
Office of External Affairs
DOE Field Office, Nevada
U.S. Department of Energy
P.O. Box 98518
Las Vegas, NV 89193-85180

12 Technical Information Officer
DOE Field Office, Nevada
U.S. Department of Energy
P.O. Box 98518
Las Vegas, NV 89193-8518

1 P. K. Fitzsimmons, Director
Health Physics & Environmental
Division
DOE Field Office, Nevada
U.S. Department of Energy
P.O. Box 98518
Las Vegas, NV 89193-8518

1 D. R. Elle, Director
Environmental Protection Division
DOE Field Office, Nevada
U.S. Department of Energy
P.O. Box 98518
Las Vegas, NV 89193-8518

1 Repository Licensing & Quality
Assurance Project Directorate
Division of Waste Management
U.S. Nuclear Regulatory Commission
Washington, D.C. 20555

1 Senior Project Manager for Yucca
Mountain Repository Project Branch
Division of Waste Management
U.S. Nuclear Regulatory Commission
Washington, D.C. 20555

1 NRC Document Control Desk
Division of Waste Management
U.S. Nuclear Regulatory Commission
Washington, D.C. 20555

1 P. T. Prestholt
NRC Site Representative
301 E. Stewart Ave.
Las Vegas, NV 89101

1 E. P. Binnall
Field Systems Group Leader
Building 50B/4235
Lawrence Berkeley Laboratory
Berkeley, CA 94720

1 Center for Nuclear Waste
Regulatory Analyses
6220 Culebra Road
Drawer 28510
San Antonio, TX 78284

3 L. J. Jardine
Technical Project Officer for YMP
Mail Stop L-204
Lawrence Livermore National
Laboratory
P.O. Box 808
Livermore, CA 94550

4 R. J. Herbst
Technical Project Officer for YMP
N-5, Mail Stop J521
Los Alamos National Laboratory
P.O. Box 1663
Los Alamos, NM 87545

1 H. N. Kalia
Exploratory Shaft Test Manager
Los Alamos National Laboratory
Mail Stop 527
101 Convention Center Dr.
Suite 820
Las Vegas, NV 89109

1 J. F. Divine
Assistant Director for
Engineering Geology
U.S. Geological Survey
106 National Center
12201 Sunrise Valley Dr.
Reston, VA 22092

6 L. R. Hayes
Technical Project Officer
Yucca Mountain Project Branch--MS 425
U.S. Geological Survey
P.O. Box 25046
Denver, CO 80225

1 V. R. Schneider
Asst. Chief Hydrologist--MS 414
Office of Program Coordination
& Technical Support
U.S. Geological Survey
12201 Sunrise Valley Drive
Reston, VA 22092

1 R. B. Raup, Jr.
Geological Division Coordinator
MS 913
Yucca Mountain Project
U.S. Geological Survey
P.O. Box 25046
Denver, CO 80225

1 D. H. Appel, Chief
Hydrologic Investigations Program
MS 421
U.S. Geological Survey
P.O. Box 25046
Denver, CO 80225

1 E. J. Helley
Branch of Western Regional Geology
MS 427
U.S. Geological Survey
345 Middlefield Road
Menlo Park, CA 94025

1 Chief
Nevada Operations Office
U.S. Geological Survey
101 Convention Center Drive
Suite 860, MS 509
Las Vegas, NV 89109

1 D. Zesiger
U.S. Geological Survey
101 Convention Center Dr.
Suite 860 - MS509
Las Vegas, NV 89109

1 R. V. Watkins, Chief
Project Planning and Management
U.S. Geological Survey
P.O. Box 25046
421 Federal Center
Denver, CO 80225

1 A. L. Flint
U.S. Geological Survey
MS 721
P.O. Box 327
Mercury, NV 89023

1 D. A. Beck
U.S. Geological Survey
1500 E. Tropicana, Suite 201
Las Vegas, NV 89119

1 P. A. Glancy
U.S. Geological Survey
Federal Building, Room 224
Carson City, NV 89701

1 Sherman S. C. Wu
Branch of Astrogeology
U.S. Geological Survey
2255 N. Gemini Dr.
Flagstaff, AZ 86001

1 J. H. Sass
Branch of Tectonophysics
U.S. Geological Survey
2255 N. Gemini Dr.
Flagstaff, AZ 86001

1 DeWayne A. Campbell
Technical Project Officer for YMP
Bureau of Reclamation
Code D-3790
P.O. Box 25007
Denver, CO 80225

1 K. W. Causseaux
NHP Reports Chief
U.S. Geological Survey
421 Federal Center
P.O. Box 25046
Denver, CO 80225

1 V. M. Glanzman
U.S. Geological Survey
913 Federal Center
P.O. Box 25046
Denver, CO 80225

1 J. H. Nelson
Technical Project Officer for YMP
Science Applications International Corp.
101 Convention Center Dr.
Suite 407
Las Vegas, NV 89109

2 SAIC-T&MSS Library
Science Applications International Corp.
101 Convention Center Dr.
Suite 407
Las Vegas, NV 89109

1 Elaine Ezra
YMP GIS Project Manager
EG&G Energy Measurements, Inc.
Mail Stop D-12
P.O. Box 1912
Las Vegas, NV 89125

1 R. E. Jackson, Program Manager
Roy F. Weston, Inc.
955 L'Enfant Plaza, Southwest
Washington, D.C. 20024

1 Technical Information Center
Roy F. Weston, Inc.
955 L'Enfant Plaza, Southwest
Washington, D.C. 20024

1 D. Hedges, Vice President,
Quality Assurance
Roy F. Weston, Inc.
4425 Spring Mountain Road, Suite 300
Las Vegas, Nevada 89102

1 D. L. Fraser, General Manager
Reynolds Electrical & Engineering Co.
Mail Stop 555
P.O. Box 98521
Las Vegas, NV 89193-8521

1 R. F. Pritchett
Technical Project Officer for YMP
Reynolds Electrical & Engineering Co.
MS 408
P.O. Box 98521
Las Vegas, NV 89193-8521

1 B. W. Colston
General Manager & President
Las Vegas Branch
Raytheon Services Nevada
Mail Stop 416
P.O. Box 95487
Las Vegas, NV 89193-5487

1 R. L. Bullock
Technical Project Officer for YMP
Raytheon Services Nevada
Suite P250, MS 403
101 Convention Center Dr.
Las Vegas, NV 89109

1 R. E. Lowder
Technical Project Officer for YMP
MAC Technical Services
101 Convention Center Drive
Suite 1100
Las Vegas, NV 89109

1 C. K. Hastings, Manager
PASS Program
Pacific Northwest Laboratories
P.O. Box 999
Richland, WA 99352

1 A. T. Tamura
Science and Technology Division
Office of Scientific and Technical Information
U.S. Department of Energy
P.O. Box 62
Oak Ridge, TN 37831

1 Carlos G. Bell, Jr.
Professor of Civil Engineering
Civil and Mechanical Engineering Department
University of Nevada, Las Vegas
4505 South Maryland Parkway
Las Vegas, NV 89154

1 C. F. Costa, Director
Nuclear Radiation Assessment Division
U.S. Environmental Protection Agency
Environmental Monitoring Systems Laboratory
P.O. Box 93478
Las Vegas, NV 89193-3478

1 ONWI Library
Battelle Columbus Laboratory
Office of Nuclear Waste Isolation
505 King Avenue
Columbus, OH 43201

1 T. Hay, Executive Assistant
Office of the Governor
State of Nevada
Capitol Complex
Carson City, NV 89710

3 R. R. Loux, Jr.
Executive Director
Nuclear Waste Project Office
State of Nevada
Evergreen Center, Suite 252
1802 North Carson Street
Carson City, NV 89710

1 C. H. Johnson
Technical Program Manager
Nuclear Waste Project Office
State of Nevada
Evergreen Center, Suite 252
1802 North Carson Street
Carson City, NV 89710

1 John Fordham
Water Resources Center
Desert Research Institute
P.O. Box 60220
Reno, NV 89506

1 Dr. Martin Mifflin
Water Resources Center
Desert Research Institute
2505 Chandler Avenue
Suite 1
Las Vegas, NV 89120

1 Eric Anderson
Mountain West Research-Southwest Inc.
2901 N. Central Ave. #1000
Phoenix, AZ 85012-2730

1 Department of Comprehensive Planning
Clark County
225 Bridger Avenue, 7th Floor
Las Vegas, NV 89155

1 Planning Department
Nye County
P.O. Box 153
Tonopah, NV 89049

1 Lincoln County Commission
Lincoln County
P.O. Box 90
Pioche, NV 89043

5 Judy Foremaster
City of Caliente
P.O. Box 158
Caliente, NV 89008

1 Economic Development Department
City of Las Vegas
400 East Stewart Avenue
Las Vegas, NV 89101

1 Community Planning & Development
City of North Las Vegas
P.O. Box 4086
North Las Vegas, NV 89030

1 Director of Community Planning
City of Boulder City
P.O. Box 367
Boulder City, NV 89005

1 Commission of the European Communities
200 Rue de la Loi
B-1049 Brussels
BELGIUM

2 M. J. Dorsey, Librarian
YMP Research and Study Center
Reynolds Electrical & Engineering Co., Inc.
MS 407
P.O. Box 98521
Las Vegas, NV 89193-8521

1 Amy Anderson
Argonne National Laboratory
Building 362
9700 So. Cass Ave.
Argonne, IL 60439

2 L. D. Foust
Nevada Site Manager
TRW Environmental Safety Systems
101 Convention Center Drive
Suite 540 - MS 423
Las Vegas, NV 89109

1 Deirdre M. Boak
Science Applications International Corp.
101 Convention Center Drive
Suite 407
Las Vegas, NV 89109

1	6300	T. O. Hunter
1	6310	T. E. Blejwas, Actg.
1	6310A	L. E. Shephard
1	6310A	A. W. Dennis
1	6312	F. W. Bingham
1	6312	W. F. Chambers
1	6312	E. Dunn
1	6312	J. H. Gauthier
1	6312	P. G. Kaplan
1	6312	F. C. Lauffer
1	6312	S. A. Shannon
1	6312	M. L. Wilson
1	6313	L. S. Costin
1	6313	M. E. Fewell
1	6313	S. R. Sobolik
1	6313	A. H. Treadway
1	6315	F. B. Nimick, Actg.
1	6315	J. Fernandez
1	6316	R. P. Sandoval
2	6318	R. J. Macer for 100/12147/SAND91-0790/QA
1	6319	R. R. Richards
1	1510	J. C. Cummings
1	1511	J. S. Rottler
1	1511	R. R. Eaton
1	1511	P. L. Hopkins
1	1511	M. J. Martinez
1	1512	A. C. Ratzel
1	1513	R. D. Skocypec
1	1514	H. S. Morgan
5	3141	S. A. Landenberger
8	3145	Document Processing for DOE/OSTI
3	3151	G. C. Claycomb
1	6257	T. E. Hinkebein
1	6310	70/12147/72-28/1.3/QA
1	6310	70/12147/72-29/1.3/QA
20	6341	WMT Library
1	6410	D. J. McCloskey, Actg.
1	8523-2	Central Technical Files

SAND91-0790

The number in the lower right-hand corner is an accession number used for Office of Civilian Radioactive Waste Management purposes only. It should not be used when ordering this publication.

END

DATE FILMED

4/17/92